Winter 2005

Halonitromethane Treatment Using Advanced Oxidation Process: Rates, Mechanisms and Kinetic Modeling

Stuart Kirkham Cole
Old Dominion University

HALONITROMETHANE TREATMENT USING ADVANCED OXIDATION PROCESS: RATES, MECHANISMS AND KINETIC MODELING

by

Stuart Kirkham Cole
B.S., May 1980, Virginia Military Institute
M.E., December 1995, Old Dominion University

A Dissertation Submitted to the Faculty of
Old Dominion University in Partial Fulfillment of the
Requirement for the Degree of

DOCTOR OF PHILOSOPHY

ENVIRONMENTAL ENGINEERING

OLD DOMINION UNIVERSITY
December 2005

Approved By:

Muìde Erten-Unal (Director)

William A. Drewry (Member)

Garv C. Schafran (Member)

William J. Cooper (Member)

ABSTRACT

HALONITROMETHANE TREATMENT USING ADVANCED OXIDATION PROCESS: RATES, MECHANISMS AND KINETIC MODELING

Stuart Kirkham Cole
Old Dominion University, 2005
Director: Dr. Mujde Erten-Unal

Halonitromethanes (HNMs) are low molecular weight halogenated disinfection-by-products (DBPs) found to be formed during ozonation, chlorination, or chloramination of waters containing natural bromide ion and nitrogenous organic matter. This work identifies the absolute rate constants for the oxidative hydroxyl radical (•OH) and reductive hydrated electron (e_{aq}^-) extinction of HNM compounds. Three forms of HNMs included in this study are the chlorinated, brominated, and mixed halogenated compounds. Electron pulse radiolysis and transient absorption spectroscopy were used to measure •OH and e_{aq}^- radical absolute reaction rate constants for a total of nine HNMs. To elucidate the decomposition reaction mechanism, six HNMs were exposed to ^{60}Co gamma (γ) irradiation at various times (absorbed doses). The disappearance of the parent compound in the ^{60}Co irradiated samples was monitored and the mass balance of ionic residuals was determined. Using reaction rate constants and the mechanistic data, a preliminary reaction mechanism was proposed and used in a kinetic model to describe the removal of the HNMs in aqueous solution. The model was then extended to simulate the electron beam process on waters of defined chemical composition and used for estimating the economics of the treatment of trichloronitromethane at large scale.

ACKNOWLEDGEMENT

Grateful appreciation is expressed to the members of my dissertation committee, Dr. William Drewry, Dr. Gary C. Schafran, Dr. Mujde Erten-Unal, of Old Dominion University, Civil and Environmental Engineering Department for reviewing this manuscript and for their invaluable help and suggestions, and Dr. William J. Cooper, Department of Chemistry and Biochemistry, University of North Carolina at Wilmington who is my mentor and guide.

I am thankful for the support provided by Dr. Robert V. Fox and Dr. Bruce J. Mincher of the Idaho National Laboratory; Dr. Piero R. Gardinali and Dr. Kevin E. O'Shea, Department of Chemistry & Biochemistry, Florida International University; and Dr. Stephen P. Mezyk, Department of Chemistry and Biochemistry, California State University at Long Beach.

Appreciation is given for the support provided in-part by the Radiation Laboratory, University of Notre Dame, and the Office of Basic Energy Sciences of the U.S. Department of Energy for use of the laboratory and facilities.

This dissertation and work is dedicated to my wife Sharon who has steadfastly given her unyielding love, devotion and support, my sister Wyc, the memory of my wonderful mother Mary and father Sam who possessed the gift of love and reason, the memory of my brother Drum, my family, and to all who have provided me encouragement along the way.

TABLE OF CONTENTS

Page

LIST OF TABLES vii

LIST OF FIGURES viii

Section

1. INTRODUCTION AND LITERATURE SEARCH 10
   - 1.1. Purpose 10
   - 1.2. Disinfection-by-products 12
   - 1.3. Overview of Free Radical Chemistry 14
     - 1.3.1. Radiation 20
     - 1.3.2. Formation 26
     - 1.3.3. Steady State Radiolysis 31
     - 1.3.4. Free Radical Characteristics 33
   - 1.4. Rate Constants 38
     - 1.4.1. Mechanistic Approach for Study of Reaction of HNMs with the Hydroxyl Radical 41
     - 1.4.2. Mechanistic Approach for Study of Reaction of HNMs with the Hydrated Electron Radical 42
   - 1.5. Halonitromethanes 42
     - 1.5.1. Formation of HNMs 43
     - 1.5.2. Drinking Water HNM Disinfection-by-products 43
     - 1.5.3. Fate and Environmental Degradation of HNMs 45
   - 1.6. Research Goals 47

2. FREE RADICAL CHEMISTRY OF HALONITROMETHANES: RATE CONSTANTS FOR REDOX REACTION OF HYDROXYL RADICAL AND HYDRATED ELECTRON IN A PULSE RADIOLYSIS STUDY 50
   - 2.1. Introduction 50
   - 2.2. Methods and Materials 51
   - 2.3. Rate Constants 53
   - 2.4. Summary 57

3. FREE RADICAL CHEMISTRY OF TRICHLORONITROMETHANE (CHLOROPICRIN): RATE CONSTANTS AND DEGRADATION MECHANISM BY OXIDATION-REDUCTION REACTIONS 59
   - 3.1. Introduction 59
   - 3.2. Methods and Materials 61
   - 3.3. Results and Discussion 64
   - 3.4. Summary 83

TABLE OF CONTENTS

Section Page

4. THE FREE RADICAL CHEMISTRY OF BROMONITROMETHANE: RATE CONSTANTS AND DEGRADATION MECHANISM BY OXIDATION-REDUCTION REACTIONS 84
4.1. Introduction 84
4.2. Rate Constant Determination 85
4.3. Mechanism 92
4.4. Summary 92

5. OVERVIEW OF REACTION MECHANISMS AND KINETIC MODELING: THE FREE RADICAL CHEMISTRY AND REACTION MECHANISMS FOR HALONITROMETHANES 93
5.1. Introduction 93
5.2. Rate Constant 94
5.3. Mechanisms 98
5.4. Dose Rate Constant 103
5.5. Simulation of Full Scale Electron Beam 104
5.6. Summary 111

6. SUMMARY 121

REFERENCES 123

APPENDICES

A. COMPUTER PROGRAMS FOR KINETIC ANALYSIS 140
A.1. Mass Action Kinetic Simulation 140

B. ANALYTICAL METHODS 144
B.1. Nuclear Magnetic Resonance 145
B.2. Gas Chromatography Mass Spectrometry 145
B.3. High Performance Liquid Chromatography 147
B.4. Ion Chromatography 149

VITA 151

LIST OF TABLES

Table		Page
1.1.	Halonitromethanes (HNMs) identified in this study	11
1.2.	Events occurring after excitation of an electron in water	17
1.3.	Known reactions in pure water resulting from radiolysis and the second-order rate constant	19
1.4.	Trichloronitromethane (Chloropicrin) found in drinking water	44
2.1.	Halonitromethane abbreviation, formula, and source	52
2.2.	Trichloronitromethane hydroxyl radical experimental data	55
2.3.	Trichloronitromethane hydrated electron radical experimental data	56
2.4.	Pseudo-second-order rate constants for reaction of hydrated electron and hydroxyl radical with halonitromethane compounds	57
3.1.	Summary of residual ion results for ^{60}Co irradiation of TCNM solutions (1.13 mM) in pure water at doses up to 8.54 kGy	69
3.2.	Linearized reaction mechanism for the free radical destruction of TCNM	77
3.3.	Comparison of experimental and model results for ^{60}Co irradiation of TCNM solutions (1.13 mM) in pure water at doses up to 8.54 kGy	81
5.1.	Summary of removal efficiency and G_D values (mol $J^{-1} \times 10^{-7}$) for initial trichloronitromethane concentration of 1.13×10^{-3} M and 1.82×10^{-8} M (3 μg L^{-1})	102
5.2.	Dose for 90% and 99% trichloronitromethane removal and equivalent energy per order (EE/O) for pure water	110
B.1.	Analytical Methods	144
B.2.	Minimum Level of Detection for GC/MS	147
B.3.	HPLC standard data for oxalic acid and formic acid	148
B.4.	Ion chromatography standard data for Cl^- and NO_3^-	150
B.5.	Ion chromatography standard data for Br^- and NO_2^-	150

LIST OF FIGURES

Figure — Page

1.1. NDRL LINAC (Model TB-8/16-1S 8 MeV S-Band) 22
3.1. Typical kinetic plot of $(SCN)_2^{\bullet -}$ formation for trichloronitromethane reaction with •OH 65
3.2. Competition kinetics plot for •OH reaction with trichloronitromethane using SCN^- as a standard 66
3.3. Typical kinetic decay profiles obtained for the hydrated electron absorbance of trichloronitromethane 67
3.4. Second-order rate constant determination for the reaction of the hydrated electron with trichloronitromethane 68
3.5. Comparison of experimental (◇) and modeled (○) data for ^{60}Co irradiated trichloronitromethane. $[TCNM]_0 = 1.13$ mM 82
3.6. Concentration of chloride ions from (□) experimental results, and (◇) model results; and nitrate ions (△) experimental results, and (○) model results; versus dose ^{60}Co irradiation 82
4.1. Competition kinetics plot for •OH reaction with bromonitromethane using SCN^- as a standard 87
4.2. Second-order rate constant for the reaction of hydrated election with bromonitromethane 88
4.3. Comparison of irradiated bromonitromethane and byproducts of irradiation 90
4.4. Steady state irradiated bromonitromethane concentration (◇) versus dose 91
5.1. Dose constant (k_D) for trichloronitromethane at ambient pH at different concentrations 103
5.2. Natural logarithm of the fraction of TCNM remaining as a function of time for $[TCNM] = 1.13 \times 10^{-3}$ M 108
5.3. Natural logarithm of the fraction of TCNM remaining as a function of time for $[TCNM] = 1.82 \times 10^{-8}$ M 109
5.4. Mass recovery of chloronitromethane, CH_2ClNO_2. Chloride (O), nitrate (Δ), and CH_2ClNO_2 (◆) 112
5.5. Mass recovery of dichloronitromethane, $CHCl_2NO_2$. Chloride (O), nitrate (Δ), and $CHCl_2NO_2$ (◆) 113
5.6. Mass recovery of dibromochloronitromethane, CBr_2ClNO_2. Bromide (■), Chloride (O), nitrate (Δ), and CBr_2ClNO_2 (◆) 114
5.7. Mass recovery of bromodichloronitromethane, $CBrCl_2NO_2$. Bromide (■), Chloride (O), nitrate (Δ), and $CBrCl_2NO_2$ (◆) 115
5.8. Dose constant (k_D) = 0.437 kGy^{-1} for logarithm chloronitromethane concentration (◇)versus dose in pure water 117
5.9. Dose constant (k_D) = 0.829 kGy^{-1} for logarithm dichloronitromethane concentration (◇)versus dose in pure water 118
5.10. Dose constant (k_D) = 0.581 kGy^{-1} for logarithm chlorodibromonitromethane concentration (◇)versus dose in pure water 119

LIST OF FIGURES

Figure Page

5.11. Dose constant (k_D) = 0.653 kGy^{-1} for logarithm bromodichloronitromethane concentration (◇)versus dose in pure water 120
B.1. Calibration curves for GC/MS 146

1. INTRODUCTION AND LITERATURE SEARCH

1.1. Purpose

Radiation chemistry has been studied extensively for many years, and in 1914 Debierne suggested that free radicals formed in the water might be responsible for the chemical action of radiation (Spinks and Woods, 1964). The study of radiation exposure to matter has been fundamental towards the advances in the nuclear power industry, radiation biology, food safety, and medicine. The interaction of radiation with water (radiolysis) provides environmental scientists and engineers a process capable of fulfilling the need for finding safe alternatives in water treatment. The exposure of water to ionizing radiation produces free radicals. Free radicals consist of an atom or group of atoms possessing one or more unpaired electrons (Leigh, 1990) and their formation is complete at 10^{-7} seconds (Buxton *et al.*, 1988), the time after the passage of ionizing particles such as gamma (γ) or fast electrons, have produced tracks and spurs within the water medium. At 10^{-5} seconds, the radicals react with the solute followed by diffusion of the radicals and molecular products in the bulk of the water (Spinks and Woods, 1964).

The purpose of this study was to investigate the degradation of halonitromethanes (HNMs) summarized in Table 1.1 as an undesired disinfection-by-product (DBP) contaminant in water by use of free radical chemistry.

Table 1.1. Halonitromethanes (HNMs) identified in this study.

	Purity (%)	CAS Number
Chlorinated Species		
Chloronitromethane	92.9[a]	1794-84-9
Dichloronitromethane	98.7[a]	7119-89-3
Trichloronitromethane (Chloropicrin)	99.4[a]	76-06-2
Brominated Species		
Bromonitromethane	99[b]	563-70-2
Dibromonitromethane	92.1[a]	598-91-4
Tribromonitromethane (Bromopicrin)	99.9[a]	464-10-8
Mixed Halogen Species		
Bromochloronitromethane	89.5[a]	135531-25-8
Bromodichloronitromethane	92.2[a]	918-01-4
Dibromochloronitromethane	91.6[a]	1184-89-0

[a]As determined by Gas Chromatography/Mass Spectrometry (GC/MS).
[b]As determined by Nuclear Magnetic Resonance (NMR).

This study includes identification of rate constants for free radical reduction-oxidation (redox) reactions with HNMs using free radicals generated by a Linear Accelerator (LINAC) and ^{60}Co irradiator. Reaction mechanisms and rate constants for destruction of HNMs were elucidated by exposure of six of nine HNM compounds to steady state ionizing radiation derived from a ^{60}Co source which emits gamma particles by its natural decay scheme. The mass production of the parent ions (chloride, bromide, and nitrate) from the HNM compound and the byproduct compounds oxalate, formate, and total organic carbon (TOC) produced were also investigated. Those mass amounts, as byproducts, found remaining in solution were then applied quantitatively in a kinetic analysis. The rate constants derived from pulse radiolysis and mass data obtained from the ^{60}Co steady state irradiations was then used in a mass action kinetic computer model

simulation to replicate and confirm a kinetic reaction mechanism. This degradation kinetic reaction mechanism was then adjusted and optimized according to known kinetic reactions. The mechanism was then incorporated into a kinetic computer model for simulation of a large scale electron beam irradiation facility. Based on these results, an energy cost for treatment of HNMs in drinking water was estimated. The reaction rate constants, degradation mechanisms, quantification of mass byproducts produced during destruction of HNM, and identification of the required radiation dose levels to degrade HNMs will directly support the needs of scientists and engineers in treatment of water.

This work was accomplished under controlled experimental conditions. Observations were made at constant temperature, pressure, and ambient pH. Solutions were prepared with ultra-pure de-ionized tap water from the Notre Dame Radiation Laboratory water treatment system to reduce potential for interference. Quality assurance and control was implemented by use of established laboratory procedures and data management practices.

1.2. Disinfection-by-products

Disinfectant chemicals are used in drinking water throughout the world as a means to maintain the health of the public and for the public's protection from waterborne microbial pathogens. Disinfection-by-products (DBPs) are formed in water from the chemical reaction of disinfection chemicals such as chlorine (Rook, 1974) and ozone (Richardson *et al.,* 1999) with natural organic materials (NOM).

Chlorine, as a chemical disinfectant, has been found to be a source of haloform DBPs identified as trihalomethanes (THM's). These THM's are produced from the interaction between chlorine and NOM in the water (Krasner *et al.,* 1996). DBP

production from use of chloramines has been found to be sensitive to pH, the chlorine-to-nitrogen ratio (Sayato *et al.,* 1982; Thibaud *et al.,* 1987), and natural bromide concentrations in the source water (Cavanagh *et al.,* 1992; Thibaud *et al.,* 1988). Recognizing the need to balance disinfection needs required for control of pathogens with DBP production, water purveyors routinely test these variables to find optimal operating conditions to minimize their formation (Diehl *et al.,* 2000). If naturally occurring bromide is present in water, it may be oxidized and react with NOM and then form brominated DBPs (Cavanagh *et al.,* 1992). The DBPs such as THMs and five haloacetic acids (HAA_5) DBPs have been found to represent a health hazard in drinking water and are regulated by the U.S. Environmental Protection Agency, Safe Drinking Water Act, Stage I Disinfection Byproducts regulations to a maximum permissible contaminant level (MCL) in drinking water of 80 and 60 $\mu g\ L^{-1}$, respectively (U.S. Environmental Protection Agency, 1997).

The use of disinfectants such as ozone, chlorine, chloramines and chlorine dioxide when used in water treatment have also been found to produce DBPs such as trichloronitromethane (TCNM) and is a chlorinated form of halonitromethane (Becke *et al.,* 1984). When ozone is used in water treatment, chemical reactions may occur with both inorganic and organic compounds to form HNM DBPs that appears in three forms: chlorinated, brominated, or mixed halogenated (Cl^-, Br^-) DBPs (Richardson *et al.,* 1999). Although these HNM DBPs are not currently regulated by the U.S. Environmental Protection Agency, they have been identified to be more potent mammalian cytotoxin and genotoxin, e.g., TCNM is 32.6 times more cytotoxic than dichloroacetic acid (DCAA) and trichloroacetic acid (TCAA) as two of the regulated HAA_5 (Plewa *et al.,*

2004). The HAA_5 compounds are currently regulated by the U.S. Environmental Protection Agency (1997).

The DBPs formed from the disinfection process can be reduced through use of treatment processes designed for the removal of the NOM, TOC, or other DBP precursors before they interact with chemical disinfectants. These water treatment processes may include physiochemical processes such as flocculation and sedimentation, membrane (direct) filtration, biological filtration, carbon absorption, or ion exchange (anion and cation resin). Other methods for control of DBPs include the use of a combination of treatment strategies. The combination strategies may include any two or more conventional treatment processes or one implemented in combination with the application of disinfection chemicals such as chloramines where it is used for residual disinfection. Chloramines, as a residual disinfectant, were found to reduce the potential for formation of THM DBPs in the water distribution system (Diehl *et al.,* 2000).

1.3. Overview of Free Radical Chemistry

With the use of chemicals disinfectants such as chlorine and the expanded use of ozone (Richardson, 1999), the formation of HNMs such as trichloronitromethane can be expected in drinking water (Hoigné and Bader, 1988). Surveys of multiple drinking waters have indicated the presence of chlorinated and brominated forms of HNMs (Weinberg *et al.*, 2002). Means for their total removal may include advanced oxidation processes (AOPs), using free radical chemistry.

Free radical AOPs have been well studied for degradation of many environmental pollutants (Cooper *et al.,* 2004) and for the elimination of NOM as precursors to

formation of THM DBPs in water (Cooper *et al.,* 1996a). The free radicals produced by the electron beam and ^{60}Co gamma (γ) irradiation have been found to effectively remove THMs in water (Cooper and Cadavid, 1993) and degrade bromate to the bromide (Br^-) ion (Siddiqui *et al.,* 1996). Electron beam irradiation, generating free radicals in water, have shown successful elimination of hazardous aqueous inorganic and organic pollutants (Mincher and Cooper, 2003), pesticides (Drzewicz *et al.,* 2004; Zona *et al.,* 2002), gasoline additive (MTBE) (Mezyk and Cooper, 2001), atrazine (Leitner *et al.,* 1999), trichloroethylene (TCE) and tetrachloroethylene (PCE) (Cooper *et al.,* 1993; Nickelsen *et al.,* 2002), chloroform (Mak *et al.,* 1996), (Tobien *et al.,* 2000; Mak *et al.,* 1997), benzene (Cooper *et al.,* 1996b; Nickelsen *et al.,* 1992), halogenated organics (ethane derivatives) (Lal *et al.,* 1988), nitromethane (Asmus *et al.,* 1964a), nitroparaffins (CH_3NO_2, $C_2H_5NO_2$, $C_3H_7NO_2$) (Sutton and Son, 1967), and organic solutes (Kalkwarf, 1968).

The basis for free radical AOP is the radiolysis of water. The purity of water used as a solvent in radiation chemistry experimentation was a major consideration when aqueous solutions are irradiated (Spinks and Woods, 1964). Water used in this experimentation was pure water filtered and produced at the Notre Dame Radiation Laboratory with tap water as the source.

Free radicals in aqueous solutions are produced by the dissociation of excited molecules and by ion reactions occurring as a dissociative, ion-molecular, or neutralization reaction in or near the tracks of ionizing particles. Radicals which do not undergo radical-radical reactions in this region of high radical concentration in the spur, diffuse into the bulk of the medium and generally react with the substrate. The initial high concentration of free radicals, close to the radiation particle tracks, can lead to radical

phenomena in radiation chemistry different from those where the radicals are formed by other means such as those produced chemically or photochemically and are more randomly distributed (Spinks and Woods, 1964).

The study of the perturbing conditions from ionizing radiation exposure to water and the resulting reactions is known as radiation chemistry. Radiation chemistry is concerned with all processes which occur following the absorption of ionizing radiation into the aqueous medium until all products have been formed and all the absorbed energy from the radioactive particle has been thermalized. This occurs at an approximate timescale of 10^{-17} seconds after the ionization event (Mozumder and Magee, 1975a).

On a nuclear particle time scale, the study of radiation chemistry includes the period of time from the moment of the interaction of the ionizing particle (electron) to a time when the particle is thermalized. The overall time period is subdivided into three distinct stages and each stage correlates to significant events exhibited by the particle in each stage. The stages are categorized into the physical, physiochemical, or chemical. Each stage and significant event is marked to the time in seconds after the interaction of an atomic particle with water medium. Several timescales describing the interaction of an electron with water have been proposed by those identified in Table 1.2. Each author identified a unique time within each stage along with a description of their respective significant events. A collective summary of these stage timescales along with their respective events was prepared and presented in Table 1.2.

Table 1.2. Events occurring after excitation of an electron in water.

Event	Time (Sec.)	Stage	Reference
Earliest discernable time based on Uncertainty Principle.	10^{-17}	Physical Stage	(Mozumder, 1969)
Ionization Event, Excitation e^- $H_2O\bullet$ ←VVVVV H_2O VVVVV→ $H_2O^+ + e^-$	10^{-16}		(Buxton ,2004)
H_2O	10^{-15}		(Buxton, 2004)
$\bullet OH + H_3O$	10^{-14}		(Buxton, 2004)
$H\bullet + \bullet OH$ $H2 + O\bullet$	10^{-13}	Physiochemical Stage	(Buxton, 2004)
Electron thermalized and hydrated "picosecond barrier". e_{aq}^-	10^{-12}		(Buxton, 2004; Mozumder and Magee, 1975b)
	10^{-11}		
Minimum time for diffusion controlled reactions in the bulk of the liquid.	10^{-10}		(Spinks and Woods, 1964)
Spur reaction complete.	10^{-9}		(Magee and Chatterjee, 1987)
Track end (blob, short track) reactions complete.	10^{-8}		(Magee and Chatterjee, 1987)
Formation of molecular products complete e_{aq}^-, $H\bullet$, $\bullet OH$, H_2, H_2O_2, H_3O^+.	10^{-7}		(Buxton, 2004)
	10^{-6}	Chemical Stage	
Reaction time for radical with solute in molar concentration.	10^{-5}		(Spinks and Woods, 1964)
Radical Reactions with scavenger at micromolar concentration.	10^{-4}		(Magee and Chatterjee, 1987)
Radiative lifetime of triplet excited state.	10^{-3}		(Spinks and Woods, 1964)
	10^{-2}		
	10^{-1}		
Chemical Reactions Complete.	$>10^{-1}$		

Mozumder and Magee (1975a) identified an upper limit or boundary of time measurement for these radiolytic events and the limit was determined to be bounded by the capability for real-time reaction measurement using photo-absorption technology. This limit is fixed by either the duration of time that the energy is deposited by the ionizing particle or the transit time of the analyzing light. When compared to the time for energy deposition, the analyzing light requires a longer time to transverse the sample and inevitably record the effects arising from the energy deposit and this occurs within a time spread of 10^{-12} seconds or more. This 10^{-12} second range of event time is referred to as the *picosecond barrier* to real-time observations (Mozumder and Magee, 1975b). Recently, the use of asynchronous laser for the radiolytic study of e^-_{aq} kinetics in water has allowed real-time measurements closer to the picosecond barrier with measurements reported in the range from 100 ps to 10 ns (Bartels *et al.*, 2000).

This research was performed predominantly in the chemical stage and this begins at a time with the completion of free radical formation and corresponds to approximately 10^{-7} seconds after the ionization event in water. To quantify the amount of free radicals formed in this time period, a yield is provided. The yield of these primary free radical species is represented by the yield (G) value. This value denotes the number of molecules changed for each 100 electron-volts (eV) of energy adsorbed (1 eV = 1.6022×10^{-19} J). It has been well established that steady state radiolysis of water produces the free radical yield in pure water for a pH range from 3 to 11 as (Buxton, 2004):

$$H_2O \text{ -}\wwvy\rightarrow [2.8]\bullet OH + [0.62]\bullet H + [2.8]\, e^-_{aq} + [0.47]H_2 + [0.73]H_2O_2 + [2.8]H^+ \qquad (1.1)$$

where the (G) value is the yield of free radicals denoted in brackets with units of mol $J^{-1} \times 10^{-7}$ (1 mol $J^{-1} \equiv 9.65 \times 10^{-6}$ molecules $(100\ eV)^{-1}$) (Buxton, 2004). Subsequent to the formation of these free radicals in pure water, the following radiolytic reactions along with their rate constants were well established and listed in Table 1.3. (Buxton *et al.*, 1988). The reactions and their respective rate constants identified in Table 1.3 were incorporated into this work.

Table 1.3. Known reactions in pure water resulting from radiolysis and the second-order rate constant. (Continued on page 19)

Reaction	Rate constant, k ($M^{-1}s^{-1}$)
$e_{aq}^- + H_2O \rightarrow H\bullet + OH^-$	1.9×10^1
$e_{aq}^- + e_{aq}^- \rightarrow OH^- + OH^- + H_2$	5.0×10^9
$e_{aq}^- + H\bullet \rightarrow H_2 + OH^-$	2.5×10^{10}
$e_{aq}^- + \bullet OH \rightarrow OH^-$	3.0×10^{10}
$e_{aq}^- + \bullet O^- \rightarrow OH^- + OH^-$	2.2×10^{10}
$e_{aq}^- + H^+ \rightarrow H\bullet$	2.3×10^{10}
$e_{aq}^- + H_2O_2 \rightarrow \bullet OH + OH^-$	1.1×10^{10}
$e_{aq}^- + HO_2^- \rightarrow \bullet OH + OH^- + OH^-$	3.5×10^9
$e_{aq}^- + O_2 \rightarrow O_2\bullet^-$	1.9×10^{10}
$e_{aq}^- + O_2\bullet^- \rightarrow O_2^{2-}$	1.3×10^{10}
$H\bullet + H_2O \rightarrow H_2 + \bullet OH$	1.0×10^1
$H\bullet + H\bullet \rightarrow H_2$	7.8×10^9
$H\bullet + \bullet OH \rightarrow H_2O$	7.0×10^9
$H\bullet + OH^- \rightarrow e_{aq}^-$	2.2×10^7
$H\bullet + H_2O_2 \rightarrow H_2O + \bullet OH$	9.0×10^7
$H\bullet + O_2 \rightarrow HO_2\bullet$	2.1×10^{10}
$H\bullet + HO_2\bullet \rightarrow H_2O_2$	1.0×10^{10}
$\bullet OH + \bullet OH \rightarrow H_2O_2$	5.5×10^9
$\bullet OH + \bullet O^- \rightarrow HO^{2-}$	2.0×10^{10}
$\bullet OH + H_2 \rightarrow H\bullet + H_2O$	4.2×10^7
$\bullet OH + OH^- \rightarrow H_2O + \bullet O^-$	1.3×10^{10}
$\bullet OH + H_2O_2 \rightarrow HO_2 + H_2O$	2.7×10^7
$\bullet OH + HO_2^- \rightarrow OH^- + HO_2\bullet$	7.5×10^9

Table 1.3. Known reactions in pure water resulting from radiolysis and the second-order rate constant. (Continued from page 19)

Reaction	Rate constant, k ($M^{-1}s^{-1}$)
$\bullet OH + H_2O_2^+ \rightarrow H_3O^+ + O_2$	1.2×10^{10}
$\bullet OH + HO_2\bullet \rightarrow H_2O + O_2$	6.0×10^{9}
$\bullet OH + O_2\bullet^- \rightarrow O_2 + OH^-$	8.0×10^{9}
$\bullet O^- + H_2O \rightarrow OH^- + \bullet OH$	1.8×10^{6}
$\bullet O^- + H_2 \rightarrow H\bullet + OH^-$	8.0×10^{7}
$\bullet O^- + H_2O_2 \rightarrow O_2\bullet^- + H_2O$	5.0×10^{8}
$\bullet O^- + HO_2^- \rightarrow O_2\bullet^- + OH^-$	4.0×10^{8}
$\bullet O^- + O_2\bullet^- \rightarrow OH^- + OH^- + O_2$	6.0×10^{8}

1.3.1. Radiation

Two types of radioactive sources were applied during this research. Experiments were conducted with each and both had a specific purpose for their application to steady state radiolysis of an aqueous medium. The first source was the pulsed electron beam, originating from a high voltage LINAC producing a constant stream of electrons. The LINAC was designed to produce a controlled pulse for radiolysis of water and in-turn generates the free radicals required for determination of the HNM rate constants. The second radiation source was the gamma particle emitted by a radioactive source. This source was contained in a lead-lined shielded cask and equipped with a trap door. The gamma irradiator was used for extended radiolysis of water and more specifically for the purpose of decomposing HNMs to their parent ions for subsequent identification of a mass balance as residual ions found remaining in solution. The gamma source was also used for the determination of HNM dose rate constant (k_D).

Pulse radiolysis is based on use of fast electrons. Electrons can originate from interaction of x-rays or γ-particles with matter or they can be generated by the LINAC.

For the purposes of experimental research, the LINAC produces a coherent beam of determinable size (5 mm wide field, 2.8 ns, and 4.4 Amps) (Whitham *et al.*, 1995). Each pulse produces a uniform radiation dose and within each pulse a stream of fast electrons at energies of up to 8 MeV is emitted (Whitham *et al.,* 1995). These fast electrons were introduced into a sample of water where their energy is dissipated into the matter resulting in excitation and ionization of atoms (Swallow, 1973). The passage of a fast electron close to an atom or molecule subjects it to an electric impulse. This passage excites or ionizes it, and eventually may cause electronic transitions involving their inner shells (Swallow, 1973). Fast electrons also interact with matter by the emission of electromagnetic radiation (Cherenkov radiation) and through inelastic and elastic scattering (Spinks and Woods, 1964).

Pulse radiolysis experiments in this work incorporated the University of Notre Dame Radiation Laboratory (NDRL) LINAC (Titan Corporation, Model TB-8/16-1S S-Band). The unit is suitable for absorption spectroscopy at 475 nm for hydroxyl radicals and 700 nm for hydrated electrons. The unit is capable to produce from 2 ns to 1.5 second pulses of 8 MeV electrons and generate free radicals at approximately 1 to 3 μM with each pulse. The range of pulse implemented during experimentation was from 0.5 to 50 μs. The LINAC system was designed to have high order of repeatable shot-to-shot radiation dose along with low pre- and post radiation. The system includes a 130 to 140 kV gridded electron gun and series of accurately aligned Helmholtz coils provided along the beam-line to transport the beam and provide a uniform beam diameter at the target area (Whitham *et al.,* 1995), as graphically depicted in Figure 1.1 (Madden, 2004).

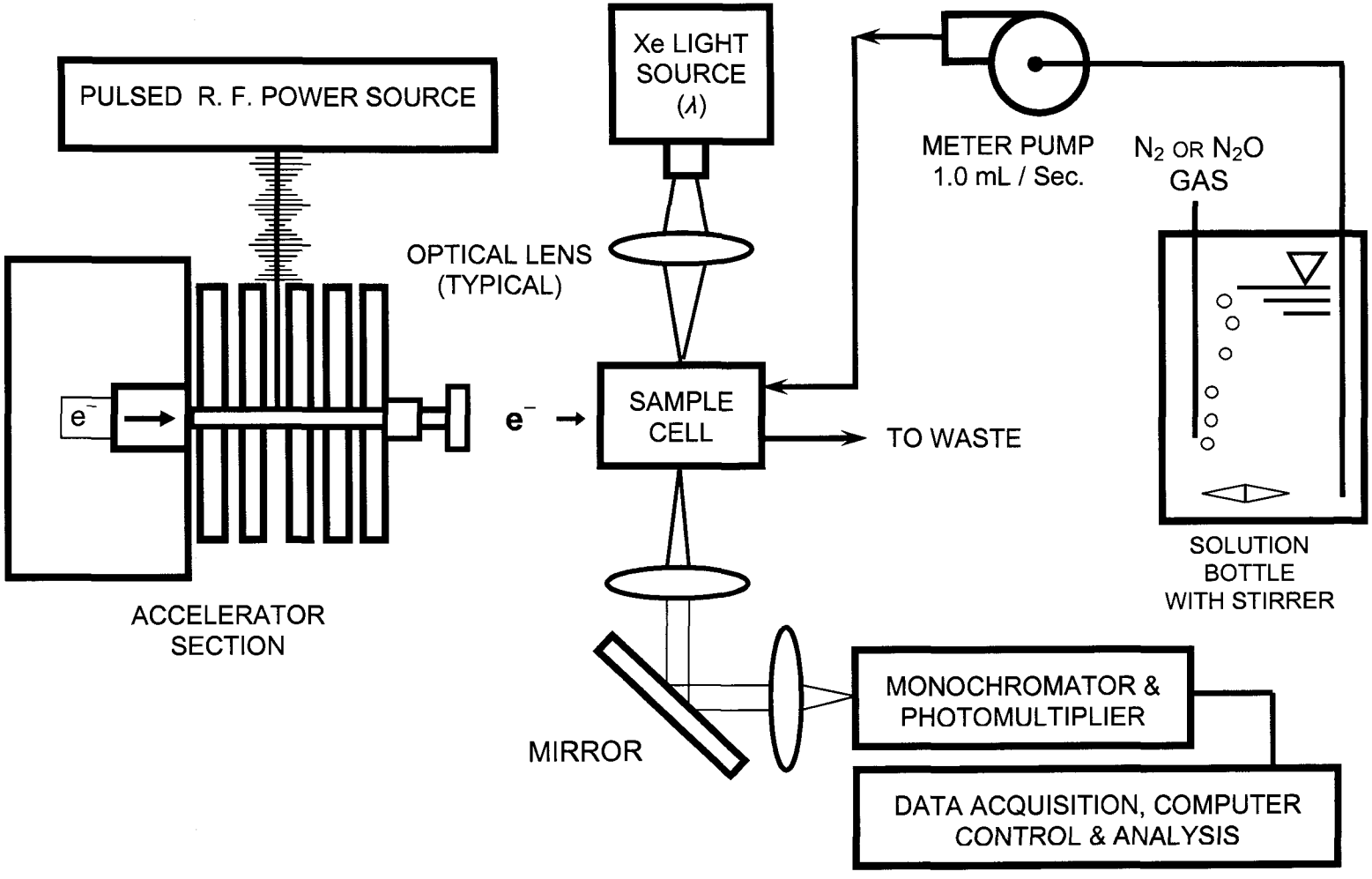

Figure 1.1. NDRL LINAC (Model TB-8/16-1S 8 MeV S-Band). (Madden, 2004)

The NDRL LINAC facility description (Schuler, 1996), equipment design and transient absorption detection system (Whitham *et al.,* 1995), pulse radiolysis equipment and dosimetry are also described elsewhere (Asmus, 1984).

During LINAC experimentation, continuously stirred solutions were pumped through glass tubing to the silica irradiation (target) cell (1 cm^3 sample volume) with pulses irradiating the solution for each experimental trace (Cooper *et al.,* 2002a). The solution was transferred from a bottle to the LINAC by a peristaltic metering pump (Cole-Palmer, Masterflex Quiet Load™ Model 7521-40) with an average pump rate of 1.0 mL s^{-1}.

All pulse radiolysis solutions were ambient pH and sparged with high purity N_2O for hydroxyl radical experimentation and N_2 for hydrated electron, with all work performed at one atmosphere and ambient room temperature (22°C). Solutions for the hydroxyl radical study were saturated with N_2O to scavenge e^-_{aq}. This N_2O saturation provides a highly reactive chemical system comprised of predominantly •OH radicals (Asmus, 1984; Janata and Schuler, 1982). Based on this scavenging of e^-_{aq} only, the •OH reactions can be observed discretely. For the hydrated electron rate constant study, high purity nitrogen gas was applied. Degassing solutions with N_2 purges or removes oxygen and thereby reduces the potential for undesired contributing byproducts or reactants from other oxygenated reactants in solution. This de-oxygenated solution then allows discrete observation of the desired reaction of solute reacting with e^-_{aq} (Buxton *et al.,* 1988). No interferences can occur or be observed from the use of nitrogen in solution because elementary nitrogen has a negative electron affinity and will not react with e^-_{aq} (Hart and Anbar, 1970).

Measurement of the radiation (dosimetry) for pulse radiolysis experiments (LINAC) is the measure of ionizing events occurring in the aqueous solution. Pulse radiolysis dosimetry was based on the standard reaction of 0.01 M thiocyanate anions (SCN^-) to $(SCN)_2^{\bullet -}$ in aqueous N_2 saturated solutions at 475 nm (Buxton and Stuart, 1995).

This study included ^{60}Co gamma irradiation for long-term exposure (maximum 70 minutes) of the HNM solute in water to ionizing (gamma) radiation. The radioactive decay of ^{60}Co to ^{59}Co produces ionizing radiation with the release of one beta particle at 0.097 MeV, and two gamma particles with one at 1.17 MeV and the other at 1.33 MeV (Spinks and Woods, 1964). The half-life (t½) of ^{60}Co was important to calibration calculations for the gamma experiments where t½ (^{60}Co) = 5.2714 years (Spinks and Woods, 1964). The beta particle does not affect the experiment because the particle is attenuated by the small thicknesses of sample container wall, distance from the source to the sample, and air. These physical shields prohibit any reaction or eliminate the effect from the beta particle on the water medium.

Gamma irradiation using ^{60}Co for radiolysis of an aqueous solution was selected based on its unique radiation ionizing property with matter. The processes by which energy is transferred from radiation to material differ for electromagnetic radiation (γ and x-ray photons), charged particles (beams of electrons) and positively charged particles (Woods, 1998). Low energy photons (below approximately 0.1 MeV for low atomic number or low Z-materials) eject an electron from an atom and are absorbed in the process, with the electron carrying off any photon energy in excess of the binding energy of the electron in the atom as a photoelectric process (Woods, 1998).

Woods (1998) identified that higher energy photons, about 0.1 to 10 MeV, use part of their energy to eject an electron and then they are deflected or scattered with the remaining energy and then exhibit Compton scattering. Photons with energy greater than 1.02 MeV can be absorbed in the vicinity of the atomic nucleus and give rise to an electron-electron pair and known as pair production. The positron eventually reacts with an electron to give two γ-photons of energy at 0.51 MeV and this action describes the condition for annihilation radiation. At energies above about 10 MeV, photons may eject a proton or neutron from the nucleus of an atom as a photonuclear reaction. In this range, photonuclear reactions may induce radioactivity in the absorbing material. For this reason, x-ray radiation energies are normally limited to a maximum of 5 MeV, and electron energies to a maximum of 10 MeV (Woods, 1998).

The ^{60}Co gamma irradiation of HNMs was used to study the effect of their degradation via free radical oxidation and reduction reactions in water. The experiment was designed to identify and quantify the remaining HNM mass of ions present after timed exposure and then apply the data in a mass balance analysis. In addition, radiolysis using the gamma irradiator allows for the determination of the total ionizing dose required for destruction of each of the HNMs to their parent ions. The point where this mineralization occurs, in terms of radiation level, was significant to this study for the determination of the dose constant. The total radiation dose was measured in units of gray (Gy). The Gy is defined as absorption of 1.0 J kg^{-1} where 1.0 gray is equal to 100 rad.

Given a ^{60}Co radioactive source, it was necessary to calculate the dose rate at the time of the experiment. The dose rate at the time of the ^{60}Co irradiation experimentation was calculated using the half-life ($t_{1/2}$) equation:

$$T_i = [T_0] \times [e^{-((0.693 \times (\Delta \text{ Days} / 365))/ t½)}] \quad (1.2)$$

where T_i (krad $min.^{-1}$) is equal to the dose rate at the time of experimentation on May 17, 2004, with posted calibration dose rate (T_0 = 12.8 krad $min.^{-1}$ for January 1, 2004) determined by NDRL using Fricke dosimetry. The number of days between dates (Δ Days) for ($T_i - T_0$) and t½ (^{60}Co) was known. The ^{60}Co radiolysis experiments were performed using the NDRL (Shepherd, Model 109-68) irradiator with a calculated exposure rate of 122 Gy $min.^{-1}$ on May 17, 2004.

Environmental application of ionizing radiation or experimental radiolysis requires a constraint in the level of nuclear particle energy applied to the target. Based on the particle's energy level, the potential exists for activation of an atomic nucleus with a photonuclear reaction in the nucleus of an atom. Photonuclear reactions will occur at particle energies greater than 10 MeV. At 10 MeV or greater, photonuclear reactions result when photons eject a proton or neutron from the nucleus of an atom (Spinks and Woods, 1964). This radiation chemistry work was performed at radiation energies well below the level of elemental activation for matter (10 MeV). Therefore, no change to the elemental state of matter or induced radioactivity can be possible.

1.3.2. Formation

Free radicals are formed in the process of energy deposition into the water medium at 10^{-7} seconds after the interaction of a nuclear particle with water. The extent of the region bounded by this energy deposition event is defined by both a characterization of the radiation interaction with water and its subsequent effect on the intra-molecular water reactions. This event characterization is primarily described in terms of the structure of

interaction of the radiation with the water, the energy lost by the ionizing particle to the water, and the free radicals produced within the event region. The introduction of an electron into water loses its energy, becomes thermalized, and this translates to a hydrated electron (Draganic and Draganic, 1971). The intra-molecular reactions are described by the concentration or yield of free radicals formed and radical scavenging.

Mozumder and Magee (1975a) described the earliest time period for the interaction of a radiation particle with water. Radiation induced reactions in water create localized event structures known as *spurs*. The driving condition for the formation and number of these spurs includes the type of radiation particle such as photons, gamma, or electrons. Other conditions that may influence the number of spurs include the number of disintegrations per unit of time or the decay rate of a radioactive material where gamma or photon particles are emitted from the nuclei of an atom. In the case of electrons, the number of electrons emitted to the water may also impact the number of spurs formed (Mozumder and Magee, 1975a).

Reducing the scope of consideration from the number of spurs formed to the proximity within a single spur's event region, the free radicals formed within that spur affect the local reaction kinetics. These local reactions kinetics will include only the independent spur, the primary radicals formed, and include the intermediate chemical radicals formed within that spur (Mozumder and Magee, 1975a). Mozumder and Magee (1975a) described the condition where these chemical primaries and intermediates formed in one spur react completely with each other and with those radical constituents within the immediate medium before they can diffuse far enough away from the localized event region to encounter intermediates or primaries from another spur or track. This

condition is required for the yield (G) of radicals to be independent of the dose rate and for continuous ^{60}Co irradiation and this condition is referred to as the *low background* case (Mozumder and Magee, 1975a). The low background case describes the condition that concentrations of intermediates do not build up outside the tracks (Mozumder and Magee, 1975a). Given that the primary and intermediate radicals (•OH and e_{aq}^-) are known from short-term observations, their various individual reactions can be determined (Mozumder and Magee, 1975a). With these known individual reactions for the low background case, the concentration of all primaries and intermediates in the track are then quantifiable at the initial time of approximately 10^{-7} seconds. Therefore, the free radical concentrations (yield) identified in equation (1.1) has been established and is based on the low background case as a condition to intra-spur kinetics (Mozumder and Magee, 1975a).

In liquid water, ionizing radiation will produce excited and ionized species (Spinks and Woods, 1964) and the yield of these products are attributed to the linear energy transfer (LET) and scavenger effects (Mozumder and Magee, 1975a). The number and extent of these resulting ionized species produced are a function of the energy level of the particles interacting with the water and the transfer of that energy along the track of the electron as LET. The LET is also known as the stopping power of a medium toward a penetrating charged particle and is the energy loss suffered by the particle per unit length measured in units of electron volts per unit path length (Mozumder and Magee, 1975a).

Mozumder and Magee (1975a) identified that the energy loss was classified into three types of ionizing particle track structures known as spurs, blobs, and short tracks. The spur conforms to an energy deposition to the water between 6 to 100 eV and the event is complete at 10^{-9} seconds. The blob is responsible for energy deposition between 100 to

500 eV, and the short track describes the energy deposited between 500 to 5000 eV. The structures are formed after the introduction of a particle into water medium where blobs and short tracks are complete within 10^{-8} seconds. Of these three track structures, the spurs represent the single structure where the very fast particles have successive energy losses and where they are separated by enough distance so that the physical and chemical processes develop occur (Mozumder and Magee, 1975a). The dissipation of the energy in water occurs at different levels for each of the track structures. For example, a 1 MeV electron theoretically expends 65% of its energy to produce isolated spurs, 15% in blobs, and 20% in short tracks (Chatterjee, 1987). The value of this stopping power (LET) in these track structures are critical to the formation and concentration of free radicals, equation (1.1). As an example of the LET scale, typical values for LET vary from 1 for gamma particles to 100 keV μm^{-1} for alpha particles (Kurucz *et al.*, 1991). For radiation of equal energy expressed in eV, LET values increase in the order of: gamma and fast electrons, beta, and then alpha particles. The higher LET value for alpha particle spurs is attributed to the close proximity of their tracks, and results in a form of a continuous column in the liquid medium, whereas gamma particles can be over 10^{-4} cm apart (Mozumder and Magee, 1975a). Kurucz *et al.*, 1991 described the net result of the energy dissipation as the production of ions, electronically excited atoms, and molecules along the path of the irradiation in water. The nature of the radiation will not influence the identity of the species formed in the water medium but does influence local radical concentrations depending on the water medium. The different chemical effects are related to the density of reactive species produced along the track of the ionizing particles. In

radiation chemistry, ionizing radiation such as gamma particles and fast electrons as exhibited in this experiment are classified as low LET in water (Kurucz *et al.*, 1991).

Within the region of the ionization event and the subsequent spur formation, free radicals are produced in combination or shared with a constituency of molecular products that will reduce the concentration of the free radicals (Spinks and Woods, 1964). These molecular products scavenge the free radicals into intermediate products, re-combine to form other complex molecular combinations, or experience geminate recombination (Spinks and Woods, 1964).

Spinks and Woods (1964) defined scavenging as a term given to a reagent that reacts rapidly with other species (primary products). Scavengers can be a reagent that may be deliberately applied to a radical reaction of a compound where it will react preferentially with the radicals. Preferential reactions will be at the expense of the normal radical reactions. In radiation-induced reactions in liquids, the reaction may take place either within spurs or close to the tracks of heavy particles, where the active intermediates are formed, or in the bulk of the medium where reactions are initiated by radicals which have diffused from the spur track zone. In the later case, the purpose for direct introduction of a scavenger into the medium was to identify the radicals taking part in the reaction and to determine what part of the over-all reaction is due to scavengeable free radicals (Spinks and Woods, 1964).

Substances used as scavengers are either stable free radicals compounds which eliminate radicals by electron transfer reactions, or compounds which react to give relatively stable free radicals in place of the active radicals originally present (Draganic

and Draganic, 1971). For example, this research used nitrous oxide as a scavenger for e^-_{aq} to determine the rate constants for •OH reaction with HNMs.

1.3.3. Steady State Radiolysis

This experimentation applied steady state radiolysis using an electron beam and ^{60}Co gamma irradiation, as low LET radiation. Steady state radiolysis of an aqueous system is the steady chemical yield and concentration of stable primary free radical products within that system when exposed to ionizing radiation. These primary free radicals are described with their indicated yield in equation (1.1) for the reactions at 10^{-7} seconds after the ionizing event.

Within the event region of the spur, steady state radiolysis depends on several conditions and these include the dose rate, scavenger concentration, reaction rate with the radical observed (Draganic and Draganic, 1961), LET, density of the aqueous medium, and the condition that the concentration of free radicals identified in equation (1.1) was constant over the pH range from 3 to 11 (Buxton, 1987). Although the yield of these primary radicals were found to decrease over time as they reacted with scavengers (Schwarz, 1968), the steady state condition exists where intermediates are not in significant amount and the period leading to build-up or period post build-up was not considered (Wright, 2004).

The steady state condition and this research were premised on the radiolysis of pure water in which the only radical scavengers are the expected molecular decomposition products H_2, H_2O_2, and O_2. Magee and Chatterjee (1987) identified that decomposition of pure water may occur for low LET radiation (γ and e^-). If the tracks produce more

radicals (H, OH) than molecules (H_2, H_2O_2), a chain *back-reaction* destroys the molecules (H_2, H_2O_2) and limits their build-up. A steady state condition implies one where there is no net decomposition of free radicals. If the molecular yields are larger that the radical yields, as in the case of heavy particle (γ) tracks, the back-reaction is not effective at first and a net decomposition of water occurs. In the case of water under the influence of low LET radiation, very little water decomposes. In the early phase of a heavy particle (γ) irradiation, some decomposition of water occurs as the stationary (steady) state is further into time (Magee and Chatterjee, 1987).

Properties such as pressure, temperature and concentration of the solvent (water) were constant. Draganic and Draganic (1971) confirmed that no effects from pressure were known to be identified in the production of free radicals. However, in the case of the e_{aq}^-, the diffusion coefficient of reactants were noted to change under pressure (Hart and Anbar, 1970). Experiments conducted in this research were at atmospheric pressure and therefore pressure was of no consequence. Experiments were performed at 20°C. Draganic and Draganic (1961) and Meesungnoen *et al.* (2002) confirmed that water temperature exhibits no effect on measured yields of the primary products identified in equation (1.1) for temperature range from 2° to 65°C.

When dilute aqueous solutions are irradiated practically all the energy absorbed is deposited in water molecules and the observed chemical changes are brought about indirectly via the molecular and radical products. Direct action due to energy deposited directly in the solute is generally unimportant in dilute solutions with concentrations below about 0.1 M. At higher solute concentrations direct action may be significant and there is some evidence that excited water molecules may transfer energy directly to the

solute (Spinks and Woods, 1964). All concentrations of solute in this research were below 0.1 M, therefore no direct action was considered applicable.

1.3.4. Free Radical Characteristics

Of the primary free radicals identified to be formed during steady state radiolysis, the hydroxyl radical and hydrated electron are significant to HNM degradation. These two free radicals represent the most reactive free radicals over the remaining others produced in the radiolysis of water with the hydroxyl radical providing oxidation reactions and the hydrated electron as the reducing species with each produced in nearly equal amounts (Mincher and Cooper, 2003). The hydroxyl radical oxidizes halide ions (Buxton, 1987) and has a standard reduction potential of 1.89 V in neutral solution (Schwarz and Dodson, 1984). In strongly alkaline solutions OH is rapidly converted to anionic form O^- where OH behaves as an electrophile and O^- as a nucleophile. Both forms of the radical can abstract H from C–H bonds (Buxton, 1987). The hydrated electron is a powerful reducing agent and reacts rapidly, as a nucleophile with halides and nitro compounds (Buxton, 1987).

Reactions of the hydroxyl radical ($^{\bullet}OH$) with inorganic and organic compounds have been well documented (Buxton *et al.,* 1988; Haag and Yao, 1992). The $^{\bullet}OH$ radical can undergo several types of reactions with chemicals in aqueous solution, notably addition, hydrogen abstraction, and electron transfer. On addition of N_2O, e^-_{aq} is converted to OH (Buxton, 1987):

$$e^-_{aq} + N_2O \rightarrow N_2 + O^- \xrightarrow{H_2O} OH + OH^- \qquad (1.3)$$

Addition reactions occur readily with aromatic and unsaturated aliphatic compounds to give hydroxylated radicals (Cooper *et al.*, 2004):

$$^{\bullet}OH + CH_2{=}CH_2 \rightarrow HOCH_2\text{-}CH_2^{\bullet} \quad (1.4)$$

Electron transfer need not always result in radical destruction. In aqueous solutions, electron transfer between halide ions and hydroxyl radicals gives halogen atoms (Spinks and Woods, 1964):

$$^{\bullet}OH + Br^- \rightarrow Br^{\bullet} + OH^- \quad (1.5)$$

Bromide ions are even more readily oxidized by hydroxyl radicals. In the presence of air, the reactions taking place in neutral solutions, the typical reactions are (Spinks and Woods, 1964):

$$^{\bullet}OH + Br^- \rightarrow Br^{\bullet} + OH^- \quad (1.6)$$

$$H^{\bullet} + O_2 \rightarrow H_2O^{\bullet} \quad (1.7)$$

$$Br^{\bullet} + H_2O^{\bullet} \rightarrow H^+ + Br^- + O_2 \quad (1.8)$$

The hydrated electron (e_{aq}^-) was postulated by Stien and Platzman in the early 1950's (Hart and Anbar, 1970). In 1952, Stein considered that the hydrated electron polarizes the water and creates a potential well (Hart and Anbar, 1970). The earliest time in the event of an electron in water occurs at 10^{-16} seconds where the most probable energy of a spur in water is about 20 eV. At 10^{-12} seconds, the electron has become thermalized to an aqueous electron (e_{aq}^-) and local diffusion processes begin (Mozumder and Magee, 1975b). The e_{aq}^- is a powerful reducing reagent with a standard-state cell potential (E^o) of 2.77 V as exemplified by the hydrated electron and hydrogen reaction ($e_{aq}^- + H \rightarrow \frac{1}{2} H_2$) (Hart and Anbar, 1970). The reaction of e_{aq}^- with organic and inorganic compounds has been studied

extensively (Hart and Anbar, 1970; Bensasson *et al.,* 1983). Hydrated electrons can be un-reactive, slow reactive, or reactive to a variety of compounds. Reaction of e_{aq}^- with halogenatated compounds occurs where there is detachment of negative ions on monochloroacetic acids (Hart and Anbar, 1964):

$$ClCH_2COOH + e_{aq}^- \rightarrow Cl^- + CH_2COOH \quad (1.9)$$

The hydrated (solvated) electron produced in pulse radiolysis of nitrous oxide in aqueous solutions is scavenged with a bimolecular rate constant of $k_2 = 9.1 \times 10^9\ M^{-1}s^{-1}$ according to (Janata and Schuler, 1982):

$$e_{aq}^- + N_2O + H_2O \rightarrow N_2 + OH^- + \bullet OH \quad (1.10)$$

and produces oxidizing scavengers for removing oxygen.

Kinetic data for e_{aq}^- radiolytic reduction of brominated compounds has been investigated and shown to provide the following reaction mechanism and their respective bimolecular rate constants for halogens such as bromate and bromide (Siddiqui *et al.,* 1996):

BrO_3^- to BrO_2^-, (k not reported) (1.11)

$e_{aq}^- + BrO_3^- + 2H^+ \rightarrow BrO_2^{\bullet} + H_2O$, $k = 3 \times 10^9\ M^{-1}s^{-1}$ (1.12)

$e_{aq}^- + BrO_2^{\bullet} \rightarrow BrO_2^-$, $k = 1 \times 10^{10}\ M^{-1}s^{-1}$ (1.13)

BrO_2^- to BrO^- (1.14)

$e_{aq}^- + BrO_2^- \rightarrow BrO^{\bullet} + O_2^-$, $k = 1 \times 10^{10}\ M^{-1}s^{-1}$ (1.15)

$e_{aq}^- + BrO^{\bullet} \rightarrow BrO^-$, $k = 1 \times 10^{10}\ M^{-1}s^{-1}$ (1.16)

and for

BrO^- to Br^-, (Not reported) (1.17)

$$e_{aq}^{-} + BrO^{-} \rightarrow Br^{-} + O^{-}, \qquad k = 2 \times 10^{10}\ M^{-1}s^{-1} \qquad (1.18)$$

The most characteristic property of free radicals is the instability associated with the presence of an unpaired electron. Hydrated electron radicals (e_{aq}^{-}) are often extremely reactive, reacting in such a manner that the odd electron is paired with a similar electron in another radical or eliminated by an electron-transfer reaction. Alternately, the radical may react so as to produce a second, more stable, free radical (Spinks and Woods, 1964).

There are seven factors that affect a radical's reactivity and chemical stability, and these include (Spinks and Woods, 1964):

- The stability of an organic radical is increased when a hydrogen attached to the carbon atom carrying the free electron is replaced by any other atom or group,
- Radical stability increases in with the following molecular series as

  primary ($-CH_2\bullet$) < secondary ($=CH\bullet$) < tertiary ($\equiv C\bullet$),
- Radical stability is increased in the halogen series given by F < Cl < Br < I,
- Selectivity: Cl^{-} is more selective in attack on substrate than H, but less than Br^{-},
- Dissociation energies of the bonds broken and formed,
- Reactivities of the attacking and displaced radicals, and
- Polar effects

Free radicals formed during the radiolysis of water react with a chemical (R) as a solute in the following general free radical reactions (Buxton *et al.,* 1988):

$$e_{aq}^{-} + R \rightarrow {}^{\bullet}R \qquad \text{(dissociative electron attachment; electron addition)} \qquad (1.19)$$

$$^{\bullet}OH + R \rightarrow {}^{\bullet}R \qquad \text{(hydrogen atom abstraction; electron abstraction; addition)} \qquad (1.20)$$

$$^{\bullet}H + R \rightarrow {}^{\bullet}R \qquad \text{(hydrogen atom abstraction; addition)} \qquad (1.21)$$

Oxygenated reactions occur along with primary free radicals in aqueous solutions and these lead to the formation of peroxyl radicals. These peroxyl radicals are highly reactive and contribute to the overall reaction mechanism for the degradation of HNMs. Reaction of oxygen to free radicals in radiation induced reactions results in stable peroxy radicals. Molecular oxygen as a diradical (•O—O•) in recognition of its triplet ground state, the reaction can be identified by (Spinks and Woods, 1964):

$$R\bullet + \bullet O—O\bullet \rightarrow R—O—O\bullet \qquad (1.22)$$

Peroxy radicals are influenced by halogen groups attached to the same carbon and are often unstable, breaking down with cleavage of bonds and the loss of the halogen. These peroxyl radical reactions may be slow as compared to other peroxyl reactions. For example, most carbon centered radicals react with molecular oxygen with rate constants which are close to the diffusion-controlled limit, equal to $k = 2–4 \times 10^{-9}$ $M^{-1}s^{-1}$, to form peroxyl radicals, as described by the peroxylation reaction (Alfassi, 1997):

$$R + O_2 \rightarrow RO_2 \qquad (1.23)$$

Halogen atoms, particularly chlorine atoms, have been found to react very fast with RO_2 radicals ($k > 10^{-10}$ cm^{-3} $molecule^{-1}$ s^{-1}) if not scavenged by precursors. The principal product of the Cl^- atom reaction with perhalogenated peroxyl radicals is ClO, along with the corresponding oxyl radical (Lescluax, 1997). Chlorine atoms appear to be set free in the bimolecular decay of peroxyl radicals and exhibit C-Cl bond cleavage leading to the formation of phosgene with slow hydrolysis (9 s^{-1} at 25°C) and a precursor to CO_2 (von Sonntag and Schuchmann, 1997). Coupling of •OH with $•NO_2$ generates almost equal amount of peroxynitrite ($ONOOH/ONOO^-$) and NO_3^- + H^+ (Merényi *et al.,* 1999).

When primary free radicals are formed in water, competing reactions and radicals then react either with the aqueous parent solute materials or other species present to give stable reaction byproducts or intermediates. Subsequent reactions of these byproducts with the reactive water radiolysis species can eventually degrade the parent material to its constituent ions and the final product such as CO_2 can be formed. The destruction process is commonly referred to as mineralization (Neta *et al.,* 1990).

1.4. Rate Constants

Chemical kinetics may be broadly defined as the study of systems whose chemical composition of energy distribution is changing with time. The study of these systems in detail includes a series of reactions and this collection represents the mechanism of the reaction (Weston and Schwarz, 1972). Experimental rate laws often point to complex mechanisms as a sequence of elementary steps or two or more sequences in parallel. Complex environmental mechanisms may also introduce intermediate species (Stumm and Morgan, 1996). In radiation chemistry, the kinetics of formation and decay of the various reactive species in a given irradiated medium (charged species, excited states, radicals) is partially interlinked and can be complex (Hummel, 1987).

This experimentation used pulse radiolysis to form both •OH and e^-_{aq} as primary free radicals for the determination of rate constants in the destruction of TCNM. In elucidation of the decay mechanism for a given reaction of e^-_{aq} with species of HNM present in an aqueous solution, the reaction was described by a first-order reaction for species *A* reacting with species *B* (Hart and Anbar, 1970):

$$e^-_{aq} + A \rightarrow A^- \qquad (1.24)$$

$$e^-_{aq} + B \rightarrow B^- \tag{1.25}$$

The case of a first-order reaction where A disappears by the combination process where product *B* is formed, allows a differential equation to be written for C_t as the concentration at the time of interest and C_0 is the initial concentration (Hart and Anbar, 1970):

$$\ln\frac{C_t}{C_0} - [k_A(A) + k_B(B)]t \tag{1.26}$$

where (A) is concentration of species A and (B) is concentration of species B and k_A and k_B are first-order rate constants.

The optical density (*OD*) as measured in the absorption spectrophotometer of the LINAC can be translated by the molar extinction coefficient $\epsilon(e^-_{aq})$,concentration (C) of e^-_{aq} at time *t*, and the optical path length (*d*) by (Hart and Anbar, 1970):

$$OD = \epsilon\,(e^-_{aq})C\,d \tag{1.27}$$

The ratio of the concentrations equals that of the optical densities (Hart and Anbar, 1970):

$$\frac{C_t}{C_0} = \frac{(OD)_t}{(OD)_0} \tag{1.28}$$

Substituting, the derivation follows (Hart and Anbar, 1970):

$$\ln\left[\frac{(OD)_t}{(OD)_0}\right] = -[k_A(A) + k_B(B)]\,t \tag{1.29}$$

From this equation, the rate constants may be then be derived from a linear plot of the first-order rate constants at each time increment (Hart and Anbar, 1970).

The basis for kinetics measurement in pulse radiolysis (LINAC) was a measurement of the change in voltage on a photomultiplier tube. When a solution of interest is irradiated, species are created that can absorb visible light at different wavelengths. When less light is transmitted through a crystal target cell, graphically represented in Figure 1.1, holding the irradiated solution, the electron current on the photomultiplier tube is correspondingly less. The absorbed light intensity (absorbance or optical density) drops with respect to the formation of transient species (Swallow, 1973) and the concentration of species created can then be calculated by the Lambert-Beer law (Draganic and Draganic, 1971).

When the formation of solutes can not be measured directly, as in the case of the reactions in this study for •OH and HNM, then competition kinetics were used. Competition kinetics was described by the general form of the equation for primary radicals, $R\bullet$ interacting with solutes, S and product, P (Buxton *et al.,* 1988):

$$R\bullet + S_1 \xrightarrow{k_1} P_1 \tag{1.30}$$

$$R\bullet + S_2 \xrightarrow{k_2} P_2 \tag{1.31}$$

where $R\bullet$ represents the primary radical, so that if P_1 is the observable product, and S_1 and S_2 are chosen so that there is a complete reaction, and $[S_1]/[S_2]$ is varied, but $\sum k_i [S_i]$ kept constant so that $G[S_i]$ does not vary by the equation (Buxton *et al.,* 1988):

$$\frac{G(R\bullet)}{G(P_1)} - 1 = \frac{k_2 [S_2]}{k_1 [S_1]\bullet} \tag{1.32}$$

then k_2 can be determined when k_1 is known.

Conflicts with extraneous or competing reactions were avoided in experimentation. This was accomplished by sparging all solutions with pure form of nitrous oxide or

nitrogen gas during the pulsed irradiations (LINAC). High purity N_2O gas was applied for hydroxyl radical experimentation and N_2 gas for hydrated electron at atmospheric pressure. Solutions saturated with N_2O scavenge e_{aq}^- and provides a highly reactive chemical system comprised of predominantly •OH radicals (Janata and Schuler, 1982). Degassing solutions with N_2 purges or removes oxygen thereby reducing the potential for contribution from reactants other than the solute reacting with e_{aq}^- (Buxton *et al.*, 1988).

1.4.1. Mechanistic Approach for Study of Reaction of HNMs with the Hydroxyl Radical

The radical reaction rate constant for reaction of •OH with HNM was determined using pulse radiolysis and an aqueous solution of thiocyanate (SCN^-) for use in competition kinetics based on the competing reactions:

$$\bullet OH + HNM \rightarrow \text{Products} \qquad (1.33)$$

$$\bullet OH + SCN^- \text{ -WWW-}\rightarrow OH^- + (SCN)_2^{\bullet -} \qquad (1.34)$$

The change in the visible light absorption or intensity was monitored for reactions of $(SCN)_2^{\bullet -}$ at a wavelength of 475 nm. These changes in light absorption values were recorded in a computer and the data was subsequently processed and provided as hard copy print.

The following method and analytical expression applies to competition kinetics study of •OH reaction with HNMs (Buxton *et al.*, 1988; Mezyk *et al.*, 2004):

$$\frac{\left[(SCN)_2^{\bullet -}\right]_0}{\left[(SCN)_2^{\bullet -}\right]} = 1 + \frac{k_{33}\left[HNM\right]}{k_{34}\left[SCN^-\right]} \qquad (1.35)$$

where $[(SCN)_2^{\bullet -}]_0$ is the final yield of $(SCN)_2^{\bullet -}$ measured for only the 0.1 M SCN^- solution and $[(SCN)_2^{\bullet -}]$ is the reduced yield of this transient when HNM is present. The

ratio of $[(SCN)_2^{\bullet -}]_0$ / $[(SCN)_2^{\bullet -}]$ to the ratio of [HNM] / $[SCN^-]$ should present a linear relation of slope k_{33} / k_{34}. Based on the established rate constant for hydroxyl radical reaction with SCN^-, $k_{34} = 1.1 \times 10^{10}$ $M^{-1}s^{-1}$ (Mezyk *et al.,* 2004), the second-order rate constant (k_{33}) for HNM may then be determined (Buxton *et al.,* 1988).

1.4.2. Mechanistic Approach for Study of Reaction of HNMs with the Hydrated Electron Radical

Hydrated electrons (e_{aq}^-) generated by pulse radiolysis were introduced in N_2 saturated HNM solutions. These HNM solutions included *tert*-butyl alcohol (2-methyl-2 propanol, *t*-ButOH) to scavenge •OH radicals. In the ultra-violet to visible light range, only the very strong absorption of hydrated electrons will be observed with the hydrated electron decay dependent on the HNM concentration (Tobien *et al.,* 2000). The decay of the *t*-ButOH was proportional to the irradiated HNM and its concentration for a pseudo-second-order rate constant follows for the reaction

$$e_{aq}^- + \text{TCNM} \rightarrow \text{Products} \qquad (1.36)$$

Typical kinetic data for hydrated electron reaction with HNMs were obtained using direct observations at 700 nm and was obtained for three consecutive readings then averaged (Mezyk *et al.,* 2004). The direct observations of e_{aq}^- were based on the optical absorption spectra for the free radicals (Hug, 1981).

1.5. Halonitromethanes

The HNMs are a low molecular weight colorless liquid and hydrolyze very slowly. They are DBPs and currently unregulated in water (U.S. Environmental Protection Agency,

1997). The most studied HNM was frequently found to be trichloronitromethane (TCNM). It was described as a strong irritant, possessed lacrimatory activity, and exposure of rats for possible carcinogenicity was inconclusive as the short survival time of the animals to TCNM did not permit conclusive evidence (U.S. Department of Health, Education and Welfare, 1978).

1.5.1. Formation of HNMs

Chemical disinfectants (chlorine) applied at drinking water treatment facilities contributes to the formation of disinfection-by-products known as halonitromethanes (HNMs) (Merlet *et al.,* 1985; Thibaud et *al.,* 1987; Richardson *et al.,* 2000). HNMs are becoming the focus of new research for emerging contaminants to be studied (Richardson, 2003) and were identified as disinfection-by-products in drinking water treatment (U.S. Environmental Protection Agency, 1999). HNMs can also be formed by the reaction of ozone with high molecular nitrogenous organic compounds occurring in natural waters (Hoigné and Bader, 1988) and when pre-ozonation is followed by chloramines, the levels of HNMs can increase (Weinberg *et al.,* 2002). The formation of TCNM was found in pre-chlorinated waters. Its precursors include nitrite (Duguet *et al.,* 1984), bromide (Thibaud *et al.,* 1988), and organic compounds such as humic acids, amino acids, and nitrophenols (Sayato *et al.,* 1982).

1.5.2. Drinking Water HNM Disinfection-by-products

Becke *et al.* (1984) identified that trichloronitromethane (chloropicrin, TCNM) was formed by the chlorination of nitro-containing compounds, and later pre-ozonation was

also attributed to its formation in water (Hoigné and Bader, 1988). As one of the HNMs, TCNM was identified frequently in the open literature as compared to the other HNMs. TCNM has been found in various locations throughout the world. A survey of the literature indicates that TCNM was found as a DBP in drinking water. The locations and range of concentrations where TCNM was found are presented in Table 1.4.

Table 1.4. Trichloronitromethane (Chloropicrin) found in drinking water.

Location	Concentration Range, Min. to Max. ($\mu g\ L^{-1}$)	Number of Source Water Samples In Study	Reference
Australia	<0.01 to 0.4	7	(Simpson and Hayes, 1998)
Canada	<0.1 to 2.5	53	(Williams *et al.*, 1997)
France	1 to 6	2	(Duguet *et al.*, 1984)
	<3		(Thibaud *et al.*, 1987)
Greece	0.02 to 0.12	13	(Golfinopoulos *et al.*, 2003)
	ND to 0.26	15	(Kampioti and Stephanou, 2002)
Israel	NR	1	(Richardson *et al.*, 2003)
Japan	3.0	7	(Sayato *et al.*, 1982)
Korea	0.03 to 2.31	15	(Shin *et al.*, 1999)
Netherlands	0.01 to 3.0	20	(de Greef *et al.*, 1980)
Switzerland	0.4 to 2	2	(Hoigné *et al.*, 1988)
	2[(a)] to 6[(a)]		
U.S.	ND to 0.05	10	(Keith *et al.*, 1976)
	ND to 3	5	(Coleman *et al.*, 1976)
	ND to 3[(b)]	12	(Weinberg *et al.*, 2002)
	0.07 to 0.57[(a)]	4	(Jacangelo *et al.*, 1989)

[(a)] Values increased when water was pre-ozonated.
[(b)] Value reflects maximum for simulated distribution systems.
ND: Not Detected.
NR: Concentration value not reported.

TCNM has been investigated and applied as a commercial fungicide and fumigant (Thies and Nelson, 1982) and TCNM's possible reductive analogue

(dichloronitromethane) has been claimed to be identified in rain and snow in the northern hemisphere (Laniewski *et al.,* 1998).

TCNM has also been identified throughout the world in waters from treatment facilities using chlorine and ozone as a disinfectant (Hoigné and Bader, 1988). The highest reported TCNM levels were observed where increased levels of natural organic matter was found in polluted rivers and used as drinking water source (Shin *et al.,* 1999). Richardson *et al.* (1999) identified new brominated HNM DBPs where ozone was applied to drinking water, and then Weinberg *et al.* (2002) later found the occurrence of HNMs in a nationwide survey of water treatment plants across the United Stated with the highest brominated HNM levels found at the sites surveyed using pre-ozonation (Weinberg *et al.,* 2002; Richardson *et al.,* 2002).

The emergence of HNMs as a DBP has only recently been identified as a concern in drinking water. Not since Sayato (1982) and Becke *et al.* (1984) identified TCNM as a DBP in water were these HNMs addressed in the open literature with respect to presence in drinking water. Subsequently, Richardson *et al.* (1999) identified bromonitromethane, dibromonitromethane, and tribromonitromethane, as HNMs and listed these compounds as an emerging DBP found in water. This was followed later by Weinberg *et al.* (2002) in the nationwide survey, and then by Plewa *et al.* (2004) where he performed quantitative comparative cytotoxicity and genotoxicity testing of HNMs.

1.5.3. Fate and Environmental Degradation of HNMs

The fate and environmental degradation of HNMs were important criteria for understanding HNM decomposition kinetics and for elucidation of a possible degradation

mechanism. A survey of the literature indicated that the fate and environmental degradation of TCNM was established previously by several types of mechanisms. These include photolysis, alkylation, chemical reduction, biodehalogenation, and ultrasonic degradation. Recognition of these mechanisms and degradation pathways provided some assistance in the development of a degradation mechanism established in this study.

Photolysis of HNMs, such as TCNM, produces phosgene (Moureu *et al.,* 1950; Moilanen *et al.,* 1978) and nitrosyl chloride (Wade *et al.,* 2002). Exposure to a xenon light source, decomposed TCNM to carbon dioxide, (bicarbonate, carbonate), chloride, nitrate, and nitrite with a half-life of 31.1 hours and in the absence of light, TCNM did not undergo hydrolysis (Wilhelm *et al.,* 1996). The photolic ultra-violet (254 nm) half-life of TCNM was observed from 18 hours (Carter *et al.,* 1997) to 20 days (Moilanen et *al.,* 1978) with the deference in owing to the type of light source. Two mechanistic alternatives for degradation of TCNM by ultra-violet (254 nm) were suggested by Carter *et al.* (1997):

$$CCl_3NO_2 + h\nu(+O_2) \rightarrow Cl_2CO + ClNO(+O_2) \quad (1.37)$$

$$ClNO + hv \rightarrow Cl\bullet + NO, \text{ or} \quad (1.38)$$

$$CCl_3NO_2 + hv \rightarrow Cl_3C\bullet + NO_2 \quad (1.39)$$

As a measure of biological potency in the environment over time, TCNM was observed to provide a two fold reduction in nematode numbers and 10 fold reductions in the ratio of total fungal to total bacterial biomass after a 9 to 12 month period after application to the area around stumps (Ingham and Thies, 1996).

Ferruginous soils injected with TCNM produced dichloronitromethane (DCNM) and chloronitromethane (CNM) (Cervini-Silva *et al.,* 2001). Dehalogenation was also

observed in Fe(II) containing soils with reduction of TCNM to yield of 80% DCNM and CNM within 30 minutes (Cervini-Silva *et al.,* 2000). In organic soils, TCNM was reduced to bound residues by alkylation with the organic matter. Bound residues are defined as the fraction of pesticide that is non-extractable upon exhaustive extraction (Xu *et al.,* 2003). Where TCNM was used as a fumigant, the potential for leaching TCNM to groundwater was high because of TCNM's natural stability in water, and field soils with low organic matter combined with limited microbial activity reduced the potential for its degradation (Guo *et al.,* 2003). Biodehalogenation of TCNM occurred via enzymatic reactions of the cytochrome P-450 system (Castro *et al.,* 1985), microbial metabolism by *Pseudomonas sp.* (Castro *et al.,* 1983), and by *Strepomyces griseus* cells containing cytochrome P-450_{SOY} (Sariasiani and Stahl, 1990).

Of particular interest in these mechanisms previously studied was the persistence of TCNM in natural water indicating stability of the compound under dark condition. Further, the identification of TCNM degradation to phosgene in one case, and dehalogenation of TCNM to DCNM and CNM in another, provided an understanding needed for investigation of possible reaction pathways and consideration of initial reduction-oxidation processes. These processes were used as a starting point for derivation of a degradation mechanism approach used in this research.

1.6. Research Goals

The goal of this research was to identify rate constants for each of nine halonitromethanes, develop a mechanism for HNM degradation, and confirm the reaction mechanism with a kinetic model using free radicals generated in water by low LET

gamma and electrons. The results gained from this study of halonitromethanes degradation in water using free radical chemistry should ultimately provide many positive benefits. These benefits would be realized through improvements to water quality and result in an improvement to the quality of life, health, safety and welfare for all, and the environment.

The research would also contribute to future applications of advanced oxidation processes, using free radical chemistry. These AOPs would provide an alternative treatment process capable for the total removal of HNMs from drinking water with potentially no adverse impact to its quality. Overall, AOP free radical chemistry removal of hazardous substances would provide an environmentally sustainable technological process for water treatment. This sustainability would be derived from several key factors including: the absence of the need to manufacture a bulk chemical for water treatment; the elimination of a continued supply of raw materials required in the bulk chemical's manufacturing process; avoidance of pollution from the chemical's manufacture, its derivatives, or processing; and elimination of the need for any bilk chemical delivery or storage. The free radical AOP process was considered as one that essentially required no special infrastructure at the point of application such as bulk mixing, chemical reservoir, or other support infrastructure such as day-tanks, pumps, and piping. Currently, there exists no information in the open literature related to the applied use of free radical chemistry in the field or study of HNMs in aqueous solution. Therefore, support in the form of this research was necessary to provide kinetic and mechanistic information for the potential application of free radical AOP elimination of HNMs in water.

This research was structured to provide the needed data for application of free radical elimination of HNMs in water. The data and information provided could be extrapolated to meet the needed engineering design criteria in support of the AOP treatment processes.

Determination of the rates, mechanism and kinetic modeling for free radical removal of HNMs will provide substantive data and information contributing towards:

- Evaluation of alternative AOP treatment processes,
- Process optimization for pilot and large scale applications,
- Engineering principals and data needed for AOP process application, and
- Equipment sizing.

2. FREE RADICAL CHEMISTRY OF HALONITROMETHANES: RATE CONSTANTS FOR REDOX REACTION OF HYDROXYL RADICAL AND HYDRATED ELECTRON IN A PULSE RADIOLYSIS STUDY

2.1. Introduction

Halonitromethanes (HNMs) are soluble low-molecular weight compounds comprised of three primary forms and they are chlorinated, brominated, and mixed halogenated analogues. These compounds all contain a nitro group that includes a carbon-halogen bond, and several HNMs contain hydrogen as a carbon-hydrogen bond. The basis of free radical chemistry is the production of the hydroxyl radical (•OH) and hydrated electron (e_{aq}^-) for oxidation-reduction of HNM in aqueous solution and eliminate these bonds. Free radicals are formed in quantifiable yields by ionizing radiation (fast electrons). The use of free radical AOPs for elimination of HNMs in water necessitates an understanding of the rate constant for the degradation reaction of HNM to the parent ions.

The purpose of this study was to determine the rate constants for the oxidative •OH hydroxyl radical and reductive e_{aq}^- hydrated electron reaction for each of the HNMs in water. The means and equipment used for obtaining these rate constants were low LET electrons generated by a linear accelerator (LINAC) and transient absorption spectroscopy. Optical spectroscopy does not provide the means for investigating all the reactions occurring with the water matrix, however it does provide the basic tool for following the progress of free radical reactions taking place on the nanosecond and microsecond time scale (Hug, 1981).

2.2. Methods and Materials

The LINAC was coupled with optical absorption spectroscopy using a high intensity Xe lamp (172 nm) for investigations in the visible and near UV range. The high intensity lamp was pulsed and appropriately shielded for protection of the crystal target cell. This shielding will preclude any potential photolysis of the compound under investigation. The light emitted through the target cell was converted into an electrical pulse by use of a photodetector (monochromator) and photomultiplier. Optical transients were recorded and plotted according to the optical absorption derived from radical reactions occurring in the target cell and the respective concentration of solute in solution upon exposure to ionizing radiation. The accelerator's transient absorption spectroscopic detection system is capable of monitoring fast pulses of light with equipment connected to a computer for data acquisition and control of the LINAC. (Asmus, 1984)

Solutions of HNMs, Table 2.1 were prepared using nano-purified water (Millipore Milli-Q) with a resistivity ≥ 18 MΩcm at 25°C (Myron L Company, Series 750 Conductivity Monitor) and constantly illuminated by a mercury lamp source generating ultraviolet light to eliminate organic contaminant concentrations to maintain them below 13 μM as measured by an on-line TOC analyzer (Millipore TOC Monitor, Model A10, ANTEL). On May 17, 2004, the TOC analyzer reading was 23 ppb. All rate constant experiments were conducted at 20°C (ambient room temperature), one atmosphere, and ambient pH.

Table 2.1. Halonitromethane abbreviation, formula, and source.

Halonitromethane	(Abbreviation)	Formula	Mfr.
Chloronitromethane	(CNM)	CH_2ClNO_2	Helix
Dichloronitromethane	(DCNM)	$CHCl_2NO_2$	Helix
Trichloronitromethane	(TCNM)	CCl_3NO_2	Aldrich
Bromonitromethane	(BNM)	CH2BrNO$_2$	Aldrich
Dibromonitromethane	(DBNM)	$CHBr_2NO_2$	Helix
Tribromonitromethane	(TBNM)	CBr_3NO_2	Helix
Bromochloronitromethane	(BCNM)	$CHBrClNO_2$	Helix
Bromodichloronitromethane	(BDCNM)	$CBrCl_2NO_2$	Helix
Dibromochloronitromethane	(DBCNM)	CBr_2ClNO_2	Helix

The steady state radiolysis of water produces constant yield of free radical yields in the pH range from 3 to 11 for pure water as described in equation (1.1) where the yield value (G) is denoted in units of mol $J^{-1} \times 10^{-7}$ (Buxton, 2004), and represents low LET radiation with each of the number of each species formed after radiolysis of water by fast electrons as condition for steady state irradiation.

The electron pulse radiolysis system (LINAC) was used for determination of bimolecular rate constants. Dosimetry for pulse radiolysis was based on the oxidation of 1.0×10^{-2} M, KSCN solution at $\lambda = 472$ nm, ($G\epsilon = 5.09 \times 10^4$) with doses of 3 to 5 Gy per 2 to 3 ns pulse, (Schuler *et al.,* 1980) where G(X) (mol J^{-1}) is defined as the number of species produced or radiation chemical yield per 100 eV and ϵ (m^2 mol^{-1}) as the molar absorption coefficient. (Buxton and Stuart, 1995; Mezyk *et al.,* 2004) The initial

concentration for each of the respective HNMs was increased in a batch process and each batch flowed through the LINAC target cell. Solutions were continuously stirred and rigorously sparged with high purity N_2O for the •OH experiments. Solutions were pumped to the quartz target cell. For the determination of the reaction rate of e_{aq}^- with the HNMs, solutions were sparged with N_2 to remove the O_2. Removal of the •OH from solution was made possible by use of 0.50 M *tert*-butanol as a scavenger (Mezyk *et al.*, 2004).

2.3. Rate Constants

The experimental work to determine the hydroxyl radical rate constant necessitated the isolation of the hydroxyl radical reaction with HNM. Aqueous solutions were pre-saturated with N_2O, which quantitatively converts the e_{aq}^- to this radical (Buxton *et al.*, 1988):

$$e_{aq}^- + N_2O + H_2O \rightarrow N_2 + OH^- + \bullet OH, \qquad k_1 = 9.1 \times 10^9\ M^{-1}s^{-1} \qquad (2.1)$$

In the kinetics experiments, the hydroxyl radical reaction with HNMs did not result in any transient absorbance over the range 250 to 800 nm. Therefore, it was necessary to use competition kinetics using SCN^- based on the reactions:

$$\bullet OH + HNM \rightarrow \text{Products} \qquad (2.2)$$

$$\bullet OH + SCN^- + (SCN^-) \rightarrow OH^- + (SCN)_2^{\bullet -}, \qquad k_3 = 1.1 \times 10^{10}\ M^{-1}s^{-1} \qquad (2.3)$$

This can be rearranged to give the following expression:

$$\frac{[(SCN)_2^{\bullet -}]_o}{[(SCN)_2^{\bullet -}]} = 1 + \frac{k_2[HNM]}{k_3[SCN^-]} \qquad (2.4)$$

where $[(SCN)_2^{\bullet -}]_o$ is the final yield of $(SCN)_2^{\bullet -}$ measured for only the SCN^- solution, and $[(SCN)_2^{\bullet -}]$ is the yield of this transient when TCNM is added. Therefore a plot of $1/[(SCN)_2^{\bullet -}]$ against the ratio $[TCNM]/[SCN^-]$ should give a straight line of slope k_2 / k_3. From the known rate constant of $k_3 = 1.1 \times 10^{10}$ $M^{-1}s^{-1}$, the k_2 rate constant can then be calculated. (Asmus, 1984) The experimental data water obtained and the confidence limit for the each rate constant was calculated by:

$$\sqrt{\left(\frac{\text{Absorb. } S_X}{\text{Avg. Absorb.}}\right)_n^2 + \left(\frac{\text{Absorb. } S_X}{\text{Avg. Absorb.}}\right)_{n+1}^2} \qquad (2.5)$$

where n is the data for initial concentration and n+1 was the next batch concentration of TCNM. The data for ratio of $[TCNM]/[SCN^-]$ and ratio of intensity was input into a linear curve fitting program (ORIGIN 7.5™) for plotting with the confidence limits identified as one standard deviation (S_X). The hydroxyl radical decay data is presented in Table 2.3 with the linear plotting data derived from the curve fitting program.

Table 2.2. Trichloronitromethane hydroxyl radical experimental data.

[TCNM] Added ($\times 10^{-4}$)	Nrml. Dose, Volts ($\times 10^{-1}$)	Absorb. Data	Absorb. ($\times 10^{-2}$)	Avg. Absorb. ($\times 10^{-2}$)	Absorb. (One Stnd. Dev.) ($\times 10^{-5}$)	[TCNM] / [SCN^-]	Ratio of Intensity	Confidence Limit, S_X	Linear Fit, [TCNM] / [SCN^-]	Linear Fit, Ratio of Intensity
0	8.980	0.01322	1.472						-0.5	0.99966
	9.360	0.0135	1.442						-0.07895	1.0016
	9.370	0.0136	1.451						0.34211	1.00354
	9.360	0.01384	1.479	1.461	17.0896	0	1.000	0.01654	0.76316	1.00549
1.236	9.080	0.01325	1.459						1.18421	1.00743
	9.200	0.01321	1.436						1.60526	1.00937
	9.330	0.01344	1.441						2.02632	1.01131
	9.330	0.01333	1.429	1.441	13.0424	2.098	1.014	0.01479	2.44737	1.01325
2.626	8.950	0.01272	1.421						2.86842	1.01519
	9.030	0.01289	1.427						3.28947	1.01714
	9.070	0.01286	1.418						3.71053	1.01908
	9.050	0.01312	1.450	1.429	14.3327	4.458	1.02	0.0141	4.13158	1.02102
4.200	8.860	0.0126	1.422						4.55263	1.02296
	8.940	0.01262	1.412						4.97368	1.0249
	8.980	0.01266	1.410						5.3474	1.02685
	9.050	0.01273	1.407	1.413	6.7100	7.130	1.034	0.01262	5.81579	1.02879

The rate constant was determined for each HNM reaction with the e_{aq}^- by directly following the absorption at 700 nm. (Mezyk *et al.*, 2004) These solutions were saturated with nitrogen gas, to remove dissolved oxygen. The solutions also contained 0.50 M *tert*-butanol to scavenge the hydroxyl radicals and hydrogen atoms into the less-reactive *tert*-butyl alcohol radical:

$$^{\bullet}OH/H^{\bullet} + (CH_3)_3COH \rightarrow H_2O/H_2 + {}^{\bullet}CH_2(CH_3)_2COH \qquad (2.5)$$

The decay of the hydrated electron was pseudo-first-order at the higher concentrations of HNMs. The data for decay of the hydrated electron was monitored directly and the rate constant and concentration was input into a linear curve fitting program (ORIGIN 7.5™) for plotting with the confidence limits identified as one standard deviation (S_X). The hydrated electron decay data is presented in Table 2.3 with the linear plotting data derived from ORIGIN™ curve fitting program.

Table 2.3. Trichloronitromethane hydrated electron radical experimental data.

[TCNM] Added ($\times 10^{-4}$)	Nrml. Dose, Volts ($\times 10^{-1}$)	Absorb. Data	Absorb. ($\times 10^{3}$)	k' ($\times 10^{-6}$)	Confidence Limit, S_X	Linear Plot, k' ($\times 10^{-4}$)	Linear Plot, [TCNM] (mM)
0				0.1645	18400	-0.5	-0.896
1.212	1.042	-0.00005	20.84	2.777	142000	-0.210	-0.279
	1.044	0.00005	20.88			0.0078	0.337
	1.033	0.00022	4.695			0.3684	0.955
2.315	1.031	0.00079	1.305	5.224	58000	0.6578	1.572
	1.035	0.00052	1.990			0.9473	2.189
	1.041	0.00083	1.254			1.236	2.806
	1.040	0.0007	1.486			1.526	3.423
3.268	1.026	0.00067	1.531	6.948	138000	1.815	4.040
	1.035	0.00023	4.500			2.105	4.657
	1.039	0.00048	2.165			2.394	5.275
4.348	1.015	-0.00011	-9.227	9.190	146000	2.684	5.892
	1.020	0.00047	2.170			2.973	6.509
	1.025	0.00034	3.015			3.263	7.126

The calculated rate constants for hydroxyl radical and hydrated electron reaction with the HNMs were calculated and presented in Table 2.4. Other attempts to measure rate constants for hydroxyl radical with HNMs in aqueous solution of water were not found in the literature.

Table 2.4. Pseudo-second-order rate constants for reaction of hydrated electron and hydroxyl radical with halonitromethane compounds.

Halonitromethane Compound	Rate constant, k e_{aq}^- reaction ($M^{-1}s^{-1}$)	Rate constant, k •OH reaction ($M^{-1}s^{-1}$)
chloronitromethane	$(3.01 \pm 0.10) \times 10^{10}$	$(1.94 \pm 0.13) \times 10^{8}$
dichloronitromethane	$(3.21 \pm 0.01) \times 10^{10}$	$(5.12 \pm 0.51) \times 10^{8}$
trichloronitromethane	$(2.31 \pm 0.03) \times 10^{10}$	$(4.84 \pm 0.40) \times 10^{7}$
bromonitromethane	$(3.13 \pm 0.03) \times 10^{10}$	$(8.36 \pm 0.49) \times 10^{7}$
dibromonitromethane	$(3.07 \pm 0.09) \times 10^{10}$	$(4.75 \pm 0.50) \times 10^{8}$
tribromonitromethane	$(2.29 \pm 0.16) \times 10^{10}$	$(3.25 \pm 0.34) \times 10^{8}$
bromochloronitromethane	$(2.93 \pm 0.03) \times 10^{10}$	$(4.16 \pm 0.48) \times 10^{8}$
bromodichloronitromethane	$(2.68 \pm 0.08) \times 10^{10}$	$(1.02 \pm 0.13) \times 10^{8}$
dibromochloronitromethane	$(2.95 \pm 0.13) \times 10^{10}$	$(1.80 \pm 0.13) \times 10^{8}$

2.4. Summary

The reduction by e_{aq}^- of all HNMs was observed to be much faster than the oxidation reaction by •OH. For the case of brominated analog of HNM, bromonitromethane reduction by e_{aq}^- was expected to produce the bromide ion, along with the corresponding carbon-centered radical:

$$e_{aq}^- + BrH_2CNO_2 \rightarrow Br^- + H_2{}^{\bullet}CNO_2 \qquad (2.6)$$

The reaction of e^-_{aq} with TCNM, a chlorinated form of HNM, proceeded forward as a dissociative electron attachment. The reaction was considered to proceed via two main reaction pathways resulting in the formation of two different carbon-centered radicals (Løgager and Sehested, 1993a):

$$e^-_{aq} + CCl_3NO_2 \rightarrow Cl^- + \bullet CCl_2NO_2 \quad (2.7)$$

$$e^-_{aq} + CCl_3NO_2 \rightarrow NO_2^- + \bullet CCl_3 \quad (2.8)$$

Initial observation of the reaction rate constants and mass quantification results obtained from analysis of residual ions in solution suggests that the reaction of e^-_{aq} with the mixed halogenated form of halonitromethane, (bromochloronitromethane) proceeds by the following pathways:

$$e^-_{aq} + CHBrClNO_2 \rightarrow Cl^- + \bullet CHBrNO_2 \quad (2.9)$$

$$e^-_{aq} + CHBrClNO_2 \rightarrow Br^- + \bullet CHClNO_2 \quad (2.10)$$

$$e^-_{aq} + CHBrClNO_2 \rightarrow NO_2^- + \bullet CHClBr^- \quad (2.11)$$

The hydroxyl radical reaction with HNMs in aqueous solutions leads to electron transfer between halide ions and hydroxyl radical and gives halogen atoms according to (Spinks and Woods, 1964):

$$\bullet OH + BrH_2CNO_2 \rightarrow \bullet BrH_2CNO_2 + OH^- \quad (2.12)$$

The slow rate of degradation exhibited by all of the HNMs with the hydroxyl radical within this study implied formation of oxy radicals of HNM and more particularly as a type of super-oxy reaction mechanism proposed by Asmus *et al.* (1964b).

3. FREE RADICAL CHEMISTRY OF TRICHLORONITROMETHANE (CHLOROPICRIN): RATE CONSTANTS AND DEGRADATION MECHANISM BY OXIDATION-REDUCTION REACTIONS

3.1. Introduction

The objective of this study was to explore the utility of advanced oxidation/reduction processes for the treatment of trichloronitromethane (chloropicrin, TCNM) in water. Of particular interest were the reactions of the hydroxyl radical (•OH) and hydrated electrons (e_{aq}^-). The bimolecular reaction rate constants for degradation of TCNM from •OH and e_{aq}^- were determined using pulse radiolysis, while the destruction mechanism and mass balances for the reactions were studied using ^{60}Co γ-radiation. To complete the study, a kinetic model was employed using MAKSIMA-CHEMIST and the results compared to experimental observations.

Disinfectants used in water treatment, such as chlorine, chloramines, and ozone, react with natural organic matter to form what are collectively referred to as disinfection-by-products such as TTHMs (Rook, 1974; Jacangelo *et al.,* 1989) where they are regulated under the Safe Drinking Water Act (U.S. Environmental Protection Agency, 1997). One class of DBPs, not currently regulated, was the focus of recent reports and was identified as halonitromethanes (HNMs) (Richardson, 2003; Richardson *et al.,* 2000; U.S. Environmental Protection Agency, 1999). The TCNM DBP was found to be the most common HNM in drinking water (Merlet *et al.,* 1985; Becke *et al.*, 1984). When pre-ozonation was followed by chloramination, the concentrations of HNMs were found to

increase and TCNM was observed up to 1.8×10^{-2} μM (3 μg L^{-1}) in U.S. drinking waters (Weinberg *et al.,* 2002).

In addition to being found as a DBP in drinking water, TCNM has been studied for use as a component of multi-fumigant formulations (Spokas and Wang, 2003), bactericides (Malatesta *et al.,* 1951), fumigants for pathogenic fungi on Douglas Fir trees (Thies and Nelson, 1982), a pre-plant soil herbicide for peppers (Gilreath and Santos, 2004), an alternate fungicide to methyl bromide for tomatoes (Gullino *et al.,* 2002), weed control for strawberries (Haara *et al.,* 2003), and for weed and fungi control on tobacco crops (Csinos *et al.,* 2002).

The LC_{50} of TCNM was ranked second in lethality (0.49 μM) in the house fly of eleven cyanohydrins tested and ninth most lethal (LC_{50} = 7.91 μM) for the lesser grain borer (Park *et al.,* 2002). Data from its use as a World War I chemical agent suggested that an exposure of 30 minutes at 0.8 mg L^{-1} or 10 minutes at 2.0 mg L^{-1} was lethal to humans (Selala *et al.,* 1989). The TCNM DBP has been reported to be a potent mammalian cytotoxin and genotoxin and found 32.6 times more cytotoxic than dichloroacetic acid (DCAA) and trichloroacetic acid (TCAA) (Plewa *et al.,* 2004). Both DCAA and TCAA are included in the five regulated haloacetic acids (U.S. Environmental Protection Agency, 1997). TCNM is metabolized, in mammals, to thiophosgene and it is acutely toxic (Sparks *et al.,* 2000), while other studies indicated genotoxicity at 1.8 x 10^{-2} μM (Giller *et al.,* 1995). Bacterial mutagenicity studies indicated that TCNM, on addition of glutathione, was mutagenic but not toxic (Schneider *et al.,* 1999).

Limited studies have been reported for the treatment of TCNM in aqueous solutions. Ultrasound, 358 kHz, degraded 99% of a 10 μM TCNM solution with recovery ratios for Cl^- and inorganic nitrogen (as NO_3^- and NO_2^-) at 72 ±1% and 91 ±2%, respectively (Zhang and Hua, 2000).

The objective of this study was to explore the utility of advanced oxidation processes for the treatment of TCNM in water. Of particular interest were the reactions of the hydroxyl radical (•OH) and hydrated electron (e_{aq}^-) with TCNM. The bimolecular reaction rate constants for degradation of TCNM from •OH and e_{aq}^- were determined using pulse radiolysis, while the destruction mechanism and mass balances for the reactions were studied using ^{60}Co γ-radiation. To complete the study, a kinetic model was employed using MAKSIMA-CHEMIST and the results compared to experimental observations.

3.2. Methods and Materials

Solutions of TCNM (CCl_3NO_2) were used as received from manufacturers identified in Table 2.1 and prepared using nano-pure (Millipore Milli-Q) filtered tap water with a resistivity ≥18 MΩcm at 25°C was constantly illuminated by a mercury lamp (UV 185 nm and 254 nm) to eliminate microbes and maintain organic concentrations to a value below 13 μM as measured by an on-line TOC analyzer.

The experimentation included investigation of formate and oxalate as a byproduct of irradiation. Standards of organic acids used in the gas chromatography and mass spectrometry were prepared from sodium formate (certified American Chemical Society, Fisher Scientific, Fair Lawn, NJ, Lot 986590) and oxalic acid disodium salt (Sigma, St.

Louis, MO, Lot 41H0116). A 2,000 mg L^{-1} formate and a 1,000 mg L^{-1} oxalate stock solution were prepared. Standard concentrations consisted of 200, 20, and 2 mg L^{-1} formate, and 100, 10 and 1 mg L^{-1} oxalate. Standards contained both formate and oxalate. All standards were prepared in accordance with laboratory procedure. Blanks were also prepared from nano-pure water.

The radiolysis of water, for the pH range 3 to 11, can be described (Buxton, 2004) by equation (1.1). The linear accelerator (LINAC), electron pulse radiolysis system, at the U.S. Department of Energy Radiation Laboratory, University of Notre Dame was used during the experimentation. This accelerator and transient absorption spectroscopic detection system has been described in detail elsewhere (Whitham *et al.,* 1995). Dosimetry for pulse radiolysis was based on the oxidation of 1.0 x 10^{-2} M KSCN solution at $\lambda = 475$ nm, ($G\epsilon = 5.09 \times 10^4$) with doses of 3 to 5 Gy per 2 to 3 ns pulse (Mezyk *et al.,* 2004).

The TCNM and reaction products exhibited no significant transient absorbance over the range 250 to 800 nm. Therefore, the hydroxyl radical rate constant determination required competition kinetics, based on the competing reactions:

$$\bullet OH + TCNM \rightarrow \text{Products} \tag{3.1}$$

$$\bullet OH + SCN^- (+ SCN^-) \rightarrow OH^- + (SCN)_2^{\bullet -}, \quad k_2 = (1.1 \times 10^{10})\ M^{-1}s^{-1} \tag{3.2}$$

The following analytical expression was then used:

$$\frac{[(SCN)_2^{\bullet -}]_o}{[(SCN)_2^{\bullet -}]} = 1 + \frac{k_1[TCNM]}{k_2[SCN^-]} \tag{3.3}$$

where a plot of $1/[(SCN)_2^{\cdot -}]$ with the ratio[TCNM]/[SCN^-] gave a straight line of slope k_1/k_2. Based on the rate constant for SCN^-, $k_2 = 1.1 \times 10^{10}\ M^{-1}s^{-1}$ (Mezyk *et al.*, 2004), the k_1 rate constant was readily determined (Asmus, 1984).

Aqueous solutions were pre-saturated with N_2O to isolate the reaction of the •OH with TCNM. This pre-saturation quantitatively converted the hydrated electron (e_{aq}^-) and hydrogen atom ($^{\bullet}H$) to •OH with their respective rate constant identified (Buxton *et al.*, 1988):

$$e_{aq}^- + N_2O + H_2O \rightarrow N_2 + OH^- + {\bullet}OH, \qquad k_4 = 9.1 \times 10^9\ M^{-1}s^{-1} \tag{3.4}$$

$$^{\bullet}H + N_2O \rightarrow {\bullet}OH + N_2, \qquad k_5 = 2.1 \times 10^6\ M^{-1}s^{-1} \tag{3.5}$$

For the determination of the reaction rate of TCNM and e_{aq}^-, solutions were sparged with N_2 to remove the O_2. To remove the •OH from solution *tert*-butanol in 0.50 M concentration was added as a scavenger. The effect of the reactions by the e_{aq}^- occurring in solution resulted in the change of absorbance and these changes could be observed directly at 700 nm according to the reaction:

$$e_{aq}^- + \text{TCNM} \rightarrow \text{Products} \tag{3.6}$$

A ^{60}Co γ-irradiator (Shepherd, Model 109-68) was calibrated from a certified dose rate to be 122 Gy $min.^{-1}$ at the time of the experimentation and was used for all steady state studies. Experiments were performed using sealed 47 mL glass vials at ambient room temperature (20°C) with no head space. The TCNM solutions were irradiated at six doses, 1.2, 2.4, 3.6, 6.1, and 8.5 kGy including a zero dose blank, by varying the length of time in the irradiator.

The Fricke dosimeter was used to determine dose rate of the ^{60}Co γ-irradiator. The dose rate was 2.034×10^{-4} Mrad and was converted for use in the kinetic model to 1.27×10^{19} eV $L^{-1} s^{-1}$.

Samples were analyzed using an ion chromatograph (Dionex DX-500) for the determination of Cl^- and NO_3^-. The limit of detection of the method was 0.3 μM and 0.2 μM, for Cl^- and NO_3^-, respectively. The standard deviation analytical error for Cl^- and NO_3^-, was $\pm$0.02 and $\pm$0.01 mM, respectively.

Concentrations of organic acids were determined using a high-pressure liquid chromatograph (HPLC). All standards and blanks were prepared using $\geq$18 MΩcm at 25°C nano-pure water. The limit of detection for formate and oxalate ions was 0.02 mM as the single standard deviation. The concentration of TCNM in the samples was determined using GC/MS. The lower limit of detection using GC/MS was $(1.8 \pm 0.2) \times 10^{-7}$ M for TCNM.

3.3. Results and Discussion

The kinetic data were obtained using absorption spectrometry at 475 nm for increasing TCNM concentrations and the results are graphically presented in Figure 3.1. The transformed kinetic data are graphically presented in Figure 3.2. From these data, the rate constant for the •OH reaction with TCNM was derived and found to be $k_{3.1} = (4.84 \pm 0.40) \times 10^7$ $M^{-1}s^{-1}$.

The reaction of e_{aq}^- with TCNM was determined using increasing concentrations of TCNM as graphically represented in Figure 3.3. The bimolecular rate constant for the reaction of e_{aq}^- with TCNM was determined from a plot of at least three kinetic traces.

The solid line in Figure 3.4 corresponds to a weighted linear fit with rate constant, k_6 = $(2.13 \pm 0.03) \times 10^{10}$ $M^{-1}s^{-1}$. The weighting corresponds to the S_X as applied in the ORIGIN™ graphing program.

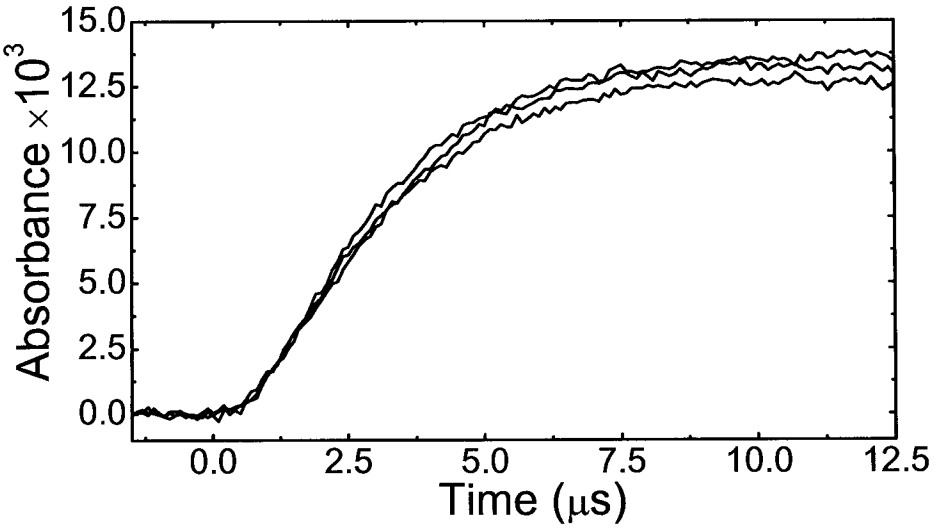

Figure 3.1. Typical kinetic plot of $(SCN)_2^{\bullet -}$ formation for trichloronitromethane reaction with •OH. Plot for 475 nm and N_2O^- saturated 5.89 × 10^{-5} M KSCN solution containing zero (top curve), 1.24×10^{-4} M (middle), and 4.20×10^{-4} M (lower curve) trichloronitromethane at ambient pH and room temperature.

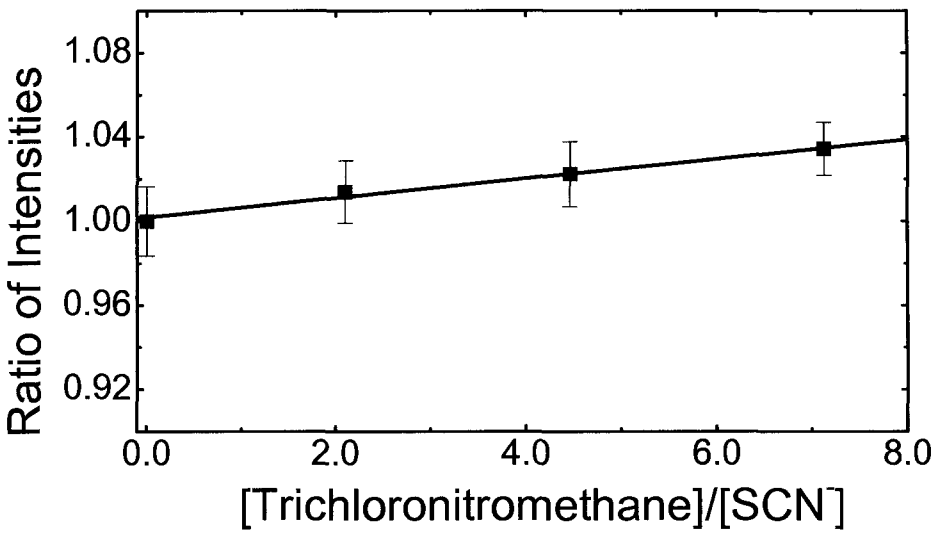

Figure 3.2. Competition kinetics plot for •OH reaction with trichloronitromethane using SCN^- as a standard. Solid line is weighted linear fit, corresponding to a slope of 0.0461 ± 0.00038. This gives a second-order rate constant for trichloronitromethane reaction as $k = (4.84 \pm 0.40) \times 10^7\ M^{-1}s^{-1}$.

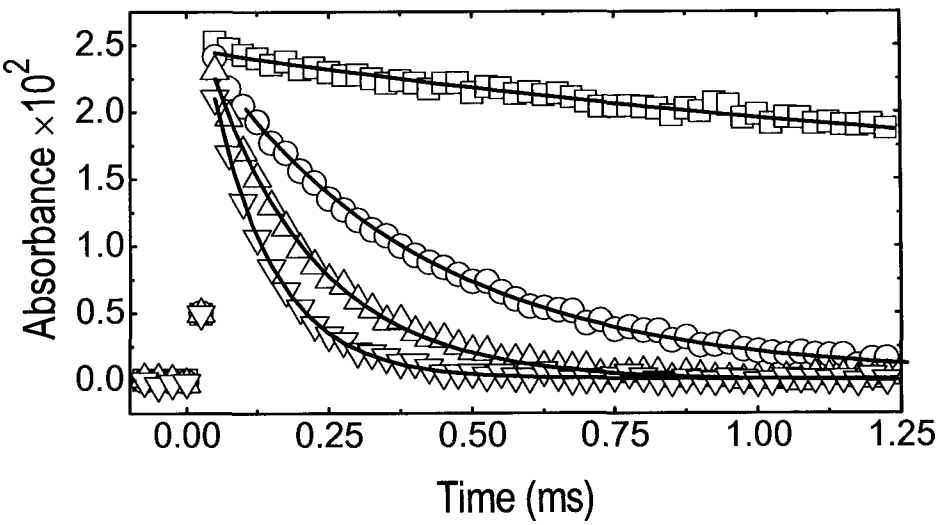

Figure 3.3. Typical kinetic decay profiles obtained for the hydrated electron absorbance of trichloronitromethane. Plot for 700 nm and electron pulse irradiated aqueous solution at ambient pH containing zero (□), 1.12×10^{-4} (O), 2.32×10^{-4} (Δ), and 4.35×10^{-4} (∇) M trichloronitromethane, respectively. Curves shown are the average of 15 individual pulses. Solid lines correspond to rate constant fitting with the pseudo-first-order values of 1.71×10^{5}, 2.64×10^{6}, 5.26×10^{6}, and 9.30×10^{6} s^{-1}, respectively.

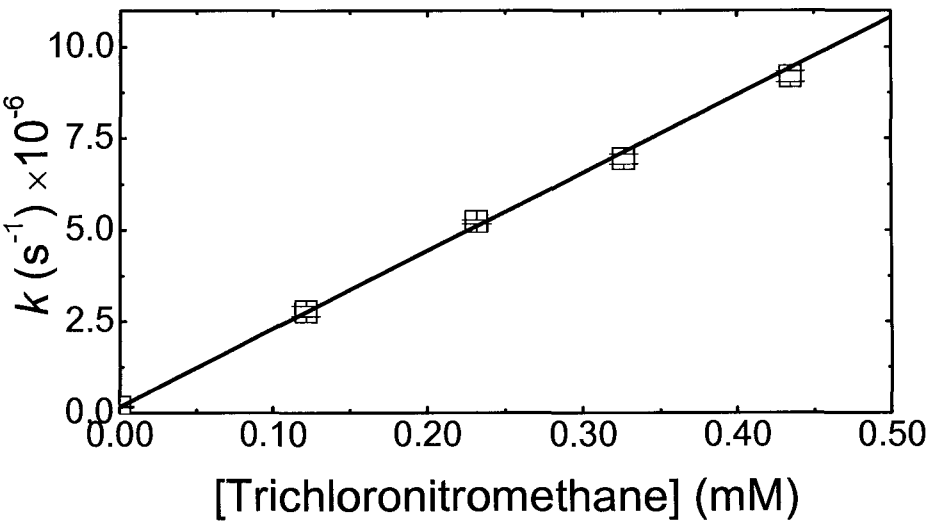

Figure 3.4. Second-order rate constant determination for the reaction of the hydrated electron with trichloronitromethane. Single point error bars are one standard deviation, as determined from the average of at least three kinetic traces. Solid line corresponds to weighted linear fit, giving $k = (2.13 \pm 0.03) \times 10^{10}\ M^{-1}s^{-1}$.

Steady state ^{60}Co gamma irradiations were performed with an initial concentration of 1.13 mM TCNM in water with an estimated dissolved oxygen concentration of 2.00×10^{-4} M as measured using the decomposition of oxygen by the hydrated electron in aqueous solution and the rate constant of $k = 1.9 \times 10^{10}$ $M^{-1}s^{-1}$. These experiments were conducted to determine the destruction of TCNM and the formation of reaction byproducts with increasing total dose to assist in elucidating a reaction mechanism. The degradation of TCNM, and the corresponding formation of chloride and nitrate ions were determined and summarized in Table 3.1. Assuming complete destruction, mass balance of the chloride ion was nearly achieved at 92% recovery at a dose of 8.5 kGy. There was no nitrite ion observed in the control or irradiated solutions. The nitrate ion was, at the highest dose, 79% of the initial TCNM-N. The irradiated samples were investigated for formate and oxalate as possible byproducts of the radiolysis. Oxalate and formate ions were below detection limits in all samples.

Table 3.1. Summary of residual ion results for ^{60}Co irradiation of TCNM solutions (1.13 mM) in pure water at doses up to 8.54 kGy.

Dose (kGy)	[TCNM] (mM)	[Cl^-] (mM)	[NO_3^-] (mM)
0	1.13	0.00	0.00
1.22	0.80	0.92	0.29
2.44	0.42	1.67	0.44
3.66	0.17	2.17	0.58
6.1	NM[a]	2.73	0.79
8.54	BMDL[b]	3.13	0.89

[a] Not measured.
[b] Below method detection limit.

From observation of the rate constant values for both hydroxyl radical and hydrated electron, it was apparent that reductive processes for the reaction with the e^-_{aq}, were primarily responsible for the destruction of TCNM. The reaction of the e^-_{aq} with TCNM, dissociative electron attachment, is expected to proceed via two main reaction pathways resulting in the formation of two different carbon-centered radicals (Hart and Anbar, 1970):

$$e^-_{(aq)} + CCl_3NO_2 \rightarrow \quad Cl^- + \bullet CCl_2NO_2 \qquad (3.7)$$

$$e^-_{(aq)} + CCl_3NO_2 \rightarrow \quad NO_2^- + \bullet CCl_3 \qquad (3.8)$$

Based on the reaction of e^-_{aq} with tetranitromethane it is possible that a third reaction may lead to other products in this system (Asmus *et al.*, 1964a; Rabani *et al.*, 1965):

$$e^-_{(aq)} + CCl_3NO_2 \rightarrow \quad \bullet NO_2 + CCl_3^- \qquad (3.9)$$

In oxygenated solutions, carbon-centered radicals react with O_2 to give peroxyl radicals (Hart and Anbar, 1970):

$$O_2 + \bullet CCl_2NO_2 \rightarrow \bullet OOCCl_2NO_2 \qquad (3.10)$$

$$O_2 + \bullet CCl_3 \rightarrow \bullet OOCCl_3, \quad k_{11} = 3.3 \times 10^9\ M^{-1}s^{-1} \quad \text{(Mönig } et\ al.\text{, 1983)} \qquad (3.11)$$

Relatively few rate constants for this general reaction (equations 3.10 and 3.11) have been measured. Most of the values that have been determined are in the range (2 – 4) $\times 10^9\ M^{-1}s^{-1}$ (Neta *et al.*, 1990).

The anion, in equation (3.9) would react with O_2:

$$O_2 + CCl_3^- \rightarrow {}^-OOCCl_3 \qquad (3.12)$$

The peroxy anion in equation (3.12) would be relatively unstable and probably spontaneously decomposes via an intramolecular reaction:

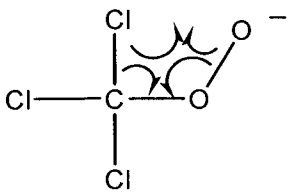

$$\longrightarrow \quad COCl_2 + OCl^- \qquad (3.13)$$

where phosgene, $COCl_2$, is unstable in aqueous solution and hydrolyzes rapidly to CO_2 and HCl (Mertens *et al.,* 1994).

In general, peroxyl radicals are relatively unreactive in aqueous solution (von Sonntag and Schuchmann, 1997). However, it is well known that the $\bullet OOCCl_3$ may react via electron transfer with a suitable electron acceptor to give $^-OOCCl_3$, e.g., I^- or aromatic thiols (Bonifačić *et al.,* 1991; Simic and Hunter, 1986; Khaikin *et al.,* 1995). In this relatively simple mechanistic solution it was not clear that such a reaction would occur. Another route that peroxyl radicals could take was to combine to form tetroxides (von Sonntag and Schuchmann, 1997). These tetroxides may then react as shown in equations (3.14) through (3.17) inclusively:

$$\xrightarrow{X} \quad R_2C{=}O + R_2CHOH + O_2 \qquad (3.15)$$

$$R_3C{-}O_4{-}CR_3 \xrightarrow{X} \quad 2R_2C{=}O + H_2O_2 \qquad (3.14)$$

$$\longrightarrow \quad 2R_3CH\dot{O} + O_2 \qquad (3.16)$$

$$\longrightarrow \quad 2\dot{R} + O_2 + 2RCH{=}O \qquad (3.17)$$

Because of the lack of hydrogen atoms on the carbon of TCNM reactions (3.14) and (3.15) was not possible and because this is a one-carbon compound reaction (3.17) can not proceed (von Sonntag and Schuchmann, 1997). Therefore, it appears that reaction (3.16) is the likely pathway and would lead to the formation of two different alkoxy radicals that would undergo intra-molecular rearrangements:

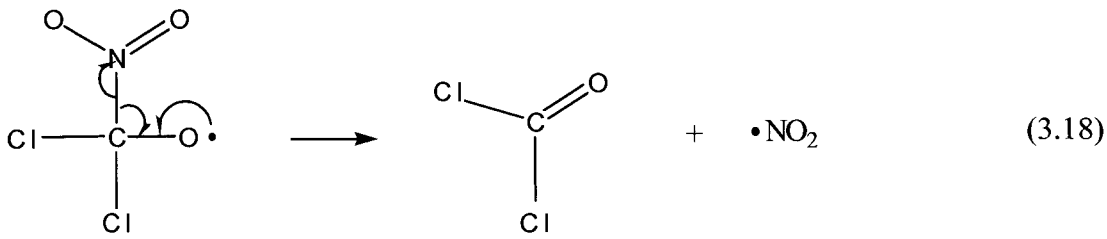

(3.18)

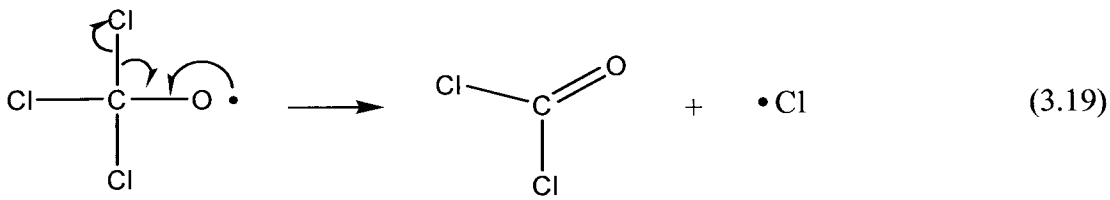

(3.19)

Phosgene is shown in both these reactions and represents an important pathway in the free radical mineralization of TCNM.

The NO_2^- formed in equation (3.8) would rapidly react with •OH and presented here as the average of seven values (Løgager and Sehested, 1993a; Barker *et al.,* 1970; Treinin and Hayon, 1970; Buxton 1969; Adams *et al.,* 1965; Adams and Boag, 1964):

$$\bullet OH + NO_2^- \rightarrow \bullet NO_2 + OH^-, \qquad k_{20} = 9.6 \times 10^9\ M^{-1}s^{-1} \tag{3.20}$$

The likely reaction of the $\bullet NO_2$ would be with the •OH leading to the formation of peroxynitrous acid (Løgager and Sehested, 1993a; Løgager and Sehested, 1993b; Merényi *et al.*, 1999)

$$\bullet OH + \bullet NO_2 \rightarrow ONOOH, \qquad k_{21} = (4.5 \pm 1.0) \times 10^9\ M^{-1}s^{-1} \tag{3.21}$$

$$ONOOH \rightleftharpoons ONOO^- + H^+ \tag{3.22}$$

As these HNMs are inorganic acids and assuming all ambient pH conditions of the experimentation are acidic, the pK_a was 6.5 to 6.8. Based on this condition, the solution would be mostly ONOOH (peroxynitrous acid) (Løgager and Sehested, 1993a; Løgager and Sehested, 1993b; Merényi *et al.,* 1999; Goldstein and Czapski, 1995; Pryor and

Squadrito, 1995). The mechanism for the (acid) hydrolysis of the ONOOH has been determined (Merényi *et al.,* 1999; Pryor and Squadrito, 1995; Kissner *et al.,* 1997) and reviewed in detail (Goldstein *et al.,* 2005):

$$OHOON \rightarrow NO_3^- + H^+ \qquad 70\% \qquad (3.23)$$

$$OHOON \rightarrow \bullet NO_2 + \bullet OH \qquad 30\% \qquad (3.24)$$

$$2\ \bullet NO_2 + H_2O \rightarrow NO_3^- + NO_2^- + H^+ \qquad (3.25)$$

$$NO_2^- + \bullet OH \rightarrow \bullet NO_2 + OH^-, \quad k_{20} = 9.6 \times 10^9\ M^{-1}s^{-1} \qquad (3.20)$$

The net reaction for the above mechanism was:

$ONOOH + H_2O \rightarrow H^+ + NO_3^-$ $\quad k_{26} = 1.25 \pm 0.05\ s^{-1}$ (Merényi *et al.,* 1999; Pryor and Squadrito, 1995; Kissner *et al.,* 1997; Goldstein *et al.,* 2005) (3.26)

All solutions in the experiment were unbuffered. Buffering would interfere with the results as it is generally known that with increasing radiation dose, the pH would have reduced (G) as identified in equation (3.1). Although at higher pH it was possible to have some NO_2^- formed, the lower the pH and thus the more complete the homolysis of ONOOH leads to only NO_3^- (Kissner *et al.,* 1997).

It is likely that the two radical products from equations (3.7) and (3.8) would also further react with •OH:

$$\bullet CCl_2NO_2 + \bullet OH \rightarrow HOCCl_2NO_2 \qquad (3.27)$$

$$HOCCl_2NO_2 \rightarrow COCl_2 + H^+ + NO_2^- \qquad (3.28)$$

$$\bullet CCl_3 + \bullet OH \rightarrow HOCCl_3, \quad k_{29} = 6.0 \times 10^9\ M^{-1}s^{-1} \text{ (Mönig } et\ al.,\ 1983) \qquad (3.29)$$

$$HOCCl_3 \rightarrow COCl_2 + H^+ + Cl^- \qquad (3.30)$$

The •Cl formed in the equation (3.19) might be expected to react as follows, where the forward and back reactions are summarized (McElroy *et al.,* 1990; Kláning and

Wolff, 1985; Cambron and Harris, 1995; Wu *et al.,* 1980; Yu *et al.,* 2004; Buxton *et al.,* 1998; Jayson *et al.,* 1973):

$$e_{aq}^- + \bullet Cl \rightarrow Cl^-, \qquad (k \text{ not reported}) \qquad (3.31)$$

$$\bullet Cl + Cl^- \rightarrow Cl_2^-\bullet, \quad k_{32} = (7.8 \pm 0.8) \times 10^9\ M^{-1}\ s^{-1} \quad \text{(Yu } et\ al.,\ 2004) \qquad (3.32)$$

$$k_{-32} = (5.7 \pm 0.4) \times 10^4\ s^{-1} \quad \text{(Yu } et\ al.,\ 2004) \qquad (-3.32)$$

$$Cl_2^-\bullet + H_2O \rightarrow \bullet ClOH^- + H^+ + Cl^-, \quad k_{33} < 100\ s^{-1} \quad \text{(Yu } et\ al.,\ 2004) \qquad (3.33)$$

$$\bullet Cl + \bullet Cl \rightarrow Cl_2, \qquad k_{34} = 8.8 \times 10^7\ M^{-1}s^{-1} \quad \text{(McElroy } et\ al.,\ 1990;$$

$$\text{Wu } et\ al.,\ 1980) \qquad (3.34)$$

$$\bullet Cl + H_2O \leftrightarrow \bullet ClOH^- + H^+, \quad k_{35} = (1.6 \pm 0.2) \times 10^5\ s^{-1} \quad \text{(Yu } et\ al.,\ 2004) \qquad (3.35)$$

$$k_{-35} = (2.6 \pm 0.6) \times 10^{10}\ M^{-1}s^{-1} \quad \text{(Yu } et\ al.,\ 2004) \qquad (-3.35)$$

$$\bullet ClOH^- \leftrightarrow \bullet OH + Cl^-, \quad k_{36} = (6.1 \pm 0.8) \times 10^9\ s^{-1} \quad \text{(Jayson } et\ al.,\ 1973) \qquad (3.36)$$

$$k_{-36} = (4.3 \pm 0.4) \times 10^9\ M^{-1}s^{-1} \quad \text{(Jayson } et\ al.,\ 1973) \qquad (-3.36)$$

The reaction of the e_{aq}^- and •Cl should proceed at diffusion controlled rates. The measurement of this reaction has eluded investigations. A rate of $5 \times 10^{10}\ M^{-1}s^{-1}$ was assumed for this reaction in the kinetic model. The rate of the radical-radical recombination of •Cl has been measured (McElroy *et al.,* 1990; Wu *et al.,* 1980) and has been determined a bimolecular reaction where the concentrations of the •Cl are relatively low. Therefore, it was not likely to be a major contributor to the loss of the •Cl. The reaction (3.34) might then contribute towards a competition with reaction (3.32). The reaction of the highly unstable $\bullet ClOH^-$ would proceed via hydrolysis, as identified in reaction (3.36) with the formation of •OH and Cl^-.

Initially the •OH reaction with the TCNM was ignored due to the relatively low reaction rate. It was possible to account for the disappearance of the TCNM, but it was

determined that the model did not predict the appearance of either the Cl^- or NO_3^- with reasonable accuracy. It was well known from other chlorinated methanes that the only reaction of the •OH is a H abstraction such as the case of $CHCl_3$ (Buxton *et al.*, 1988). Emmi *et al.* (1985) substantiated this case for CH_2Cl_2, and CCl_4 where there is no reaction. Two possible reactions were then conceived for TCNM:

$$TCNM + \bullet OH \rightarrow CCl_3OH + \bullet NO_2 \quad (3.37)$$

$$TCNM + \bullet OH \rightarrow \bullet CCl_3 + ONOOH \quad (3.38)$$

Reaction (3.37) does not seem likely as a candidate for primary reactivity because the •OH is an electrophile and would favor attack on the NO_2 moiety as evidenced in reaction (3.38). Therefore, the following mechanism was proposed for this reaction:

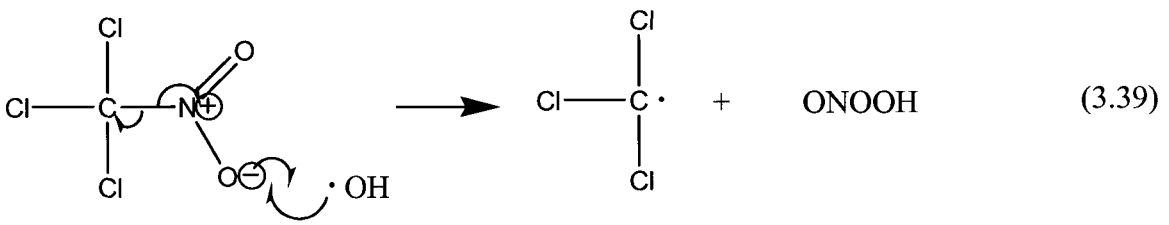

(3.39)

Bimolecular reaction rates of the TCNM and the hydrogen atom (H•) were not evaluated. However, with a molecule such as TCNM, it was apparent that it could react to give the anions:

$$TCNM + H^\bullet \rightarrow \bullet CCl_2NO_2 + H^+ + Cl^- \quad (3.40)$$

$$TCNM + H^\bullet \rightarrow \bullet CCl_3 + H^+ + NO_2^- \quad (3.41)$$

An investigation was made to find a similar case for the reactivity of the hydroxyl radical and the carbon centered halogenated compound. It was noted that the •OH is generally unreactive with CCl_4. More importantly, it was found that the reaction of $H^\bullet$ will react with CCl_4 at rate constant ranging from 3.2 to 4.4 ($\times 10^7$) $M^{-1}s^{-1}$ and result in the liberation of a Cl^- ion (Neta *et al.*, 1971; Köester and Asmus, 1971). Recently, it was

shown that $H^{\bullet}$ reacted with dichloroethanes to give exclusively Cl^- in aqueous solution (Pimblott *et al.,* 2005). The precedence for reaction (3.41) was found in the reaction of $H^{\bullet}$ liberating the nitro-moiety in the reaction rate of tetranitromethane at a range from 5.5 to 26 ($\times 10^8$) $M^{-1}s^{-1}$ (Rabani *et al.,* 1965; Asmus *et al.,* 1964a). Thus, a second reductive destruction pathway for the loss of TCNM by $H^{\bullet}$ was added to the reaction mechanism. These reactions (3.40) and (3.41) were added into the model at estimated rates of $1.0 \times 10^7\ M^{-1}s^{-1}$.

The mechanism described above for the destruction of TCNM was coded into a kinetic computer model (MAKSIMA-CHEMIST) and used to simulate the ^{60}Co irradiation (Carver *et al.,* 1979; Gear, 1971; Schwarz, 1962). The program was based on classical stiff equations which follow fast reaction transients in small integration steps. The program utilizes Gear algorithms (Gear, 1971) to produce error controlled step size equations combined with order selection, and sparse algorithms for evaluation of the Jacobian matrix as the predictor corrector equation (Carter *et al.*, 1979).

The initial computer simulations included e_{aq}^- reactions with the TCNM, reactions with O_2, and the reaction byproducts from reactions (3.7) through (3.36) in Table 3.2. This formulation was unable to account for the appearance of the Cl^- and NO_3^- with any accuracy. The reaction for the •OH with TCNM was included in the reaction mechanisms and the model over-predicted the removal of TCNM. It was found that the formation of the two anions, Cl^- and NO_3^- fit the data much better than previous attempts. An intermediate reaction was added, equation (-3.38), to establish continuity of the hydroxyl radical reaction with TCNM. In addition to the •OH, it was necessary to include a contribution of the $H^{\bullet}$.

Table 3.2. Linearized reaction mechanism for the free radical destruction of TCNM.
Rates identified by * are estimates based on model fit of the data from this study. (Continued on Page 78)

Eqn.	Reactions	k (L $M^{-1}s^{-1}$)	Reference
3.7	TCNM + e_{aq}^- → $\bullet CCl_2NO_2$ + Cl^-	1.07×10^{10}	This work
3.8	TCNM + e_{aq}^- → $\bullet CCl_3$ + NO_2^-	1.07×10^{10}	This work
3.9	TCNM + e_{aq}^- → CCl_3^- + $\bullet NO_2$	1.00×10^{1}	This work
*3.10	$\bullet CCl_2NO_2$ + O_2 → $\bullet OOCClNO_2$	3.0×10^{9}	This work
3.11	$\bullet CCl_3$ + O_2 → $\bullet OOCCl_3$	3.3×10^{9}	(Mönig *et al.*, 1983)
*3.12	CCl_3^- + O_2 → $^-OOCCl_3$	1.0×10^{9}	(Mönig *et al.*, 1983)
*3.13	$^-OOCCl_3$ + → $COCl_2$ + OCl^-	10^6 (s^{-1})	This work
*3.16	$\bullet OOCCl_2NO_2$ + $\bullet OOCCl_2NO_2$ → $2\bullet OCCl_2NO_2$ + O_2	3.0×10^{9}	This work
*3.16	$\bullet OOCCl_3$ + $\bullet OOCCl_3$ → $2\bullet OCCl_3$ + O_2	3.0×10^{9}	This work
*3.18	$\bullet OCCl_2NO_2$ + → $COCl_2$ + $\bullet NO_2$	10^6 (s^{-1})	This work
*3.19	$\bullet OCCl_3$ + → $COCl_2$ + $\bullet Cl$	10^6 (s^{-1})	This work
	$COCl_2$ + H_2O → CO_2 + $2H^+$ + $2Cl^-$	9 (s^{-1})	(Mertens *et al.*, 1994)

Table 3.2. Linearized reaction mechanism for the free radical destruction of TCNM.
Rates identified by * are estimates based on model fit of the data from this study. (Continued on Page 79)

Eqn.	Reactions	k (L $M^{-1}s^{-1}$)	Reference
3.20	$\bullet OH + NO_2^- \rightarrow OH^- + \bullet NO_2$	9.6×10^9	(Løgager and Sehested, 1993a) (Barker *et al.*, 1970) (Treinin and Hayon, 1970) (Buxton, 1969) (Adams *et al.*, 1965)
3.21	$\bullet OH + \bullet NO_2 \rightarrow ONOOH$	4.5×10^9	(Løgager and Sehested, 1993a) (Løgager and Sehested, 1993b) (Merényi *et al.*, 1999)
3.26	$ONOOH + H_2O \rightarrow H^+ + NO_3^-$	1.25 (s^{-1})	(Pryor and Squadrito,1995) (Kissner *et al.*, 1997) (Goldstein *et al.*, 2005)
*3.27	$\bullet CCl_2NO_2 + \bullet OH \rightarrow HOCCl_2NO_2$	6.0×10^9	This work
*3.28	$HOCCl_2NO_2 \rightarrow COCl_2 + H^+ + NO_2^-$	1.0×10^6 (s^{-1})	This work
3.29	$\bullet CCl_3 + \bullet OH \rightarrow CCl_3OH$	6.0×10^9	(Mertens *et al.*, 1994)
3.30	$CCl_3OH \rightarrow COCl_2 + H^+ + Cl^-$	1.0×10^6 (s^{-1})	(Mertens *et al.*, 1994)

Table 3.2. Linearized reaction mechanism for the free radical destruction of TCNM.
Rates identified by * are estimates based on model fit of the data from this study. (Continued from page 78)

Eqn.	Reactions	k (L $M^{-1}s^{-1}$)	Reference
3.31	$e_{aq}^- + \bullet Cl \rightarrow Cl^-$	5.0×10^{10}	(Buxton *et al.*, 1988)
3.32	$\bullet Cl + Cl^- \rightarrow Cl_2^-\bullet$	7.8×10^9	(Yu *et al.*, 2004)
−3.32	$Cl_2^-\bullet \rightarrow \bullet Cl + Cl^-$	5.7×10^4 (s^{-1})	(Yu *et al.*, 2004)
3.33	$Cl_2^-\bullet + H_2O \rightarrow \bullet ClOH^- + H^+ + Cl^-$	< 100 (s^{-1})	(Yu *et al.*, 2004)
3.34	$\bullet Cl + \bullet Cl \rightarrow Cl_2$	8.8×10^7	(McElroy, 1990)
3.35	$\bullet Cl + H_2O \rightarrow \bullet ClOH^- + H^+$	1.6×10^5 (s^{-1})	(Yu *et al.*, 2004)
−3.35	$\bullet ClOH^- + H^+ \rightarrow \bullet Cl + H_2O$	2.1×10^{10}	(Jayson *et al.*, 1973)
3.36	$\bullet ClOH^- + \bullet OH \rightarrow Cl^-$	6.1×10^7	(Jayson *et al.*, 1973)
−3.36	$\bullet OH + Cl^- \rightarrow \bullet ClOH^-$	4.3×10^9	(Jayson *et al.*, 1973)
3.38	TCNM + $\bullet OH \rightarrow$ Intermediate	4.84×10^7	This work
−3.38	Intermediate + TCNM $\rightarrow \bullet OH$	1.0×10^6	This work
*3.39	Intermediate + $\rightarrow \bullet CCl_3 + ONOOH$	1.0×10^5	This work
*3.40	TCNM + $H^\bullet \rightarrow \bullet CCl_2NO_2 + H^+ + Cl^-$	1.0×10^7	This work
*3.41	TCNM + $H^\bullet \rightarrow \bullet CCl_3 + H^+ + NO_2^-$	1.0×10^7	This work

With the addition of both the •OH and $H^{\bullet}$, the model over predicted the destruction of TCNM. Changes were then made in the mechanism through sequential changes in the intermediate reaction rate constants. The estimated kinetic constants presented in Table 3.2 resulted in no improvement to the model's predictive capability for TCNM elimination. The model revealed that equation (3.9) was not important in describing the results and the reaction rate was reduced to essentially zero. It was reasoned that the addition of •OH to TCNM could lead to an intermediate that is stabilized prior to collapsing to products. If this intermediate does exist, then it could either proceed to the products indicated in equation (3.39), or go in the reverse direction to the starting reactants resulting in a partial equilibrium. Therefore, the equation was written in the model to provide for these two branches, the formation of the intermediate at the measured rate, with a ratio of 10:1 of the intermediate returning to the starting reactant $k = 1.0 \times 10^{6}\ s^{-1}$ and going to products $k = 1.0 \times 10^{5}\ s^{-1}$.

The MAKSIMA-CHEMIST model was revised to include the kinetic mechanism and the HNM rate constants determined in this study. The results of the kinetic model are presented in Table 3.3 along with the experimental results for comparison. The modeled TCNM mass production results ranged from 18.3% to 48.9% difference from experimental to model. The largest percent difference (48.9%) for TCNM ion production occurred at the higher applied dose. This larger difference was expected at the region of highest dose and lower value of HNM concentration. The modeled chloride and nitrate ions production ranged from 3.3% to 36% difference from experimental to modeled results. The largest percent difference (36%) occurred for the production of ions (Cl^{-} and NO_3^{-}) in the region where it was the smallest dose and highest concentration of HNM.

The highest difference occurred where the mechanistic model simulation would exhibit the lowest numerical value for reactions indicating full mineralization at the highest radiation dose. It was believed that the overall success of the mechanism would be demonstrated for the initial reactions at the lowest dose. The lowest dose would contribute to the largest difference in results as the mechanism is highly sensitive to those intermediate reactions in the short exposure time periods. Based on the results obtained from the model for simulating the lowest dose and TCNM removal, the difference noted appeared to be reasonable and generally followed the TCNM degradation indicated by experimental results.

Table 3.3. Comparison of experimental and model results for ^{60}Co irradiation of TCNM solutions (1.13 mM) in pure water at doses up to 8.54 kGy.

	Experimental			Model		
Dose (kGy)	[TCNM] (mM)	[Cl^-] (mM)	[NO_3^-] (mM)	TCNM (mM)	[Cl^-] (mM)	[NO_3^-] (mM)
0	1.13	0.00	0.00	1.13	0.00	0.00
1.22	0.80	0.92	0.29	0.67	1.33	0.42
2.44	0.42	1.67	0.44	0.36	1.99	0.60
3.66	0.17	2.17	0.58	0.11	2.56	0.77
6.1	NM[a]	2.73	0.79	[c]	2.82	0.85
8.54	BMDL[b]	3.13	0.89	[c]	2.82	0.85

[a] Not measured.
[b] Below method detection limit.
[c] Modeled data is below detection limit.

The results of the final kinetic model are presented graphically in Figure 3.5 and Figure 3.6 with the experimental results for comparison. The kinetic model closely follows the production of residual byproducts and TCNM degradation.

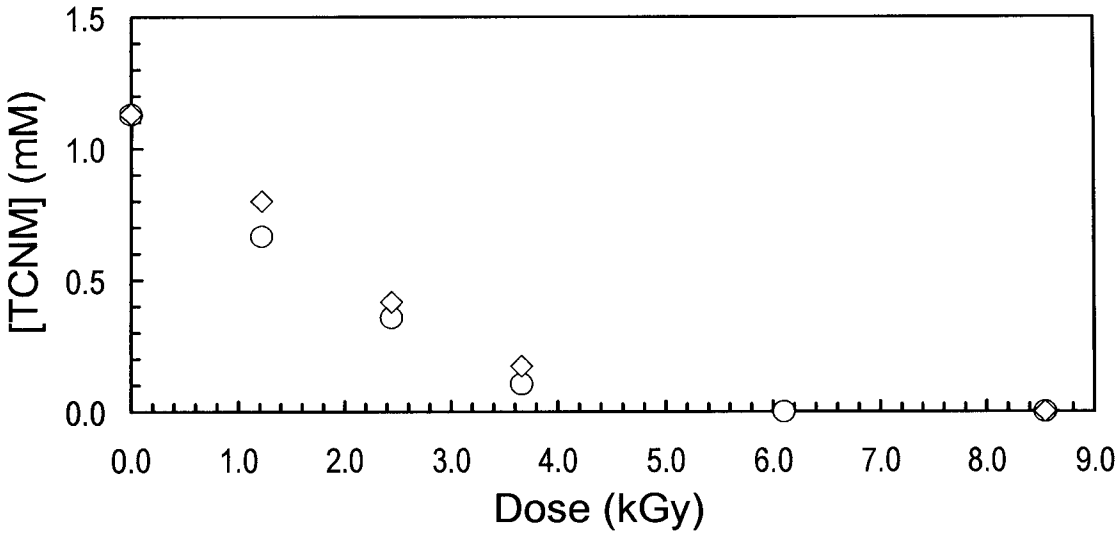

Figure 3.5. Comparison of experimental (◇) and modeled (○) data for ^{60}Co irradiated trichloronitromethane. $[TCNM]_0$ = 1.13 mM.

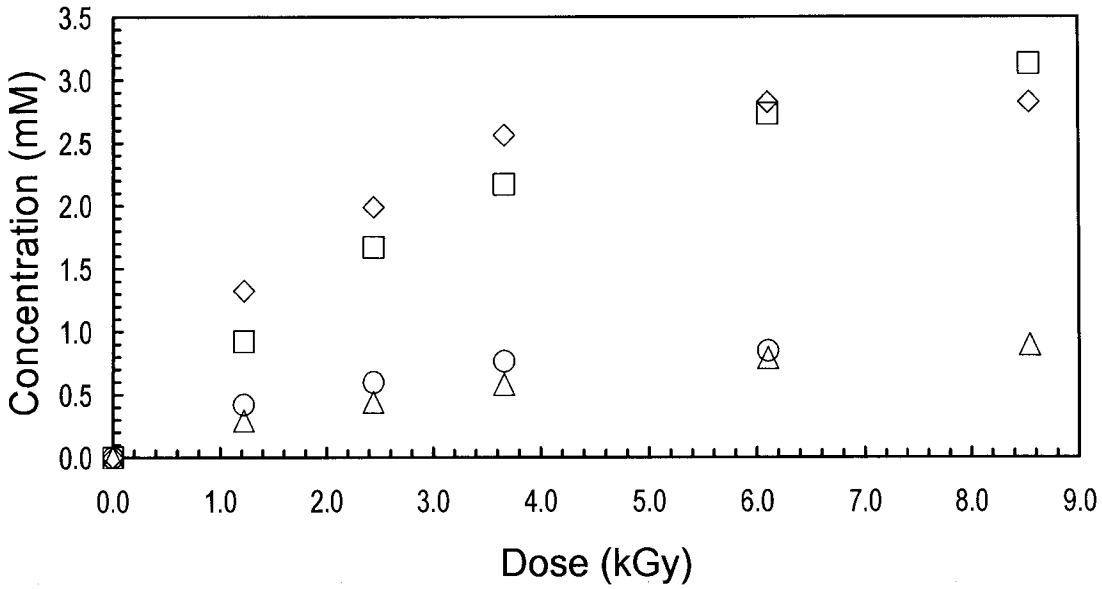

Figure 3.6. Concentration of chloride ions from (□) experimental results, and (◇) model results; and nitrate ions (△) experimental results, and (○) model results; versus dose ^{60}Co irradiation.

3.4. Summary

The kinetic model over predicted the removal of the TCNM and slightly under predicted the appearance of the two anion products, Cl^- and NO_3^-. The kinetic model was a reasonable representation of the experimental results for both the production of the residual ions in solution and for the degradation of TCNM. It was observed that the model overestimates the degradation of TCNM at lower dose owning to minor inaccuracy in the model. It also showed that both peroxynitrous acid and phosgene, potentially toxic byproducts, were formed but even with the high initial concentrations of TCNM (mM level of concentration), neither of these compounds were ever greater than 5 nM. At lease low concentrations, it would be difficult to ascertain their specific concentration. In addition, these byproducts would be found only at doses less than 3.66 kGy indicating a larger dose was to be eventually applied and their fate would be full elimination for ultimate TCNM mineralization at 6 kGy.

4. THE FREE RADICAL CHEMISTRY OF BROMONITROMETHANE: RATE CONSTANTS AND DEGRADATION MECHANISM BY OXIDATION-REDUCTION REACTIONS

4.1. Introduction

In the United States, all drinking water must be disinfected before it enters the water distribution system and is ultimately consumed by the general public. Common drinking water disinfectants include chlorine gas, ozone, chloramines, chlorine dioxide, sodium hypochlorite, or a combination of these. However, studies have found that using chlorine as a primary disinfectant may result in the production of multiple disinfection-by-products (DBPs), from the oxidation of dissolved organic matter (Rook, 1974; Krasner *et al.,* 1996). The oxidation of waters with naturally occurring levels of bromide with ozone have been found to form brominated forms of DBPs (von Gunten and Hoigné, 1996) and these halogenated compounds are regulated by the U.S. Environmental Protection Agency with a maximum concentration for bromate of 10 $\mu g\ L^{-1}$ (U.S. Environmental Protection Agency, 1997).

One emerging class of DBPs is the brominated halonitromethanes (HNMs). These contaminant chemicals are produced when chlorine (Thibaud *et al.,* 1988) or ozone (Hoigné and Bader, 1998; Richardson, 2003) are used at drinking water treatment facilities with source waters containing bromide and natural organic matter, and are of major concern as they have been shown to be cytotoxic and genotoxic (Meier, 1988; Plewa *et al.,* 2000). Naturally occurring bromide in water reacts with ozone (Richardson *et al.,* 2003) and produces brominated byproducts such as tribromonitromethane

(bromopicrin) (U.S. Environmental Protection Agency, 1999). Other brominated forms of HNMs (tribromonitromethane, dibromonitromethane, and bromodichloronitromethane) were found at 2.5, 1.5, and 0.7 $\mu g\ L^{-1}$, respectively, in finished water from a California drinking water treatment plant that used pre-ozonation and post-chlorine/chloramine disinfection on a high-bromide source water (0.14 $mg\ L^{-1}$) (Chen *et al.,* 2002).

The purpose of this study was to assess the potential of free radical chemistry to degrade bromonitromethane (BNM) in water. To assure that any treatment by advanced oxidation processes (AOPs) occurs efficiently and quantitatively, a full understanding of the radiation chemistry involved under the conditions of use was necessary. This in turn requires that absolute rate constants, and destruction mechanisms, are well understood. This study determined the rate constants for hydroxyl radical and hydrated electron reaction with HNM in water as well as steady state irradiation to identify and quantify the stable products of these reactions. Bromonitromethane (CH_2BrNO_2) was obtained from Aldrich at 90% to 95% purity and re-purified using vacuum distillation to greater than 99% purity as indicated by nuclear magnetic resonance spectroscopy.

Both the linear accelerator and ^{60}Co γ-irradiations produce •OH, e_{aq}^- , and •H as well as some molecular products according to equation (1.1) (Buxton, 2004) and considered as condition for steady state irradiation.

4.2. Rate Constant Determination

The determination of the rate constant for reaction of e_{aq}^- with BNM required isolation of the hydroxyl radical reaction. Aqueous solutions were pre-saturated with N_2O, which quantitatively converts the solvated electron, e_{aq}^- to this radical:

$$e^-_{aq} + N_2O + H_2O \rightarrow N_2 + OH^- + \bullet OH \qquad (4.2)$$

at a fast rate constant of $k_2 = 9.1 \times 10^9$ $M^{-1}s^{-1}$ (Janata and Schuler, 1982). In the kinetics experiments, the hydroxyl radical reaction with bromonitromethane did not give any significant transient absorbance over the range 250 to 800 nm, and so this rate constant was determined using SCN^- competition kinetics based on the competing reactions:

$$\bullet OH + BNM \rightarrow \text{Products} \qquad (4.3)$$

$$\bullet OH + SCN^- (+ SCN^-) \rightarrow OH^- + (SCN)_2^{\bullet -} \qquad (4.4)$$

This competition can be analyzed to give the following expression:

$$\frac{[(SCN)_2^{\bullet -}]_o}{[(SCN)_2^{\bullet -}]} = 1 + \frac{k_3[BNM]}{k_4[SCN^-]} \qquad (4.5)$$

where, $[(SCN)_2^{\bullet -}]_o$ is the final yield of $(SCN)_2^{\bullet -}$ measured for only the SCN^- solution, and $[(SCN)_2^{\bullet -}]$ is the reduced yield of this transient when bromonitromethane is added. Therefore a plot of $1/[(SCN)_2^{\bullet -}]$ against the ratio $[BNM]/[SCN^-]$ should give a straight line of slope k_3 / k_4. From the known rate constant of $k_4 = 1.05 \times 10^{10}$ $M^{-1}s^{-1}$ (Janata and Schuler, 1982), the k_3 rate constant can then be calculated. Typical kinetic data obtained at 475 nm are graphically presented in Figure 4.1.

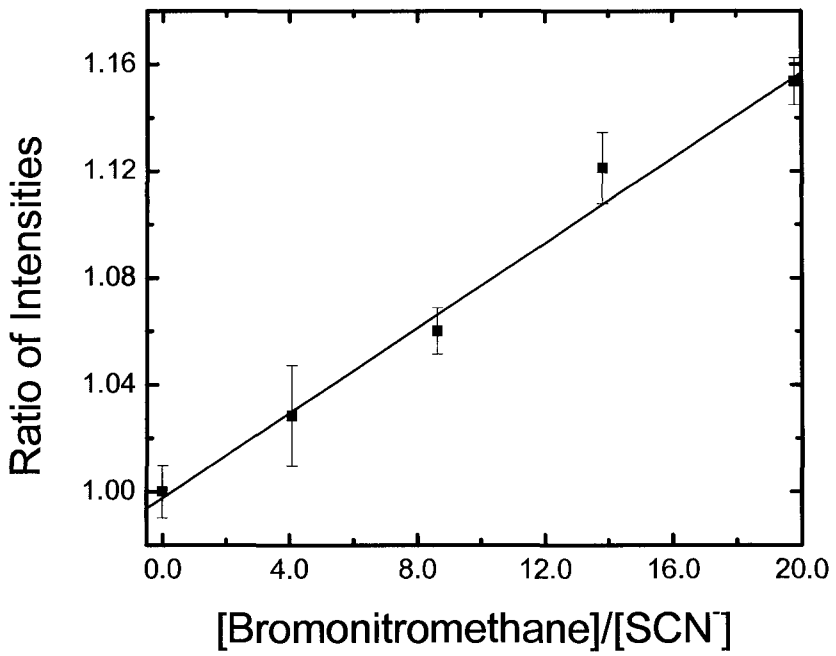

Figure 4.1. Competition kinetics plot for •OH reaction with bromonitromethane using SCN^- as a standard. The solid line is a weighted linear fit, corresponding to a slope of 0.00796 ± 6.3×10^{-4}. A second-order rate constant for bromonitromethane reaction was derived where, $k_3 = (8.36 \pm 0.49) \times 10^7\ M^{-1}s^{-1}$.

The rate constant for the hydroxyl radical reaction with calculated to be $k_3 = (8.36 \pm 0.49) \times 10^7\ M^{-1}s^{-1}$. No comparative rate constants for bromonitromethane could be found from a survey of the open literature.

The rate constant for bromonitromethane reaction with the hydrated electron rate constant was determined by directly following the absorption of the e^-_{aq} at 700 nm (Janata and Schuler, 1982). These solutions were saturated with nitrogen gas, to remove dissolved oxygen, and also contained 0.50 M *tert*-butanol to scavenge the hydroxyl radicals and hydrogen atoms and convert these highly reactive radicals into the less-reactive tert-butyl alcohol radical, and thus isolating the reducing radical:

$$^{\bullet}OH/H^{\bullet} + (CH_3)_3COH \rightarrow H_2O/H_2 + {}^{\bullet}CH_2(CH_3)_2COH \qquad (4.6)$$

The decay of the hydrated electron was found to be first-order, and to be faster with higher concentrations of bromonitromethane. By fitting exponential decays to the pseudo-first-order kinetics, the kinetic data shown in Figure 4.2 were obtained. The fitted second-order rate constant gave a reaction rate constant for this reduction process of $k = (3.13 \pm 0.03) \times 10^{10}\ M^{-1}s^{-1}$.

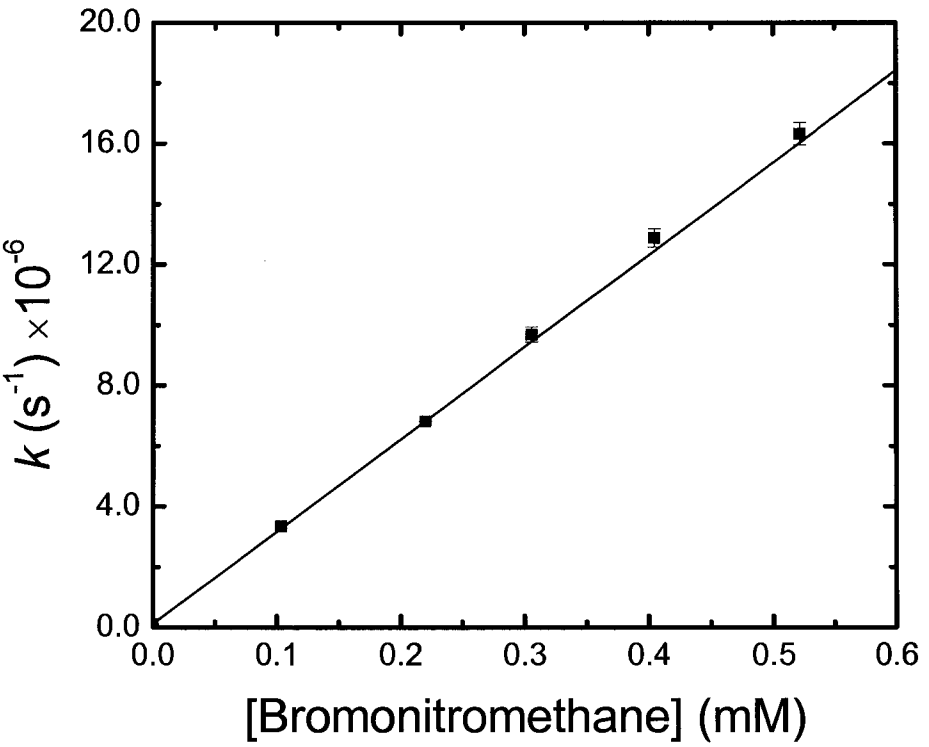

Figure 4.2. Second-order rate constant for the reaction of hydrated electron with bromonitromethane. Single-point error bars are one standard deviation, as determined from the average of at least three kinetic traces. Solid line indicates the weighted linear fit with rate constant of $k = (3.13 \pm 0.03) \times 10^{10}\ M^{-1}s^{-1}$.

As observed by the comparison of the hydroxyl and hydrated radical rate constants, the reduction of this chemical by e^-_{aq} was much faster than its oxidation by •OH. This

reduction is expected to produce the bromide ion, along with the corresponding carbon-centered radical and a nitrate ion by:

$$e_{aq}^- + BrH_2CNO_2 \rightarrow Br^- + H_2{}^{\bullet}CNO_2 \quad (4.7)$$

$$e_{aq}^- + BrH_2CNO_2 \rightarrow BrH_2C + NO_2^- \quad (4.8)$$

To determine the ultimate chemical products produced in the radiolytic destruction of bromonitromethane, steady state ^{60}Co irradiations were performed in this study. These irradiations were conducted for various concentrations of bromonitromethane in aerated water with a dissolved oxygen concentration of 2.00×10^{-4} M, ambient pH and room temperature. Under these conditions, destruction of this chemical occurred by both the oxidation and reduction pathways. Figure 4.3 shows that with increasing applied dose, the concentration of bromonitromethane decreased continuously to zero at a dose of approximately 6 kGy as interpolated from the concentration-dose curve. This removal process was found to be approximately first-order as presented in Figure 4.2. Bromide and nitrate ions were produced concomitant with bromonitromethane removal. Of interest is the observation that the yields of these two ions are very similar and this observation is graphically depicted in Figure 4.3. The production of ions as shown in Figure 4.3 indicates a suggested reaction mechanism releasing the halogen ion and nitrate ion according to equations (4.7) and (4.8).

The determination of the rate constant and degradation mechanism was necessary for application of free radical AOP treatment of BNM. A plot of the BNM concentration in the post irradiated solution of water to the dose rate is graphically presented in Figure 4.4. This graph quantitatively provides the dose constant (k_D) at 0.74 kGy^{-1} and was based on

pure water at ambient room temperature. This dose constant can be applied to large scale electron beam for free radical AOP degradation of BNM.

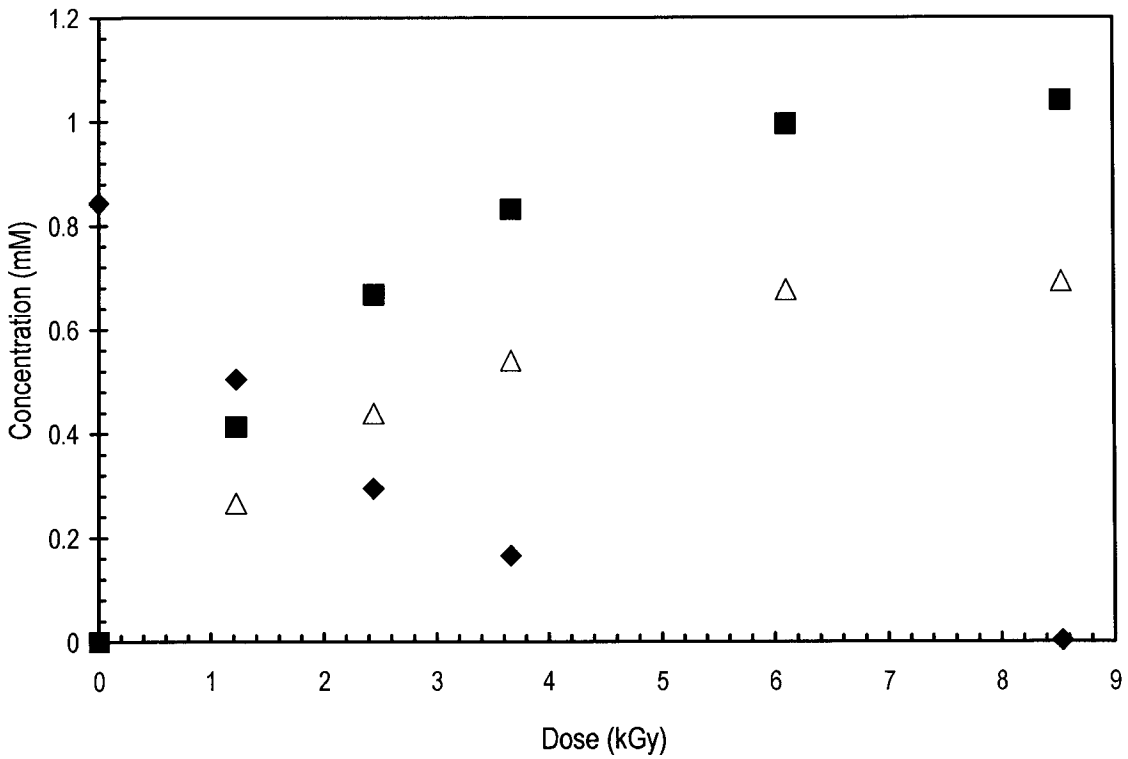

Figure 4.3. Comparison of irradiated bromonitromethane and byproducts of irradiation. Bromonitromethane (◆), and byproducts of bromide ion (■), nitrate ion (△) versus total dose. Dose rate of ^{60}Co at 122 Gy $min.^{-1}$ at ambient pH.

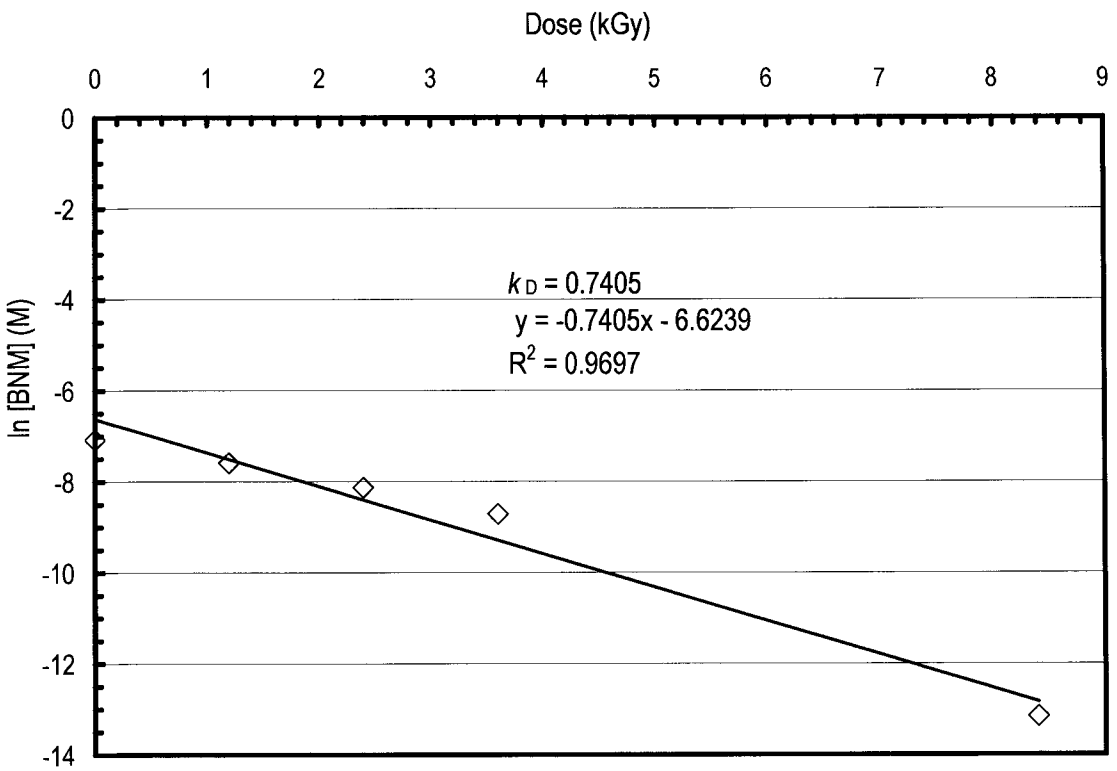

Figure 4.4. Steady state irradiated bromonitromethane concentration (◇) versus dose. Dose constant, $k_D = 0.74\ kGy^{-1}$.

4.3. Mechanism

In aerated solution, this de-halogenated radical is expected to first react with dissolved oxygen:

$$H_2{}^{\bullet}CNO_2 + O_2(g) \rightarrow {}^{\bullet}OOCH_2NO_2 \quad (4.7)$$

This peroxyl radical is not very reactive, its major fate is to dimerize:

$$2\ {}^{\bullet}OOCH_2NO_2 \rightarrow O_2NCH_2OOOOCH_2NO_2 \quad (4.8)$$

The tetroxide formed as an intermediate and the suggested fate was to break into smaller, oxygen containing compounds that ultimately yields halogen ions and nitrate.

4.4. Summary

Absolute rate constants for the reaction of the hydroxyl radical and hydrated electron were determined for bromonitromethane in water, using electron pulse radiolysis and transient absorption spectroscopy. Values of hydrated electron rate constant, $k = (3.13 \pm 0.03) \times 10^{10}$ $M^{-1}s^{-1}$ and hydroxyl radical rate constant, $k = (8.36 \pm 0.49) \times 10^{7}$ $M^{-1}s^{-1}$, were measured. Steady state ^{60}Co irradiations revealed that the radiolytic removal of bromonitromethane was approximately first order, with concomitant formation of both the bromide and nitrate ions. The dose constant for radiolysis of BNM was identified and the data could be applied at large scale.

.

5. OVERVIEW OF REACTION MECHANISMS AND KINETIC MODELING: THE FREE RADICAL CHEMISTRY AND REACTION MECHANISMS FOR HALONITROMETHANES

5.1. Introduction

The effectiveness for free radical AOP treatment of DBP pollutants in water was based on an understanding of mechanisms and the reduction-oxidation reactions occurring in the water matrix. The free radical chemistry of hydroxyl radical and the aqueous electron has been investigated for elimination of many types of pollutants and these studies provide favorable results indicating satisfactory removal of both organic and inorganic compounds (Cooper and Cadavid, 1993; Cooper *et al.,* 1993; Cooper *et al.,* 1996a; Cooper *et al.,* 1996b; Cooper *et al.,* 2001; Cooper *et al.,* 2002a; Cooper *et al.*, 2002b; Cooper *et al.,* 2004). One DBP pollutant recently identified as a concern is the halogenated nitromethanes (HNMs). These HNMs are derived from chlorine, bromine, carbon-nitro based groups and are formed by the disinfection of water using very strong oxidizing agents such as ozone, chlorine and chloramines. Nine HNM compounds were recently identified (Richardson *et al.,* 1999) in drinking water as a DBP and are believed to be a health concern (Plewa *et al.,* 2004).

Experimental investigations were performed to identify the efficacy for removal of halonitromethanes from water using free radical chemistry under steady state irradiation conditions. The experimental work included four primary components and these must be satisfied prior to identification of the treatment parameters at large scale. The four research components included determination of rate constants for degradation of the

HNMs using pulse radiolysis, identification and quantification of the residual byproducts produced by irradiation of HNMs, elucidation of a degradation mechanism, and confirmation of the degradation mechanism by mass action kinetic computer modeling that incorporates both the rate constants and mechanism. Once the suitability for use of free radical chemistry was confirmed, the data was evaluated to identify the general parameters for a large scale electron beam AOP treatment facility. Based on the experimental results obtained determined in the four research components, free radical AOP for elimination of HNMs was determined viable.

This work summarizes previous HNM experimental work and presents data needed for sizing a large scale AOP electron beam facility. To fully explore use of AOP treatment for HNMs, an understanding and a measure of the magnitude for the large scale AOP was needed. This development required an understanding of the radiation dose needed for mineralization of HNMs and the energy to attain this dose. The energy level was related to a unit energy cost expressed as electrical energy per order (EE/O). This large scale AOP treatment EE/O was exclusive of operation, maintenance, and support facilities as these parameters vary widely.

5.2. Rate Constant

Mineralization of the molecular structure of compounds into their primary ionic components and to their most stable carbon based form as found in aqueous solution was the objective for application of free radicals to HNMs. Determination of free radical rate constants for the hydroxyl radical and hydrated electron with HNM was essential towards the ultimate development of mechanism pathways leading to HNM mineralization.

Based on the rate constants obtained in pulse radiolysis experiments, the free radicals met this objective to mineralize the HNM molecular compound and the experimental work provided a unique rate constant value for each HNM. All reactants were considered distributed homogeneously in the water medium. The rate constants were obtained for the reactants, •OH and e_{aq}^- independently with HNM. Competition kinetics was applied for rate constant determination of •OH with HNM and the reaction rate constants for e_{aq}^- reaction with HNMs were obtained by direct measurement of absorption. It was possible from this work to isolate a bimolecular reaction in each case and study the reaction as a single transient with itself (Matheson and Dorfman, 1969).

No HNM free radical rate constants could be found in the open literature. Other reported HNM rate constants that were found but not applicable to this work include those reported by Porter *et al.* (2000) for bromonitromethane at (pH 5.0) with $k = 0.0365$ $M^{-1}s^{-1}$ determined for the reaction with glucose oxidase substrate, and those rate constants identified by Carter *et al.* (1997) for atmospheric photodecomposition of trichloronitromethane.

As a measure of comparison, the rate constants for these HNM reactions were found consistent with other rate constants of halogenated compounds in aqueous solution. A search of the literature for analogous reactions showed that a decreased rate constant for fully halogenated compounds was observed in the hydrated electron reduction of chlorinated ethanes and methanes (Buxton *et al.,* 1988). However, for both series of halogenated organic compounds, there was first a consistent increase in the measured rate constant with the number of chlorine atoms. This was not the case for those observations made of the halonitromethanes in this study. The change in rate constant for the hydrated electron

reaction with chloromethane 1.1×10^9 $M^{-1}s^{-1}$ (Balkas *et al.,* 1970), dichloromethane 5.45×10^9 $M^{-1}s^{-1}$ and 6.3×10^9 $M^{-1}s^{-1}$ (Balkas *et al.,* 1972), and trichloromethane 1.38×10^{10} $M^{-1}s^{-1}$ (Tobien *et al.,* 2000); 3.0×10^{10} $M^{-1}s^{-1}$ (Hart and Anbar, 1964) was fairly linear with number of chlorine atoms. This rate constant then drops by about 30% to 50% for hydrated electron reaction with carbon tetrachloride and the rate constant values generally range from $(1.3 \text{ to } 2.4) \times 10^{10}$ $M^{-1}s^{-1}$ (Buxton *et al.,* 1988).

The analogous literature data for the brominated compounds was much more scattered, with no consistent trends evident (Mezyk *et al.,* 2005). No hydrated electron reaction rate constant for bromomethane or tetrabromomethane was found in the literature, and the value for dibromomethane 2.0×10^{10} $M^{-1}s^{-1}$ (Hayes *et al.,* 1989) splits the two values reported for tribromomethane 1.0×10^{10} $M^{-1}s^{-1}$ (Lal and Mahal, 1992), and 2.6×10^{10} $M^{-1}s^{-1}$ (Tobien *et al.,* 2000).

The literature data for the hydrated electron reaction with the mixed halogenated methanes such as bromodichloromethane 2.1×10^{10} $M^{-1}s^{-1}$ and chlorodibromomethane 2.0×10^{10} $M^{-1}s^{-1}$ (Tobien *et al.,* 2000) suggests that the type of halogen substitution does not significantly affect the rate constant for this process. This condition was in agreement with the observed data for the HNMs. In addition, the analogous rate constants for nitromethane 2.2×10^{10} $M^{-1}s^{-1}$ (Wallace and Thomas, 1973) and tetranitromethane 4.6×10^{10} $M^{-1}s^{-1}$ (Rabani *et al.,* 1965) shows that the nitro group significantly activates this substituted methane, again consistent with the HNM rate constants being faster than the analogous halogenated methanes. The one available rate constant for the hydrated electron reaction with trichloroacetonitrile 3.2×10^{10} $M^{-1}s^{-1}$ (Lal *et al.,* 1988) is similar to HNM

values in this research, indicating the cyanide group also activates a substituted methane significantly (Mezyk *et al.*, 2005).

The reaction of the hydrated electron with halogenated compounds was believed to exhibit release of a halogen in the free radical reaction. These typical reactions involving e_{aq}^- and a release of a halogen ion were widely noted in the literature. Wu *et al.* (1980) identified the release of the chloride ion by reaction of the e_{aq}^- with an aqueous halide solution at a bimolecular rate constant of $(1.49 \text{ to } 7.12) \times 10^{-4}$ s^{-1}. The release of bromide ion by interaction of e_{aq}^- was established by Siddiqui *et al.* (1996) in the reduction of BrO^- at 2.0×10^{-4} s^{-1}. Matheson *et al.* (1966) established the rate constant for reaction of e_{aq}^- with aqueous KBr solution with the release of Br_2^- $(1.3 \pm 0.5) \times 10^{-4}$ $M^{-1}s^{-1}$. Lal *et al.* (1986) established a rate constant of 2.8×10^{-4} s^{-1} for the bromide radical release from 1, 2-dibromoethane for the reaction with the e_{aq}^-. These reactions indicated a cleavage of the halogen ion from the parent compound.

The reaction rate of the hydroxyl radical with halogenated compounds was notably slower when compared to e_{aq}^- reactions. The HNM experiments were conducted at ambient pH with no buffering. One explanation for the slower hydroxyl reaction was the inability of the radical to abstract ions from the HNM molecule. At the molecular level, no high potential valence sites predominate on HNM to initiate rapid degradation by the hydroxyl radical. This condition could change with lower pH of the solution. Matheson *et al.* (1966) indicated that the interaction of the hydroxyl radical with bromine ion increases at low pH and decreases markedly at high pH. Therefore, the ambient pH condition of HNM solutions was not expected to markedly affect the brominated HNMs

release of a Br^- from interaction with the hydroxyl radical. Upon release of the Br^- to solution, the ion was noted to involve additional intermediate steps as Zehavi and Rabani, (1972) reported that the reaction of Br^- in solution was not a simple electron transfer reaction, but transfers to an intermediate $BrOH^-$, and then another electron change, with a possible end point being a reversible reaction. Attempts were made in the mechanism to adjust the ion reaction mechanism to account for these intermediate steps and reversible reactions. These reversible reactions were subsequently removed from the model without affecting the results.

The second-order rate constants obtained for HNMs using pulse radiolysis methods clearly reflect continuity with similar published rate conditions for the •OH and e_{aq}^- with halogenated and nitro-group compounds. These HNM rate constants were determined reasonable and suitable for further use and application in a kinetic model.

5.3. Mechanisms

Given the relatively simple molecular structure of the HNMs, the mechanism for their degradation by free radicals, •OH and e_{aq}^- was unique and not straightforward. The free radical chemistry degradation of HNMs included multiple path reactions occurring both in series and in parallel whereby some or all of these reactions included reduction, oxidation, abstraction, electron exchange, reversible, and substitution reactions. The degradation of trichloronitromethane included the formation of peroxyl radicals degrading intermediates to halogen ions, and nitrate products. Carbon centered halogen groups demerize to oxygenated radicals by several stepped reactions involving multiple oxidation reactions, electron abstraction reactions, and formation of peroxyl radicals.

Although hydrogen rate constants were not known, hydrogen radical reactions were included and their rate constants were estimated.

The nitro group within HNMs was particularly challenging for its mechanistic reaction. The HNM degradation was modeled to form peroxynitrite and these reactions were modeled in the mechanism to contribute towards the formation of NO_3^-. It was known that these peroxynitro-based radical compounds provided acidic type reactions within the water matrix (Goldstein *et al.,* 2005). Similarity of this acidic condition was noted by Wagnière (1969) where the NO_2^- group in nitroalkanes exhibit pseudo-acid properties in water. The molecular properties of the nonbonding electrons in the nitro group oxygen pair were preserved. Cleavage of the nitro-group from the carbon was anticipated due to its bond length. Wagnière (1969) identified that tribromonitromethane has a C-N bond length of 1.59 Angstroms.

Analysis of ^{60}Co irradiated samples was performed in an attempt to understand the degradation intermediates and irradiation byproducts in HNM mineralization. This data was used in the development of the degradation mechanism and confirmation of mass balance. In addition to Gas Chromatography/Mass Spectrometry (GC/MS), electrospray ionization/mass spectrometry (ESI/MS) was used in an attempt to identify intermediates and residual ions. A TOC analyzer (Shimadzu, Model 5000) was used in the attempt to identify carbon based intermediates and byproducts. It was determined that the ESI-MS was not successful for identification of ion byproducts. The ESI-MS results positively revealed that there was no oxalic acid and formic acid production as none could be detected. The TOC results obtained were inconclusive and therefore not used. Given the challenges experienced in the analytical work, GC/MS provided the ion mass for Cl^-,

Br^-, NO_2^- and NO_3^-. All parent ions were identified as residual except NO_2^-. No nitrite was identified as a residual ion in solution for any HNMs.

The approach for solving the mechanism included the development of pathways for formation of intermediates with their end-point adjusted towards achieving a mechanistic problem solution with the results optimized towards satisfying the final ionic mass balance. This effort included a stepped process and included selectively alternating suitable branching ratios and follow reaction pathways until the mechanism was complete. Branching ratios of the peroxynitrous reaction decay scheme and the addition of a chloride decay scheme were adjusted and a ratio of 10:1 ultimately provided reasonable results. It was recognized that a degradation mechanism scheme may include an environmentally sensitive compound such as the case for the formation of phosgene, nitrite, or nitrate. Formation of phosgene was identified by Getoff (1997) for a degradation mechanism of chloroform. One of the pathways in the degradation scheme in this research reduced the parent compounds to phosgene. Based on the quantities of HNM and the dose levels required for phosgene formation, it was concluded that there will be almost no discernable quantities of phosgene formed in HNM degradation. It was confirmed by kinetic modeling that if phosgene was formed the relative mass generated in real world application would be far below a level of concern as further radiolysis would follow with its ultimate elimination. Using the mass recovery data and the degradation schemes, a mechanistic kinetic model was accomplished and found to work reasonably well.

The kinetic modeling study included use of a computer program (MAKSIMA-CHEMIST) developed by Carver *et al.* (1979). The program functions as a mass action

kinetic computer model suitable for simulations on a personal computer. The kinetic computer model utilizes rate constants, degradation mechanism scheme, radiation dose rate, timing step, the standard hydrolysis reactions presented in Table 1.3, and the free radical yield concentrations identified in equation (1.1) to solve for the residual concentration of the reactants. The modeling for TCNM included an input of 80 chemical reactions and 57 reactants. All simulations were performed using pure water conditions. The mass action kinetic computer model results output were in units of molar concentration versus dose. These results were then input into a spreadsheet computer graphing program EXCEL® for visual interpretation. Comparisons of model to experimental analytical results for TCNM indicated reasonable results.

Based on the kinetic model results for TCNM, the removal efficiency was calculated as a measure of the efficiency of HNM destruction by free radicals. The model results indicated results of >6-Log removal at >8 kGy with an initial concentration of 1.13×10^{-3} M. The MAKSIMA-CHEMIST program was then revised to include a new concentration of HNM at 1.82×10^{-8} M (3 μg L^{-1}) to represent the concentration found in drinking water from the national survey conducted by Weinberg *et al.,* (2002) for water plants using ozone treatment practices. Model prediction for removal of the lower HNM concentration was greater than 6-Log removal at a radiation dose above 6 kGy. The results presented in Table 5.1 identify and compare the removal efficiency for TCNM with both experimental and computer model results.

In radiation chemistry study, the removal efficiency can be quantitatively described in terms of a yield expressed as G_D, in units of mol $J^{-1} \times 10^{-7}$. The G_D value is the

concentration of solute removed by radiation dose. The G_D was determined by the following (Nickelsen *et al.*, 2002):

$$G_D = \frac{\Delta R \times N_A}{D\ 6.24\times10^{19}} \tag{5.1}$$

where Δ R is the change in organic solute solution at a given dose, D in units of kGy, 6.24×10^{19} is the constant to convert kGy to 100 eV L^{-1}, and N_A is Avogadro's number. Table 5.1 presents the G_D for the respective dose for both HNM concentrations and experimental and model results.

Table 5.1. Summary of removal efficiency and G_D values (mol $J^{-1} \times 10^{-7}$) for initial trichloronitromethane concentration of 1.13×10^{-3} M and 1.82×10^{-8} M (3 μg L^{-1}).

	[TCNM] = 1.13×10^{-3} M				[TCNM] = 1.82×10^{-8} M	
Dose (kGy)	Experiment (% rmvl.)	Experiment $(G_D) \times 10^{-3}$	Computer model (% rmvl.)	Computer model $(G_D) \times 10^{-3}$	Computer model (% rmvl.)	Computer model $(G_D) \times 10^{-3}$
1			19.4	2.1	76.6	5.1
1.22	29.2	3.7				
2			34.4	1.9	93.7	5.8
2.44	63.2	3.0				
3			50.9	1.9	98.1	5.9
3.66	84.7	2.6				
4			63.9	1.8	99.4	6.3
5			73.8	1.6	99.8	6.8
6			81	1.5	99.9	7.4
6.1	100	1.8				
7			86.5	1.4	100	8
8			90.4	1.2	100	8.9
8.54	100	1.3				
9			100	1.1	100	9.7
10			100	1	100	10.5

5.4. Dose Rate Constant

The dose rate constant (k_D) provides a quantitative value for evaluating removal efficiency of HNMs in irradiated aqueous solution at different doses. The dose constant is the slope of the line obtained by plotting ln[HNM] versus dose, where [HNM] is the concentration of HNM in the post irradiated solution (Mak *et al.*, 1996). The dose constant for TCNM is graphically represented in Figure 5.1 and presents the experimental results and kinetic computer model results. The graphical depiction indicates the dose required to obtain a desired concentration of solute in solution.

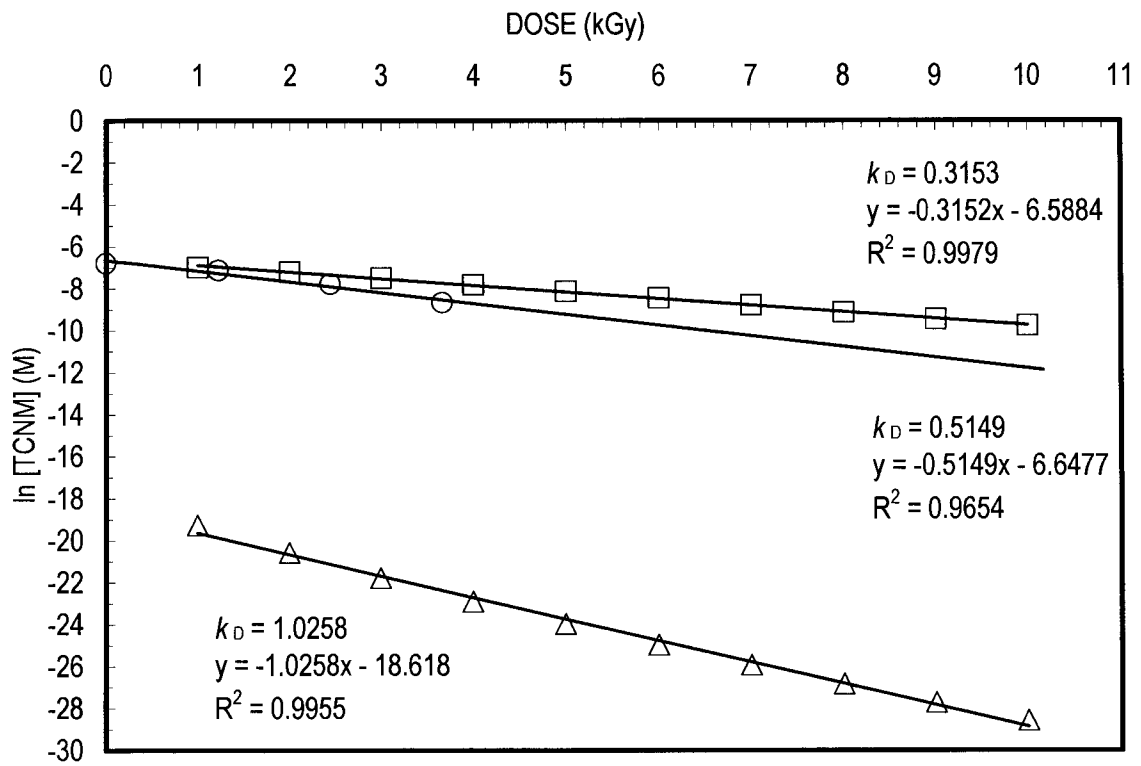

Figure 5.1. Dose constant (k_D) for trichloronitromethane at ambient pH at different concentrations. Initial experimental concentration of 1.13×10^{-3} M (O) with $k_D = 0.5149$ kGy^{-1}, computer model simulation concentration (□) 1.13×10^{-3} M with $k_D = 0.3152$ kGy^{-1}, and computer model simulation concentration 1.82×10^{-8} M (3 $\mu g\ L^{-1}$) with $k_D = 1.0258$ kGy^{-1} (Δ).

Both experimental and MAKSIMA-CHEMIST computer based results for the dose constant determination were in general agreement at the initial TCNM concentration of 1.13×10^{-3} M. Therefore, the TCNM degradation mechanism included in the model was considered suitable for extrapolation to lower trichloronitromethane concentration levels typically found in drinking water supplies. Based on the dose constant presented in Figure 5.1 and the removal efficiency (Table 5.1), a dose of greater than 6 kGy will exceed 6-Log removal of [TCNM] = 1.82×10^{-8} M (3 μg L^{-1}) in pure water. Using the dose rate constant, k_D = 1.0258 kGy^{-1} ([TCNM] =3 μg L^{-1}) or k_D = 0.5149 kGy^{-1} ([TCNM] =1.13×10^{-3} M) (Figure 5.1), the dose required to remove 90%, and similarly 99% of pollutant is determined by (Mak *et al.*, 1996):

$$D_{0.90} = \frac{\ln 10}{k_D} \tag{5.2}$$

$$D_{0.99} = \frac{\ln 100}{k_D} \tag{5.3}$$

It was important to recognize that these removal efficiencies and dose constants are based on ^{60}Co irradiation. These results can be used to describe the radiation level required for removal of TCNM in a large scale electron beam.

5.5. Simulation of Full Scale Electron Beam

The U.S. Food and Drug Administration (1997) approved the use of irradiation for foods as human food stuffs, with poultry at 3 kGy, 4.5 kGy for fresh meat, and 7 kGy for frozen meat because the primary necessity for food irradiation was the elimination of harmful bacteria. Electron beam treatment technology represents a state-of-the-art AOP treatment process and well known to be used for irradiation of mail and sterilization of medical

supplies. Based on a search of the open literature, currently there are no known large scale water treatment facilities in operation using an electron beam AOP process.

Electron beam irradiation has been applied at large scale for the Miami-Dade Water and Sewer Authority's Virginia Key Wastewater Treatment Plant in Miami, Florida and consisted of a 1.5 MeV, 75 kW electron accelerator and described by Kurucz *et al.* (1990) where the overall efficiency of the energy transfer was identified at approximately 65% (Kurucz *et al.,* 1991; Kurucz *et al.,* 1995; Kurucz *et al.,* 2002). The efficiency of an AOP treatment process must account for a number of factors before the process was sized and an estimated energy value assigned. The efficiency considerations to be made for an AOP treatment of water at a large scale facility include the difference in the type of radiation applied during the bench scale testing, the level of treatment required for the pollutant to be removed, and electrical energy losses (Cooper and Tobien, 2001).

Kurucz *et al.* (2002) investigated the efficiency between bench scale gamma irradiation and electron beam radiation and a unique condition was found where gamma irradiation was more efficient for degradation of organic compounds over the electron beam. Kurucz *et al.* (2002) also identified during a comparison study of ^{60}Co bench scale work and electron beam irradiations that the required dose for electron beam treatment ranged from 1.2 to 2.5 times the gamma bench scale study. These differences were described in this work as *removal quality*.

The difference in the removal quality for these two radiation types and their respective efficiencies for removal of HNMs in aqueous solutions were suggested to be derived from the likely occurrence that gamma particles are heavy and their energy transfer is larger for gamma particles when compared to electrons (Kurucz *et al.,* 1991).

The LET value for gamma (LET_{γ} = 1) (Kurucz *et al.*, 1991) is notably a larger value when compared to the electron, prior to the electron's total thermalization and later hydration (LET_{e^-} = 0.24 at 1 MeV) (Spinks and Woods, 1964). Other likely cause for the difference in the removal quality is the density of gamma spur formation (Chatterjee, 1987). Gamma formation of spurs in the water matrix is close together and they interact as they expand. The density of free radicals increases in the closer cores of these heavy particle spurs. This density for gamma is in contrast to electrons where the LET is smaller in comparison and their spurs are farther apart (Chatterjee, 1987).

In addition to LET differences and free radical density affecting the removal quality, a condition was believed to exist where heavy γ-particles interact in the core of the water matrix with a high number of events. This increase in the number of events corresponds to a reduction in the distance between these reactive zones of the spur thus allowing higher frequency and numbers of free radical formation to result in an increased number of reactions before chain back reactions have time to occur (Magee and Chatterjee, 1987). The limitation of diffusion control free radical reactions may be overcome by this higher radical flux. Steady state irradiation conditions may be considered when the flux is constant. An analogous condition was observed by Trumbore *et al.* (1988) for competition effects observed between the un-solvated electron and the solvated (hydrated) electron. Trumbore et al. (1988) identified the condition where the hydrated electron at low solute concentration was not large enough to compete effectively with reactions both in the spur and in the region of expanding spurs (high spur density region). These qualitative conditions were considered in the selection of a removal quality factor (Q_f) at 2.0 for HNMs.

Electrical energy losses can be accounted for systematically from the point of electron production to the target. Generally, the power transfer loss from the point where the electron is generated to the point of application was approximately 20% (Schuetz and Vroom, 1998). The power requirement or efficiency for production of ionizing electrons, losses from scattering at the window of the beam accelerator, requirement for over-scanning of the beam due to distance from the beam source to the edge of the target area will total an additional amount of 10% to 15% (Schuetz and Vroom, 1998).

The concentration of the pollutant was a factor in the energy efficiency required for its removal from the water. The removal efficiency does not always follow the pattern established for HNMs (increasing dose and decreased concentration of pollutant). Kurucz *et al.* (2002) noted that low radiation dose may result in higher removal efficiency for some pollutants and in some cases a higher dose would be needed. Therefore, the radiation dose required for removal of each pollutant must be determined individually. Removal efficiency for HNMs follows the pattern of increased removal efficiency with increase dose as was revealed in the molecular degradation of high and low concentrations for TCNM indicated in Figure 5.1.

The electrical energy per order (EE/O) is unique to each pollutant and based on a logarithmic relationship between the change in pollutant concentration and the electron beam dose (Mincher and Cooper, 2003). The EE/O accurately compares AOP technologies for treatment efficiency and energy cost uniformly as the value was based on the definition of efficiency of kilowatt-hours of electricity required to reduce the concentration of a pollutant one order of magnitude (90% or $D_{0.90}$) (Mincher and Cooper,

2003). Smaller EE/O values are considered to indicate a more efficient process, because less energy would be required (Bolton *et al.,* 1998).

Using the MAKSIMA-CHEMIST program and the kinetic mechanism, the degradation of TCNM was found to be described by first-order kinetics in terms of TCNM concentration and presented in Figure 5.2 for [TCNM] = 1.13×10^{-3} M and Figure 5.3 for [TCNM] = 1.82×10^{-8} M. The degradation rate constant determined for each concentration and the results will be applied in the determination of the EE/O (Bolton *et al.,* 1998).

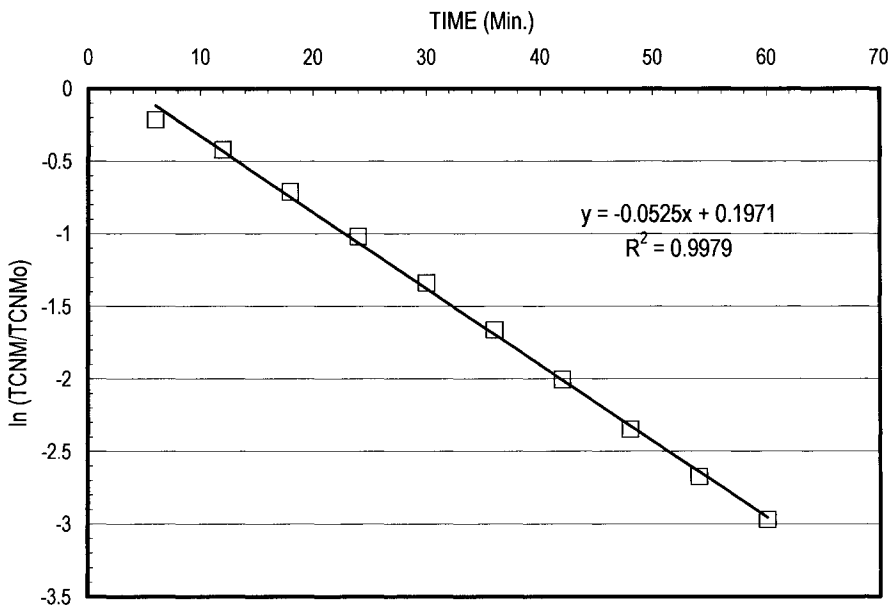

Figure 5.2. Natural logarithm of the fraction of TCNM remaining as a function of time for [TCNM] = 1.13×10^{-3} M. Fraction remaining based on computer simulation where k = 0.0525 $min.^{-1}$.

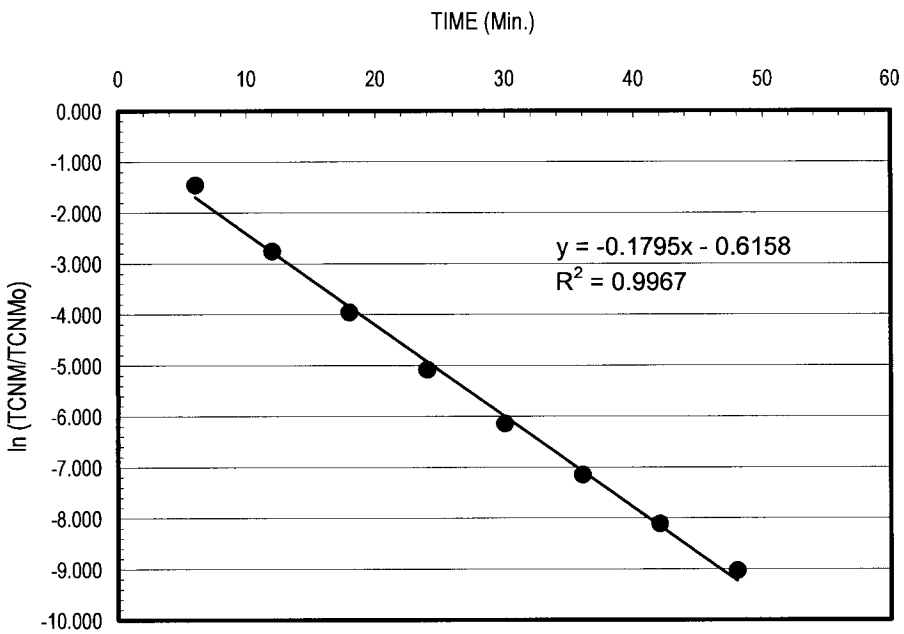

Figure 5.3. Natural logarithm of the fraction of TCNM remaining as a function of time for [TCNM] = 1.82×10^{-8} M. Fraction remaining based on computer simulation where k = 0.1795 $min.^{-1}$.

The EE/O was determined for TCNM and presented in Table 5.2. For comparison, the $D_{0.90}$ and $D_{0.99}$ (dose required for 90% and 99% HNM removal) was presented. HNM removal at a large scale facility would require inclusion of both the $D_{0.99}$ and consideration for use of a removal quality factor ($Q_f = 2.0$). In addition, a safety factor of 1.1 should be added measure to account for unknowns.

The EE/O required to remove water with [TCNM] = 1.82×10^{-8} M (3 μg L^{-1}) was expressed in units of kWh/1000 Liters/order of magnitude (Bolton *et al.*, 1998; Mincher and Cooper, 2003) where an electron beam unit at 150 kW suitable for 6 kGy at 2,200 gpm (8,330 L $min.^{-1}$) (Pikaev, 1998). The EE/O calculated was also based on an extrapolation of ^{60}Co bench scale testing from a higher concentration to a lower modeled concentration. The lower concentration 1.82×10^{-8} M would require an electron beam unit at 65 kW suitable for 2 to 3 kGy at 2,200 gpm (8,330 L $min.^{-1}$) (Pikaev, 1998). The EE/O was determined by (Bolton *et al.*, 1998; Mincher and Cooper, 2003):

$$EE/O = \frac{38.4 \times \text{Power (kWhrs)}}{\text{Volume (Liters)} \times k_1} \tag{5.4}$$

Table 5.2. Dose for 90% and 99% trichloronitromethane removal and equivalent energy per order (EE/O) for pure water.

TCNM Concentration =	1.13×10^{-3} M	1.82×10^{-8} M
Dose (kGy) 90% Removal =	4.5	2
Dose (kGy) 99% Removal =	8.9	5
EE/O (kWh per order per m^3) =	3.8	1.9

Price of treatment is dependant upon several items in addition to the AOP equipment and these items vary widely based on facility parameters, location and the time when the

treatment facility would be constructed (Zimek and Chmielewski, 1998). Pricing should include engineering cost, allowances for work performed at an existing facility versus new, pumping, piping, ancillary support equipment cost, market conditions that affect current interest rates, the size of the treatment facility, permitting costs, pilot plant study cost that has been found to be approximately 1% of the total project cost, land and easements, cost to bring electrical power to the site, site development, administration, staffing, and training, and replacement cost. Kurucz *et al.* (1995) found that an electron beam irradiation treatment system characterized as a 1.5 MeV, 50 mA producing 50 krad (0.5 kGy) at an interest rate of 15% for 20 years operating for 8,000 hours per year treating 2,100 gallons per minute would cost approximately $0.76 per 1,000 gallons of water in year 1995 dollars.

5.6. Summary

The study of free radical degradation of HNM was accomplished as four primary research components with the determination of the rate constants using pulse radiolysis performed first. The literature was surveyed to ascertain reasonableness of those experimentally obtained values and these rate constants were found satisfactory. The second research component included irradiation of HNMs using a ^{60}Co gamma irradiator to mineralize the HNMs under varied gamma dose. The third component included an evaluation of HNMs to ascertain recovery of the degradation products and for mass balance. The mass recovery results are graphically presented by Figure 5.4 chloronitromethane, Figure 5.5 dichloronitromethane, Figure 5.6 dibromochloronitromethane, and Figure 5.7 bromodichloronitromethane.

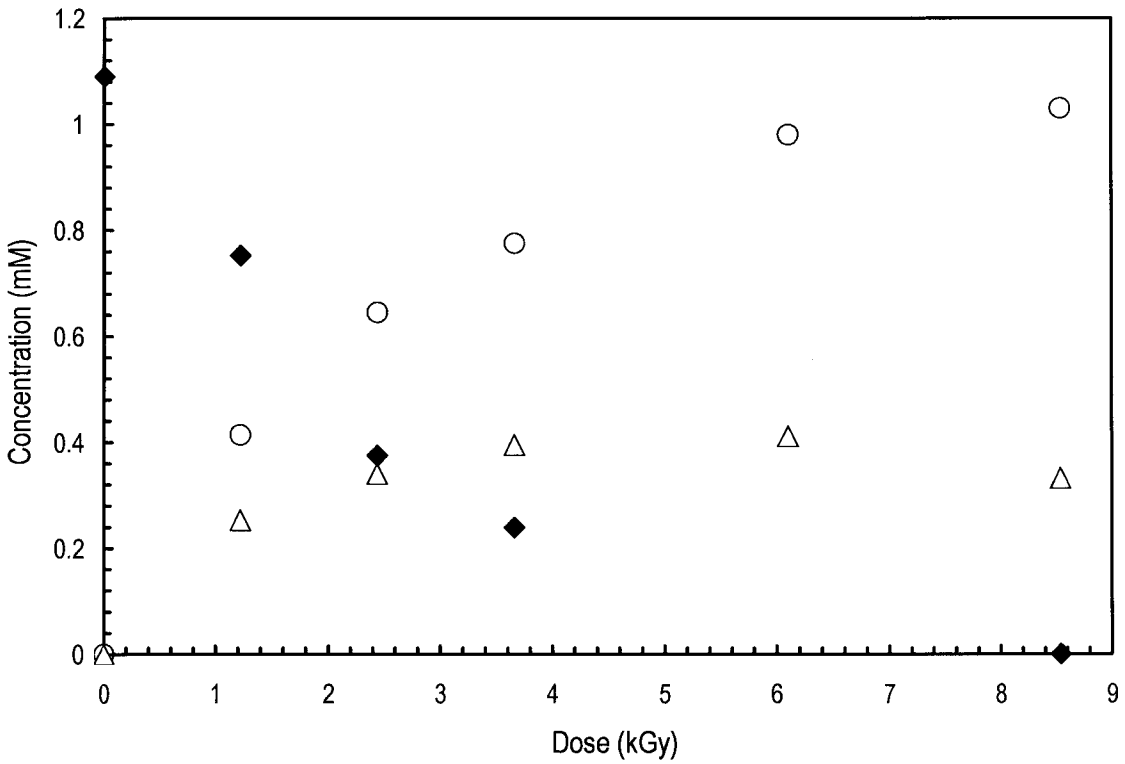

Figure 5.4. Mass recovery of chloronitromethane, CH_2ClNO_2. Chloride (O), nitrate (Δ), and CH_2ClNO_2 (◆).

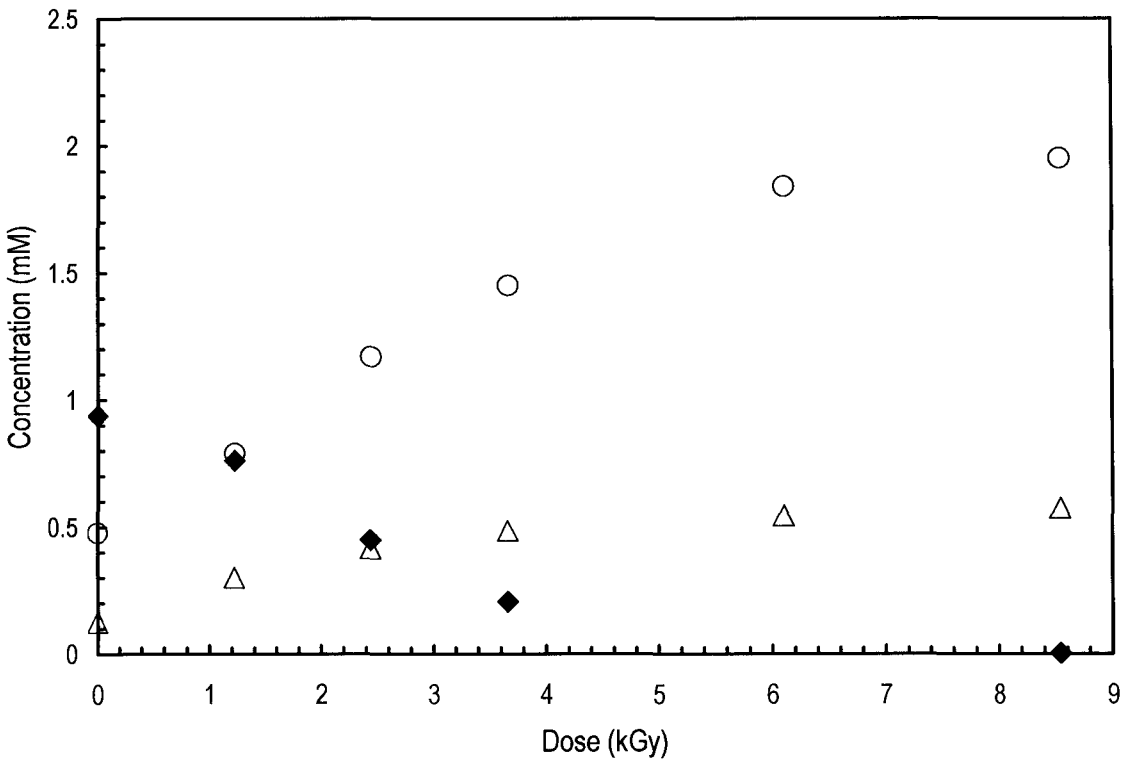

Figure 5.5. Mass recovery of dichloronitromethane, $CHCl_2NO_2$. Chloride (O), nitrate (Δ), and $CHCl_2NO_2$ (◆).

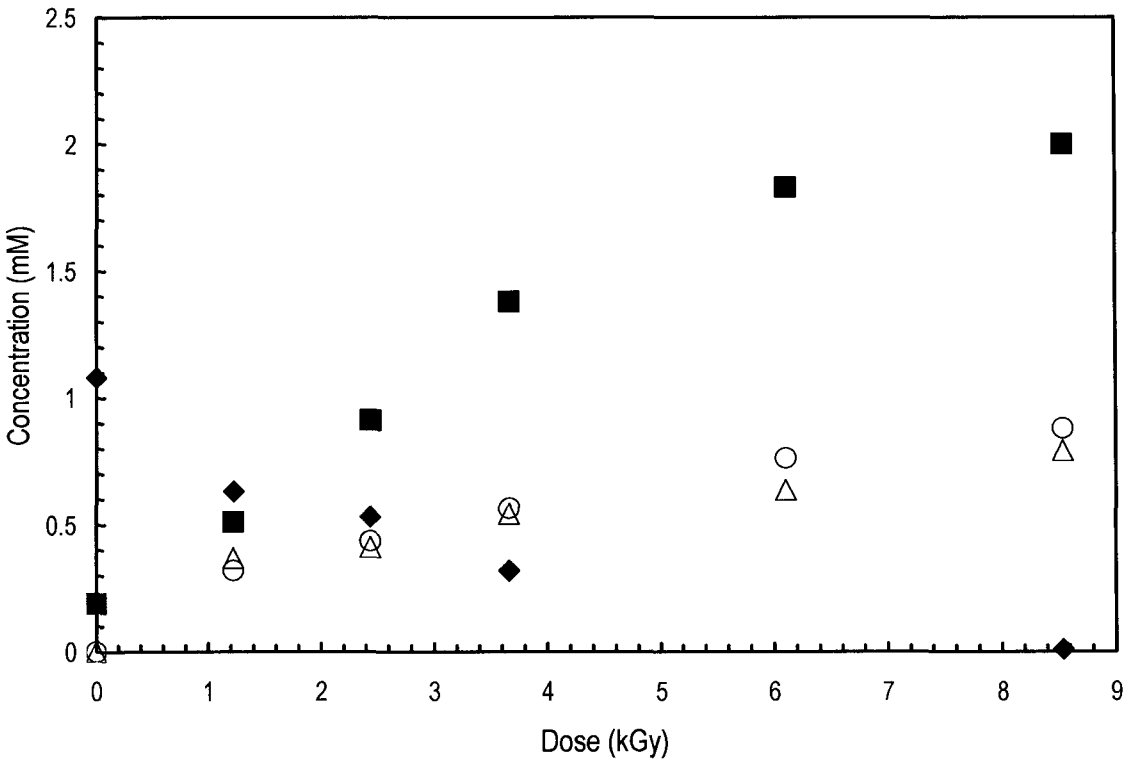

Figure 5.6. Mass recovery of dibromochloronitromethane, CBr_2ClNO_2. Bromide (■), Chloride (O), nitrate (Δ), and CBr_2ClNO_2 (◆).

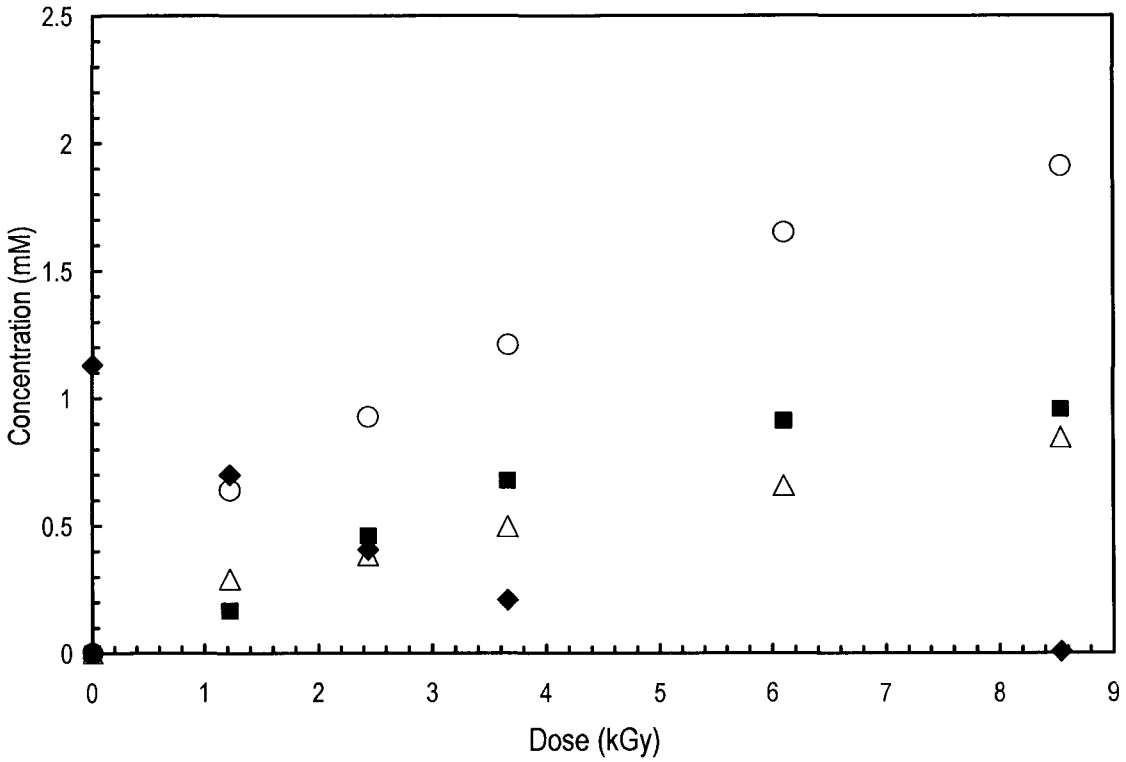

Figure 5.7. Mass recovery of bromodichloronitromethane, $CBrCl_2NO_2$. Bromide (■), Chloride (O), nitrate (Δ), and $CBrCl_2NO_2$ (◆).

The fourth component included a compilation of the experimental results and those results input into a mechanism developed for the HNM degradation. For TCNM, the model simulation results obtained were compared to the experimental mass recovered. The model indicated the production of chloride and nitrate ions in proportion to the experimental results. Irradiated solutions were analyzed for nitrite (NO_2^-), however no nitrite was detected. Overall, the results were noted to be reasonable for the postulated degradation mechanism as evidenced by comparisons of the simulated mass recovery to experimental results.

The data obtained in these four experimental research components were then applied to large scale electron beam treatment of HNMs in water. The dose constant was identified for large and small concentration of HNM and the results indicated that increasing dose would degrade HNM. The dose constant (k_D) for the following HNMs are graphically presented in Figure 5.8 for chloronitromethane, Figure 5.9 dichloronitromethane, Figure 5.10 chlorodibromonitromethane, and Figure 5.11 bromodichloronitromethane.

The removal quality and safety factors were addressed to identify requirement for large scale AOP. In addition to the energy cost identified as EE/O, a price for free radical AOP treatment using 65 kW electron beam was estimated at $0.51 per 1,000 gallons of water for a 2.5 MGD water plant operating 14 hours per day in year 2005 dollars.

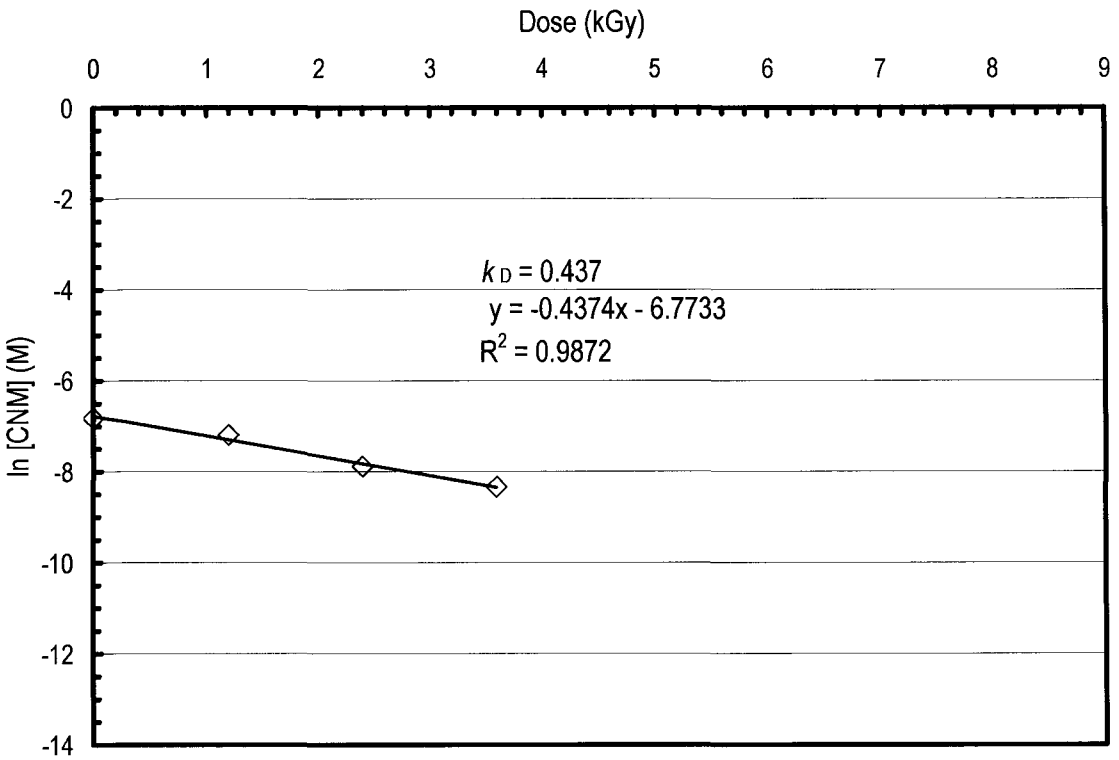

Figure 5.8. Dose constant (k_D) = 0.437 kGy^{-1} for logarithm chloronitromethane concentration (◇)versus dose in pure water.

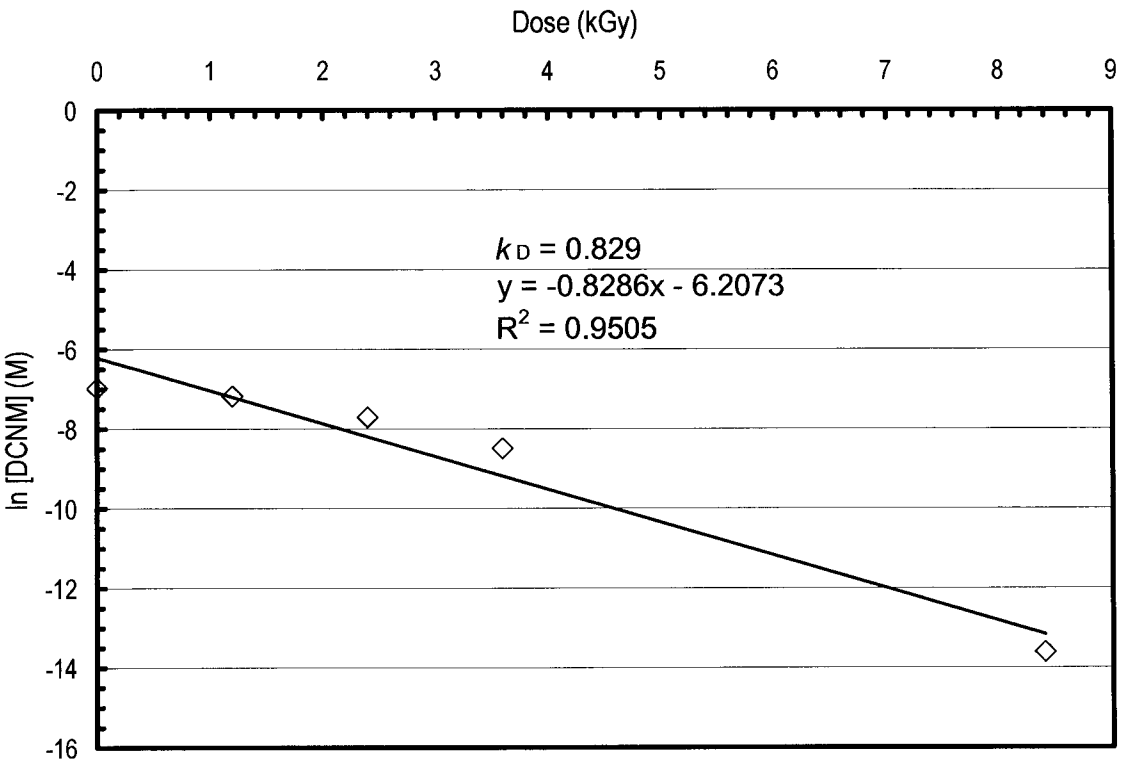

Figure 5.9. Dose constant (k_D) = 0.829 kGy^{-1} for logarithm dichloronitromethane concentration (◇)versus dose in pure water.

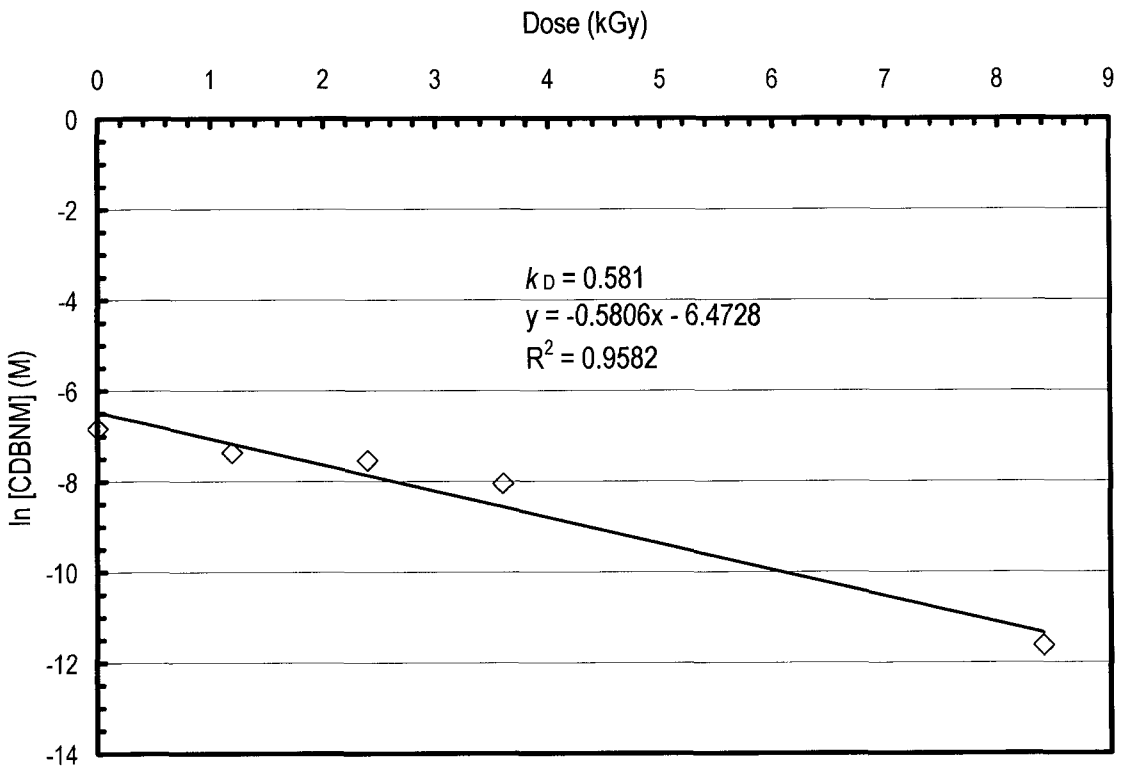

Figure 5.10. Dose constant (k_D) = 0.581 kGy^{-1} for logarithm chlorodibromonitromethane concentration (◇)versus dose in pure water.

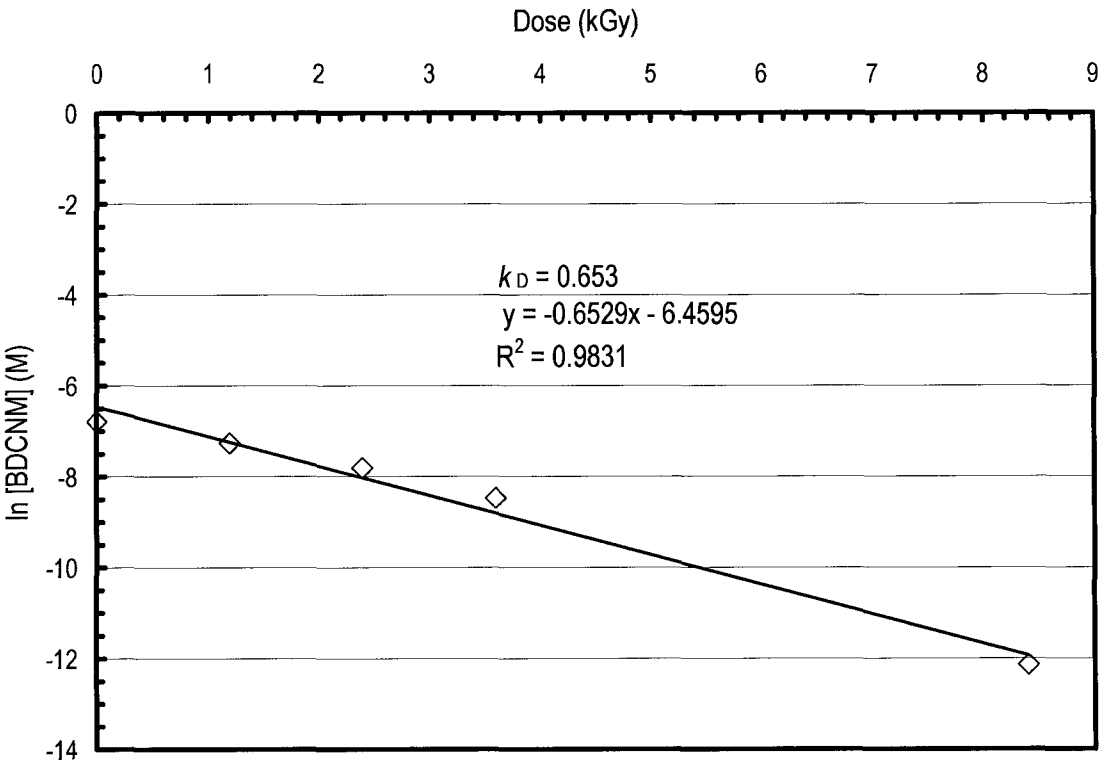

Figure 5.11. Dose constant (k_D) = 0.653 kGy^{-1} for logarithm bromodichloronitromethane concentration (◇) versus dose in pure water.

6. SUMMARY

Drinking water professionals possess a continuous need to explore advanced treatment options for elimination of pollutants and disinfection-by-products found in drinking water. Drinking water disinfectants have been in use for a long time as a means for protecting the public health from microbial pathogens, however studies have shown that disinfection-by-products have been found (Rook, 1974). As a result of this use, DBP reduction or elimination has been identified necessary to maintain the public's health, safety, and welfare. Each treatment option for removal of these DBPs must be understood and well developed prior to acceptance for use with the public's drinking water.

The purpose of this study was to assess the potential for use of free radical Advanced Oxidation Processes (AOPs) in the degradation of halonitromethanes (HNMs) in water. The results obtained from this study will assist with an understanding for use of free radicals in the removal of these HNMs. Further, this research was designed to acquire the data needed for understanding free radical destruction of HNMs. The HNM destruction method included the use of hydroxyl radical and hydrated electron applied in an aqueous solution and the results were satisfactory.

Two primary goals were initially identified and subsequently accomplished in this research. They were to ascertain the efficacy of free radicals for destruction of halonitromethanes and the identification of implications for water treatment using free radical AOP. The first goal identified was achieved by satisfactory identification of rate constants for halonitromethane compounds and their degradation byproducts. A kinetic

mechanism for the degradation reactions was established and then confirmed by kinetic computer model simulation. The results of this research indicated that free radicals, •OH and e^-_{aq} were found reasonable for the removal of HNMs in aqueous solution. The accomplishment of the second goal was substantiated by identification of removal efficiencies for different HNM concentrations in solution, their dose rate constants, removal quality factor, and the electrical energy per order (EE/O).

The research provided a unique contribution of data and information required for treatment of water. Prior to this research, there were no known free radical kinetic or mechanistic data for halonitromethane degradation in water. These research results should support scientists and engineers with the kinetic information needed for removal of HNMs in aqueous solutions.

The HNMs represent DBPs that will not be eliminated by current conventional water treatment processes. Given that the use of ozone in the treatment of water continues along with the use of chlorine and chloramines, free radical AOP may provide an alternative method for removal of HNMs from water. The free radical AOP could provide a sustainable treatment process with potentially no adverse impact to water quality. Overall, free radical AOP was considered a viable process for degradation of HNMs in water.

REFERENCES

Adams, G. E. and Boag, J. W. (1964) Spectroscopic Studies of Reactions of the OH Radical. *Proc. Chem. Soc.* 112.

Adams, G. E., Boag, J. W. and Michael, B. D. (1965) Reactions of the Hydroxyl Radical Part 2. Determination of Absolute Rate Constants. *Trans. Faraday Soc.* **61**, 1417-1424.

Alfassi, Z., Huei, R. E. and Neta, P. (1997) Kinetic Studies of Organic Peroxyl Radicals in Aqueous Solutions and Mixed Solvents. In *The Chemistry of Free Radicals: Peroxyl Radicals* (Edited by Z. Alfassi). John Wiley and Sons, New York.

Asmus, K. -D. (1984) Methods in Enzymology. In *Pulse Radiolysis Methodology. Vol. 105, Chapter 20.* Academic Press, Burlington, Massachusetts.

Asmus, K. -D., Henglein, A. and Beck, G. (1964a) Pulsradiolytiche Untersuchung der Reaktion des hydratisierten Elektrons mit Nitromethan. Berichte der Bunsen Gesellschaft Fur Physikalische Chemie **70**, 459-466.

Asmus, K. -D., Henglein, Ebert, M., and Keene, J. P. (1964b) Pulsradiolytiche Untersuchung schneller Reaktionen von hydratisierten Elektronen, freien Radikalen und Ionen mit Tetranitromethan in wäBriger Lösung. Berichte der BunsenGesellschaft Fur Physikalische Chemie **68**, 657-663.

Balkas, T. I. (1972) The radiolysis of aqueous solutions of methylene chloride. *Int. J. Radiat. Phys. Chem.* ***4***, 199-208.

Balkas, T. I., Fendler, J. H. and Schuler, R. H. (1970) Radiolysis of Aqueous Solutions of Methyl Chloride. The Concentration Dependence for Scavenging Electron within Spurs. *J. Phys. Chem.* **74**, 4497-4505.

Barker, G. C., Fowles, P. and Stringer, B. (1970) Pulse radiolytic Induced Transient Electrical Conductance in Liquid Solutions. *Trans. Faraday Soc.* **66**, 1509-1519.

Bartels, D. M., Cook, A. R., Mudaliar, M. and Jonah, C. D. (2000) Spur Decay of the Solvated Electron in Picosecond Radiolysis Measured with Time-Correlated Adsorption Spectroscopy. *J. Phys. Chem. A* **104**, 1686-1691.

Becke, C., Maier, D. and Sonthheimer, H. (1984) Herkunft von Trichlornitromethan im Trinkwasser, Origin of Trichloronitromethane in Drinking Water. *Vom Wasser* **62**, 125-135.

Bensasson, R. U., Land, E. J. and Truscott, T. G. (1983) *Flash Photolysis and Pulse Radiolysis, Contributions to the Chemistry of Biology and Medicine.* Pergamon Press, New York.

Bolton, J. R., Valladares, J. E., Zanin, J.P., Cooper, W. J., Nickelsen, M. G., Kajdi, D.C., Waite, T. D. and Kurucz, C. N. (1998) Figures-of-Merit for Advanced Oxidation Technologies: A Comparison of Homogeneous UV/H_2O_2, Heterogeneous UV/TiO_2 and Electron Beam Processes. *Science and Technology Integration, Journal of Advanced Oxidation Technology* **3**, 174-181.

Bonifačić, M., Schöneich, C. and Asmus, K. -D. (1991) Halogenated peroxyl radicals as multi-electron oxidants: Pulse radiolysis study on the reactions of trichloromethyl peroxyl radicals with iodide. *J. Chem. Soc., Chem. Commun.* 1117-1119.

Buxton, G. V. (1969) Pulse Radiolysis of Aqueous Solutions. *Tran.s Faraday Soc.* **65**, 2150-2158.

Buxton, G. V. (1987) Radiation Chemistry of the Liquid State: (1) Water and Homogeneous Solutions. In *Radiation Chemistry: Principals and Applications* (Edited by M. A. Farhataziz and J. Rodgers). VCH Publishers, New York.

Buxton, G. V. (2004) The Radiation Chemistry of Liquid Water: Principles and Applications. In *Charged Particle and Photon Interactions with Matter, Chemical, Physiochemical, and Biological Consequences with Applications* (Edited by A. Mozumder and Y. Hatano). Marcel Dekker, Inc., New York.

Buxton, G. V., Bydder, M. and Salmon, G. A. (1998) Reactivity of chlorine atoms in aqueous solution Part 1 The equilibrium $Cl^{\bullet} + Cl^{-} \leftrightarrow Cl_2^{\bullet-}$. *J. Chem. Soc., Faraday Trans.* **94**, 653-657.

Buxton, G. V., Greenstock, C. L., Helman, W. P. and Ross, A. B. (1988) Critical Review of Rate Constants for Reactions of Hydrated Electrons, Hydrogen Atoms and Hydroxyl Radicals (OH/O^{-}) in Aqueous Solutions, Reprint No. 343. *J. Phys. Chem. Ref. Data* **17**, 513-886.

Buxton, G. V. and Stuart, C. R. (1995) Re-evaluation of the thiocyanate dosimeter for pulse radiolysis. *J. Chem. Soc., Faraday Trans.* **91**, 279-281.

Cambron, R. T. and Harris, J. M. (1995) Photothermal investigation of chlorine photodissociation and nongeminate recombination in liquids. *J. Phys. Chem.* **99**, 695-706.

Carter, W. P., Luo, D. and Malkina, I. L. (1997) Investigation of the atmospheric reactions of chloropicrin. *Atmos. Env.* **31**, 1425-1439.

Carver, M. B., Hanley, D. V. and Chapin, K. R. (1979) *MAKSIMA-CHEMIST, A program for mass action kinetic simulation manipulation and integration using STIFF techniques. Chalk River Nuclear Laboratories Report.* Atomic Energy of Canada, Ltd. Available from W. J. Cooper, University of North Carolina, Wilmington, Center for Marine Science, 5600 Marvin K. Moss Lane, Wilmington, North Carolina.

Castro, C. E., Wade, R. S. and Belser, N. O. (1983) Biodehalogenation: The Metabolism of Chloropicrin by Pseudomonas sp. *J. Agric. Food. Chem.* **31**, 1184-1187.

Castro, C. E., Wade, R. S. and Belser, N. O. (1985) Biodehalogenation: Reactions of Cytochrome P-450 with polyhalomethanes. *Biochem.* **24**, 204-210.

Cavanagh, J. E., Weinberg, H. S., Gold, A., Sanalah, R., Marbury, D., Glaze, W. H., Collette, T. W., Richardson, S. D. and Thruston, A. D. (1992) Ozonation Byproducts: Identification of Bromohydrins from the Ozonation of Natural Water with Enhanced Bromide Levels. *Environ. Sci. Technol.* **27**, 1658-1662.

Cervini-Silva, J., Larson, R. A., Wu, J. and Stucki, J. W. (2001) Transformation of Chlorinated Aliphatic Compounds by Ferruginous Smectite. *Environ. Sci. Technol. (Article)*, **35**, 805-809.

Cervini-Silva, J., Wu, J., Larson, R. A. and Stucki, J. W. (2000) Transformation of Chloropicrin in the Presence of Iron-Bearing Clay Minerals. *Environ. Sci. Technol. (Communication)* **34**, 915-917.

Chatterjee, A. (1987) Interaction of Ionizing Radiation with Matter. In *Radiation Chemistry Principals and Applications* (Edited by M. Farhataziz and J. Rodgers). VCH Publishers, New York.

Chen, P.H., Richardson, S.D., Krasner, S.W., Majetich, G. and Glish, G. L. (2002) Hydrogen abstraction and decomposition of bromopicrin and other trihalogenated disinfection byproducts by GC/MS. *Environ. Sci. Technol.* **36**, 3362-3371

Coleman, W. E., Lingg, R. D., Melton, R. G. and Kopfler, F. C. (1976) The Occurrence of Volatile Organics in Five Drinking Water Supplies Using GC/MS. In *Identification and Analysis of Organic Pollutants in Water* (Edited by K. L. Keith). Ann Arbor Science, Ann Arbor, Michigan.

Cooper, W. J. and Cadavid, E. (1993) Removing THMs from Drinking Water Using High-Energy Electron Beam Irradiation. *J. Am. Water Works Assoc.* **69**, 105-112.

Cooper, W. J., Dougal, R. A., Nickelsen, M. G., Waite, T. D., Kurucz, C. N., Lin, K. and Bibler, J. P. (1996b) Benzene Destruction in Aqueous Waste-I. Bench–Scale Gamma Radiation Experiments. *Radiat. Phys. Chem.* **48**, 81-87.

Cooper, W. J., Gehringer, P., Pikaev, A. K., Kurucz, C. N. and Mincher, B. J. (2004) Radiation Process. In *Advanced Oxidation Processes for Water and Wastewater Treatment* (Edited by S. Parson). International Water Association, Ashland, Ohio.

Cooper, W. J., Meacham, D. E., Nickelsen, M. G., Lin, K., Ford, D. B., Kurucz, C. N. and Waite, T. D. (1993) The Removal of Tri- (TCE) and Tetrachloroethylene (PCE) from Aqueous Solution Using High Energy Electrons. *Journal of Air and Waste Management*, **43**, 1358-1366.

Cooper, W. J., Mezyk, S. P. and Bartels, D. M. (2002b) The Free Radical Chemistry of tert-butyl formate: Rate Constants for hydroxyl radical, hydrated electron and hydrogen atom reaction in aqueous solution. *Radiat. Phys, Chem.* **65**, 309-315.

Cooper, W. J., Sawal, K. L., Hoogland, Y. S., Slifker, R., Nickelsen, M. G., Kurucz, C. N. and Waite, T. D. (1996a) Disinfection By-Product Precursor Removal from natural Waters Using Gamma Radiation to Simulate an Innovative Water Treatment Process. In *Disinfection Byproducts in Water Treatment, The Chemistry of Their Formation and Control* (Edited by R. A. Minear and G. L. Amy). Lewis Publishers, New York.

Cooper, W. J. and Tobien, T. (2001) The Application of the Electron Beam Process in water and Wastewater treatment: Fundamental and Applied Studies. In *Use of irradiation for Chemical and microbial decontamination of water, wastewater and sludge.* International Atomic Energy Agency, Austria.

Cooper, W. J., Tobien, T., Mezyk, S. P., Adams, J. W., Nickelsen, M. G., O'Shea, K. E., Inclan, G., Tornatore, P. M., Hajali, P. and Weidman, D. J. (2002a) The Electron-Beam Process for the Destruction of Methyl tert-Butyl Ether. In *ACS Symposium Series 799, Oxygenates in Gasoline Environmental Aspects* (Edited by A. F. Diaz and D. L. Drogos). American Chemical Society, Washington, DC.

Csinos, A. S., Webster, T. M., Sumner, D. R., Johnson, A. W., Dowler, C. C. and Seebold, K. W. (2002) Application and crop safety parameters for soil fumigants. *Crop Protection* **21**, 973-982.

de Greef, E. J., Morris, J. C., van Kreijl, C.F. and Morra, C. F. H., (1980) Health Effects in the Chemical Oxidation of Polluted Waters. In *Water Chlorination: Environmental Impacts and Health Effects* (Edited by R. L. Jolley, W. A. Brungs, R. B. Cumming, and V. A. Jacobs). Ann Arbor Science, Ann Arbor, Michigan.

Diehl, A. C., Speitel, Jr., G. E., Symons, J. M., Krasner, S. W., Hwang, C. J. and Barrett, S. E., (2000), DBP Formation during Chloramination. *J. Am. Water Works Assoc.* **92**, 76-90.

Draganic, I. G. and Draganic, Z. D. (1971) *The Radiation Chemistry of Water, Physical Chemistry, Vol. 26* (Edited by E. M. Loebil). Academic Press, New York.

Drzewicz, P., Trojanowicz, M., Zona, R., Solar, S. and Gehringer, P. (2004) Decomposition of 2,4-dichlorophenooxyactetic acid by ozonation, ionizing radiation as well as ozonation combined with ionizing radiation. *Radiat. Phys. Chem.* **69**, 281-287.

Duguet, J.P., Tsutsumi, Y., Bruchet, A. and Mallevialle, J. (1984) Chloropicrin in Potable Water: Conditions for Formation and Production During Treatment. In *Proceedings of the 5th Conference on Water Chlorination: Environmental Impact and Health Effects Williamsburg, Virginia, June 3-8.* Lewis Publishers, Chelsa, Michigan.

Emmi, S. S., Beggiato, G., Casalbore-Miceli, G. and Fuochi, P. G. (1985) $^{\bullet}OH$ radical reaction with CH_2Cl_2: Direct spectrophotometric observation of $^{\bullet}CHCl_2$ radical formation. *J. Radioanal. Nucl. Chem., Lett.* **93**, 189-197.

Gear, C. W. (1971) Automatic Integration of Ordinary Differential Equations. *Comm. ACM*, **14**, 176.

Getoff, N. (1997) Peroxyl Radical in the Treatment of Waste Solutions. In *The Chemistry of Free Radicals: Peroxyl Radicals* (Edited by Z. Alfassi). John Wiley and Sons, New York.

Giller, S., Le Curieux, F., Gauthier, L., Erb, F. and Marzin, D. (1995) Genotoxicity assay of chloral hydrate and chloropicrin. *Mutat. Res.* **348**, 147-152.

Gilreath, J.P. and Santos, B. M. (2004) Herbicide dose and incorporation depth in combination with 1,3-dichloropropene plus chloropicrin for Cyperus rotundas control in tomato and pepper. *Crop Protection* **23**, 205-210.

Goldstein, S. and Czapski, G. (1995) The reaction of NO• with $O_2^{\bullet -}$ and $HO_2^{\bullet -}$: A pulse radiolysis study. *Free Radical Biol. Med.* **19**, 505-510.

Goldstein, S., Lind, J. and Merényi, G. (2005) Chemistry of peroxynitrites as compared to peroxynitrates. *Chem. Rev.* Manuscript submitted for publication.

Golfinopoulos, S. K., Nikolaou, A. D. and Lekkas, T. D. (2003) The occurrence of disinfection byproducts in the drinking water of Athens, Greece. *Environ. Sci. Pollut. Res.* **10**, 368-372.

Gullino, M. L., Minuto, A., Gilardi, G., Garibaldi, A. and Ajwa, H., Duafala, T. (2002) Efficacy of preplant soil fumigation with chloropicrin for tomato production in Italy. *Crop Protection* **21**, 741-749.

Guo, M., Papiernik, S. K., Zheng, W. and Yates, S. R. (2003) Formation and Extraction of Persistent Fumigant Residues in Soils. *Environ. Sci. Technol.* **37**, 1844-1849.

Haag, W. R. and Yao, C. C. D. (1992) Rate Constants for Reaction of Hydroxyl Radicals with Several Drinking Water Contaminants. *Environ. Sci Technol.* **26**, 1005-1013.

Haara M. J., Fennimore, S. A., Ajwa H. A. and Winterbottom, C. Q. (2003) Chloropicrin effect on weed seed viability. *Crop Protection* **22**, 109–115.

Hart, E. J. and Anbar, M. (1970) *The Hydrated Electron*. Wiley-Interscience, New York.

Hart, E. J., Gordon, S. and Thomas, J. K. (1964) Rate constants of hydrated electron reactions with organic compounds. *J. Phys. Chem.* **68**, 1271-1274.

Hayes, D., Schmidt, K. H. and Meisel, D. (1989) Growth Mechanisms of Silver Halide clusters from the Molecule to the Colloidal Particle. *J. Phys. Chem.* **93**, 6100-6109.

Hoigné, J. and Bader, H. (1988) The Formation of Trichloronitromethane (Chloropicrin) and Chloroform in a Combined Ozonation/Chlorination Treatment of Drinking Water. *Wat. Res.* **22**, 313-319.

Hug, G. L. (1981) Optical Spectra of Nonmetallic Inorganic Transient Species in Aqueous Solution. In *National Standard Reference Data System NSRDS-NBS 69*. U. S. Department of Commerce, National Bureau of Standards, Washington, DC.

Hummel, A. (1987) Kinetics in Radiation Chemistry. In *Radiation Chemistry Principals and Applications* (Edited by M. A. Farhataziz and J. S. Rodgers). VCH Publishers, New York.

Ingham, E. R. and Thies, W. G. (1996) Responses of soil foodweb organisms in the first year following clearcutting and application of chloropicrin to control laminated root rot. *Applied Soil Ecology* **3**, 35-47.

Jacangelo, J. G., Patania, N. L., Reagan, K. M., Aieta, E. M., Krasner, S. W. and McGuire M. J. (1989) Impact of Ozonation on the Formation and Control of Disinfection Byproducts in Drinking Water. *J. Am. Water Works Assoc.* **81**, 74-83.

Janata, E. and Schuler, R. H. (1982) Rate Constant for Scavenging e_{aq}^- in N_2O-Saturated Solutions. *J. Phys. Chem.* **86**, 2078-2084.

Jayson, G. G., Parsons, B. J. and Swallow, A. J. (1973) Some Simple, Highly Reactive, Inorganic Chlorine Derivatives in Aqueous Solution Their Formation using Pulses of Radiation and Their Role in the Mechanism of the Fricke Dosimeter. *J. Chem. Soc. Faraday Trans. I* **69**, 1597-1607.

Kalkwarf, D. R. (1968) Absolute Rate constants for the Reaction of Organic Solutes with Hydroxyl Radicals in Aqueous Solution. In *AEC Research and Development Report, Pacific Northwest Laboratory Annual Report for 1967 to the AEC, Division of Biology and Medicine, Vol. II, Part 2, Physical Sciences*. Atomic Energy Commission, Richland, Washington.

Kampioti, A. A. and Stephanou, E. G. (2002) The Impact of Bromide on the Formation of Neutral and Acidic Disinfection Byproducts (DBPs) in Mediterranean Chlorinated Drinking Water. *Wat. Res.* **36**, 2596-2606.

Keith L. H. (1976) Identification of Organic Compounds in Drinking Water From 13 U.S. Cities. In *Identification and Analysis of Organic Pollutants in Water* (Edited by K. L. Keith). Ann Arbor Science, Ann Arbor, Michigan.

Khaikin, G. I., Alfassi, Z. B. and Neta, P. (1995) Formation and reaction of halogenated phenylperoxyl radicals in aqueous alcohol solutions. *J. Phys. Chem.* **99**, 11447-11451.

Kissner, R., Nauser, T., Bugnon, P., Lye, P. G. and Koppenol, W. H. (1997) Formation and properties of peroxynitrite as studied by laser flash photolysis, high-pressure stopped-flow technique, and pulse radiolysis. *Chem. Res. Toxicol.* **10**, 1285-1292.

Kláning, U. K. and Wolff, T. (1985) Laser flash photolysis of HClO, $ClO^{\cdot}$, HBrO, and $BrO^{\cdot}$ in aqueous solution reactions of Cl^{-} and Br^{-} atoms. *Ber. Bunsenges. Phys. Chem.* **89**, 243-245.

Köester, R. and Asmus, K.-D. (1971) Die Reduktion von Tetrachlorkohlenstoff durch hydratisierte Elektronen, H-Atome und reduzierende Radikale. *Z. Naturforsch. Teil B* **26**, 1104-1108.

Krasner, S. W., Sclimenti, M. J., Chinn, R., Chowdbury, Z. K. and Owen, D. M. (1996) The Impact of TOC and Bromide on Chlorination By-Product Formation. In *Disinfection Byproducts in Water, the Chemistry of Their Formation and Control* (Edited by R. A. Minear and G. L. Amy). CRC Press, Boca Raton, Florida.

Kurucz, C. N., Waite, T. D. and Cooper, W. J. (1995) The Miami Electron Beam Research Facility: A Large Scale Wastewater Treatment Application. *Radiat. Phys. Chem.* **45**, 299-308.

Kurucz, C. N., Waite, T. D., Cooper, W. J. and Nickelsen, M. G. (1990) Full Scale Electron Beam Treatment of Hazardous Wastes – Effectiveness and Costs. In *Proceedings of the 45th Industrial Waste Conference, May 8-10.* Purdue Research Foundation, Lewis Publishers, Michigan, 539-545.

Kurucz, C. N., Waite, T. D., Cooper, W. J. and Nickelsen, M. J. (1991) High Energy Beam Irradiation of Water, Wastewater and Sludge. In *Advances in Nuclear Science and Technology, 22* (Edited by J. Lewins and M. Becker). Plenum Press, New York.

Kurucz, C. N., Waite, T. D., Otaño, Cooper, W. J., and Nickelson, M. G. (2002) A comparison of large-scale electron beam and bench-scale ^{60}Co irradiations of simulated aqueous waste streams. *Radiat. Phys. Chem.* **65**, 367-378.

Lal, M. and Mahal, H. S. (1992) Reactions of alkylbromides with free radicals in aqueous solutions *Radiat. Phys. Chem.* **40**, 23-26.

Lal, M., Mönig, J. and Asmus, K.-D. (1986) Free Radical Induced Degradation of 1,2-dibromoethane. Generation of Free Br• Atoms. *Free Rad. Res. Comms.* **4**, 235-241.

Lal, M., Schoneich, C., Monig, J. and Asmus, K. -D. (1988) Rate Constants for the Reactions of Halogenated Organic Radicals. *Inter. J. Radiat. Bio.* **54**, 773-785.

Laniewski, K., Boren, H. and Grimvall, A. (1998) Identification of Volatile and Extractable Chloroorganics in Rain and Snow. *Environ. Sci. Technol.* **32**, 3935-3940.

Leigh, G. J. (1990) Nomenclature of Inorganic Chemistry Recommendations 1990 (Edited by G. J. Leigh). International Union of Pure and Applied Chemistry, Blackwell Scientific Publications, Oxford, England.

Leitner, N. K. V., Berger, P. and Gehringer, P. (1999) γ-irradiation for the removal of atrazine in aqueous solution containing humic substances. *Radiat. Phys. Chem.* **55**, 317-322.

Lesclaux, R. (1997) Combination of Peroxyl Radicals in the Gas Phase. In *The Chemistry of Free Radicals* (Edited by Z. Alfassi). John Wiley and Sons, New York.

Løgager, T. and Sehested, K. (1993a) Formation and decay of peroxynitrous acid: A pulse radiolysis study. *J. Phys. Chem.* **97**, 6664-6669.

Løgager, T. and Sehested, K. (1993b) Formation and decay of peroxynitric acid: A pulse radiolysis study. *J. Phys. Chem.* **97**, 10047-10052.

Madden, K. P. (2004) Graphic Figure: NDRL LINAC (Model TB-8/16-1S 8 MeV S-Band). U.S. Department of Energy, Notre Dame Radiation Laboratory, South Bend, Indiana.

Magee, J. L. and Chatterjee, A. (1987) Track Models and Radiation Chemical Yields. In *Radiation Chemistry Principles and Applications* (Edited by Farhataziz and A. J. Rodgers). VCH Publishers, New York.

Mak, F. T., Cooper, W. J., Kurucz, C. N., Nickelsen, M. G. and Waite, T. D. (1996) Removal of Chloroform from Drinking Water Using High-Energy Electron Beam Irradiation. In *Disinfection Byproducts in Water Treatment Their Chemistry of Their Formation and Control* (Edited by R. A. Minear and G. L. Amy). Lewis Publishers, New York.

Mak, F. T., Zele, S., Cooper, W. J., Kurucz, C. N., Waite, T. D. and Nickelsen, M. G. (1997) Kinetic Modeling of Carbon Tetrachloride, Chloroform, and Methylene Chloride Removal from Aqueous Solution using the Electron Beam Process. *Wat. Res.* **31**, 219-228.

Malatesta, P., Scuro, L.A. and Sorice, F. (1951) Sull'Attivita Antibatterica Di Alcuni Alogeno-Derivati Alifatici E. In Particolare Della Cloro E Bromopicrina, antibacterial activity of aliphatic halogen derivatives. *Il Farmaco: Science a technica* **6**, 137-141.

Matheson, M.S. and Dorfman, L. M. (1969) Pulse Radiolysis, Research Monographs. In *Radiation Chemistry*. M.I.T. Press, Cambridge, Massachusetts.

Matheson, M. S., Mulac, W. A., Weeks, J. L. and Rabani, J. (1966) The Pulse Radiolysis of Deaerated Aqueous Bromide Solutions. *J. Phys. Chem.* **70**, 2092-2099.

McElroy, W. J. (1990) A laser photolysis study of the reaction of SO_4^- with Cl^- and the subsequent decay of Cl_2^- in aqueous solution. *J. Phys. Chem.* **94**, 2435-2441.

Meesungnoen, J. M., Jay-Gerin, J., Filali-Mouhim, A. and Mankhekorn, S. (2002) On the temperature dependence of the primary yield and the product $G\epsilon_{max}$ of hydrated electrons in the low-LET radiolysis of liquid water. *Can. J. Chem.* **80**, 767-773.

Meier, J. R., (1988) Genotoxic activity of organic chemicals in drinking water. *Mutat. Res.* **196**, 211-245.

Merényi, G., Lind, J., Goldstein, S. and Czapski, G. (1999) Mechanism and Thermochemistry of Peroxynitrite Decomposition in Water. *J. Phys. Chem.* **103**, 5685-5691.

Merlet, N., Thibaud, H. and Dore, M. (1985) Chloropicrin Formation During Oxidative Treatments in the Preparation of Drinking Water. *Science of the Total Environment* **47**, 223-228.

Mertens, R., von Sonntag, C., Lind, J. and Merenyi, G. (1994) A kinetic study of the hydrolysis of phosgene in aqueous solution by pulse radiolysis. *Chem. Int. Ed. Engl.* **33**, 1259-1261.

Mezyk, S. P. and Cooper, W. J. (2001) Radiation chemistry of alternative fuel oxygenates - Substituted Ethers. *J. Phys. Chem. A*, **105**, 3521-3526.

Mezyk, S. P., Cooper, W. J., Madden, K. P. and Bartels, D. M. (2004) Free Radical Destruction of N-Nitrosodimethylamine in Water. *Environ. Sci. Technol.* **38**, 3161-3167.

Mincher, B. J. and Cooper, W. J. (2003) The Electron Beam Process for the Radiolytic Degradation of Pollutants. In *Chemical Degradation Methods for Wastes and Pollutants* (Edited by M. A. Tarr). Marcel Dekker, Inc., New York.

Mezyk, S. P., Helgeson, T., Cole, S. K., Cooper, W. J., Fox, R. V., Gardinali, P. R. and Mincher, B. J. (2005) Free Radical Chemistry of Disinfection By-Products 1: Kinetics and Hydrated Electron and Hydroxyl Radical Reactions with Halonitromethanes in Water. *J. Phys. Chem.* Manuscript submitted for publication.

Milosavljevic, B. H., LaVerne, J. A. and Pimblott, S. M. (2005) Rate Coefficient Measurements of Hydrated Electrons and Hydroxyl Radicals with Chlorinated Ethanes in Aqueous Solutions. *J. Phys. Chem. A.* **109**, 7751-7756.

Moilanen, K. W., Crosby, D. G., Humphrey, J. R. and Giles, J. W. (1978) Vapor-phase photodecomposition of chloropicrin (Trichloronitromethane). *TETRA* **34**, 3345-3349.

Mönig, J., Bahnemann, D. and Asmus, K. -D. (1983) One-Electron Reduction of CCl_4 in Oxygenated Aqueous Solutions. A CCl_3O_2• Free Radical Mediated Formation of Cl- and CO_2. *Chem. Biol.* **47**, 15-27.

Moureu, H., Chovin, P. and Truffert, L. (1950) Sur la transformation photochimique de la chloropicrine en phosgene. *Archives des Maladies professionelles de m'edecine du travail et s'ecurit'e sociale* **11**, 445-452.

Mozumder, A. (1969) Charged Particle Tracks and Their Structure. In *Advances in Radiation Chemistry, Vol. 1* (Edited by M. Burton and J. L. Magee). John Wiley and Sons, New York.

Mozumder, A. and Magee, J. L. (1975b) The Early Events of Radiation Chemistry. *Int. J. Radiat. Phys. Chem.* **7**, 83-93.

Mozumder, A. and Magee, J. L. (1975a) Radiation Chemistry in Condensed Phases. In *Physical Chemistry An Advanced Treatise, Reactions in Condensed Phases, Vol. 7* (Edited by H. Eyring, D. Henderson, and W. Jost). Academic Press, New York.

Neta, P., Fessenden, R. W. and Schuler, R. H. (1971) An Electron Spin Resonance Study of the Rate Constants for Reaction of Hydrogen Atoms with Organic Compounds in Aqueous Solution. *J. Phys. Chem.* **75**, 1654-1666.

Neta, P., Huie, R. E. and Ross, A. B. (1990) Rate constants for reactions of peroxyl radicals in fluid solutions. *J. Phys. Chem. Ref. Data* **19**, 413-513.

Nickelsen, M. G., Cooper, W. J., Kurucz, C. N. and Waite, T. D. (1992) Removal of Benzene and Selected Alkyl-Substituted Benzenes from Aqueous Solution Utilizing Continuous High-Energy Electron Irradiation. *Environ. Sci. Technol.* **26**, 144-152.

Nickelsen, M. G., Cooper, W. J., Secker, D. A., Rosocha, L. A., Kurucz, C. N. and Waite, T. D. (2002) Kinetic Modeling and Simulation of PCE and TCE Removal In Aqueous Solutions by Electron-Beam Irradiation. *Radiat. Phys. Chem.* **65**, 579-587.

Park, D.-S., Grodnitzky, J. A. and Coats, J. R. (2002) QSAR Evaluation of Cyanohydrins' Fumigation Toxicity to House Fly (Musca domestica) and Lesser Grain Borer (Rhyzopertha dominica). *J. Agric. Food Chem.* **50**, 5617-5620.

Pimblott, S., Milosavljevic, B. H. and LaVerne, J. A. (2005) Radiolysis of aqueous solutions of 1, 1- and 1, 2-dichloroethane. *J. Phys. Chem. A.* Manuscript submitted for publication.

Pikaev, A. K. (1998) Electron-Beam Purification of Water and Wastewater. In *Environmental Applications of Ionizing Radiation* (Edited by W. J. Cooper, R. D. Curry and K. E. O'Shea). John Wiley and Son, New York.

Plewa, M. J., Kargalioglu, Y., Vankerk, D., Minear, R. A. and Wagner, E. D. (2000) Development of Quantitative Comparative Cytotoxicity and genotoxicity Assays for Environmental Hazardous Chemicals. *Wat. Sci. Tech.* **42**, 109-116.

Plewa, M. J., Wagner, E. D., Jazwierska, P., Richardson, S.D., Chen, P.H. and McKague, A B. (2004) Halonitromethane drinking water disinfection byproducts: Chemical characterization and mammalian cell cytotoxicity and genotoxicity. *Environ. Sci. Technol.* **38**, 62-68.

Porter, J. T., Voet, J. G. and Bright, H. J. (2000) Active Site Generation of a Protonically Unstable Suicide Substrate from a Stable Precursor: Glucose Oxidase and Dibromonitromethane. *Biochem.* **39**, 11808-11817.

Pryor, W. A. and Squadrito, G. L. (1995) The chemistry of peroxynitrite: a product from the reaction of nitric oxide with superoxide. *Am. J. Physiol. (Lung Cell. Mol. Physiol.)* **12**, L699-722.

Rabani, J., Mulac, W. A. and Matheson, M. S. (1965) The pulse radiolysis of aqueous tetranitromethane. I. Rate constants and the extinction coefficient of e^-_{aq}. II. Oxygenated solutions. *J. Phys. Chem.* **69**, 53-70.

Richardson, S. D., Thruston, Jr., A. D., Caughran, T. V., Chen, P. H., Collette, T. W., Floyd, T. L., Schenck, K. M., Lykins, Jr., B. W., Sun, G-R., and Majetich, G. (1999) Identification of New Ozone Disinfection Byproducts in Drinking Water. *Environ. Sci. Technol.* **33**, 3368-3377.

Richardson, S. D., Thruston Jr., A. D., Rav-Acha, C., Groisman, L., Popilevsky, I., Juraev, O., Glezer, V., McKague, A. B., Plewa, M. J. and Wagner, E. D. (2003) Tribromopyrrole, brominated acids, and other disinfection byproducts produced by disinfection of drinking water rich in bromide. *Environ. Sci. Technol.* **37**, 3782-3793.

Richardson, S. D. (2003) Water Analysis: Emerging Contaminants and Current Issues. *Anal. Chem.* **75**, 2831-2857.

Richardson, S. D., Simmons, J. E. and Rice, G. (2002) Disinfection Byproducts: Next Generation. *Environ. Sci. Technol.* **62**, 198-205.

Richardson, S. D., Thruston Jr., A.D., Caughran, T. V., Chen, P. H., Collette, T. W., Schenck, K. M., Lykins, Jr., B. W., Rav-Acha, C. and Glezer, V. (2000) Identification of new drinking water disinfection byproducts from ozone, chlorine dioxide, chloramines and chlorine. *Water Air Soil Pollut.* **123**, 95-102.

Richardson, S.D., Thruston, Jr., A. D., Caughran, T. V., Chen, P. H., Collette, T. W., Floyd, T. L., Schenck, K. M. Lykins, Jr., B. W., Sun, G-R. and Majetich, G. (1999) Identification of New Ozone Disinfection Byproducts in Drinking Water. *Environ. Sci. Technol.* **33**, 3368-3377.

Rook, J. J. (1974) Formation of Haloforms During Chlorination of Natural Waters, Water Treatment and Examination, Chorleywood, England (PT. 2). *Society for Water*, **23**, 234-243.

Sariasiani, S. and Stahl, Jr., R. G., (1990) Activation of promutagenic chemicals by Streptomyces griseus containing cytochrome P-450soy. *Biochem. Biophys. Res. Commun.* **166**, 743-749.

Sayato, Y., Nakmuro, K. and Matsui, S. (1982) Studies on Mechanism of Volatile Chlorinated Organic Compound Formation (III). Mechanism of Formation of Chloroform and Chloropicrin by Chlorination of Humic Acid, Suishitsu Odaku Kenkyu. *Japan Journal of Water Pollution Research* **5**, 127-128.

Schneider, M., Quistad, G. B. and Casida, J. E. (1999) Glutathione activation of chloropicrin in the Salmonella mutagenicity test. *Mutat. Res.* **439**, 233-238.

Schuler, R. H. (1996) Radiation Chemistry at Notre Dame 1943-1994. *Radiat. Phys. Chem.* **47**, 9-17.

Schuler, R. H., Patterson, L. K. and Janata, E. (1980) Yield for the Scavenging of OH Radicals in the Radiolysis of N2O-Saturated Aqueous Solutions. *J. Phys. Chem.* **84**, 2088-2089.

Schuetz, M. N. and Vroom, D. A. (1998) Radiation Chemistry and Its Application to Environmental Pollution. In *Environmental Applications of Ionizing Radiation* (Edited by W. J. Cooper, R. D. Curry and K. E. O'Shea). John Wiley and Son, New York.

Schwarz, H. A. (1962) A Determination of Some Rate Constants for the Radical Processes in the Radiation Chemistry of Water. *J. Phys. Chem.* **66**, 255-262.

Schwarz, H. A. (1968) Applications of the Spur Diffusion Model to the Radiation Chemistry of Aqueous Solutions. *J. Phys. Chem.* **73**, 1928-1937.

Schwarz, H. A. and Dodson, R. W. (1984) Equilibrium between Hydroxyl Radicals and Thallium (II) and the Oxidation Potential of OH (aq). *J. Phys. Chem.* **88,** 3643-3647.

Selala, M. I., Janssens, J. J., Jorens, Ph. G., Bossaert, L. L., Beaucourt, L. and Schepens, P. J. C. (1989) An improperly labeled container of chloropicrin: A farmer's nightmare. *Bulletin Environmental and Contamination Toxicology* **42**, 202-208.

Shin, D., Chung, Y., Choi, Y., Kim, J., Park, Y. and Kum, H. (1999) Assessment of disinfection byproducts in drinking water in Korea. *Journal of Exposure Analysis and Environmental Epidemiology* **9**, 192-199

Siddiqui, M. S., Amy, G. L., Cooper, W. J., Kurucz, C. N., Waite, T. D. and Nickelsen, M. G. (1996) Bromate ion Removal by HEEB irradiation. *J. Am. Water Works Assoc.* **10**, 90-101.

Simic, M. G. and Hunter, E. P. L. (1986) Reaction mechanisms of peroxyl and C-centered radicals with sulfhydryls. *Free Radical Biol. Med.* **2**, 227-2

Simpson, K. L. and Hayes, K. P. (1998) Drinking water disinfection byproducts: An Australian perspective. *Wat. Res.* **32**, 1522-1528.

Sparks, S.E., Quistad, G. B., Li, W. and Casida, J. E. (2000) Chloropicrin in Relation to Toxic Action. *J. Biochem. Molecular Toxicology* **14**, 26-32.

Spinks, J. W. T. and Woods, R. J. (1964) *An Introduction to Radiation Chemistry*. John Wiley and Sons, New York.

Spokas, K. and Wang, D. (2003) Stimulation of nitrous oxide production resulted from soil fumigation with chloropicrin. *Atmos. Env.* **37**, 3501-3507.

Stumm W. and Morgan, J. J. (1996) *Aquatic Chemistry: Chemical Equilibria and Rates in Natural waters.* 3rd ed. John Wiley and Sons, New York.

Sutton, J. and Son, T. D. (1967) Vitesses De Reaction de Trois Nitroparaffines Avec Les Atomes D'Hydrogene Et Les Electrons Solvates En Milieu Aqueux. *Journal de Chemie Physique* **64**, 688-690.

Swallow, A. J. (1973) *Radiation Chemistry.* John Wiley and Sons, New York.

Thibaud, H., De Laat, J. and Doré, M., (1988) Effects of bromide concentration on the production of chloropicrin during chlorination of surface waters. Formation of brominated trihalomethanes. *Wat. Res.* **22**, 381-390.

Thibaud, H., Laat, D. J., Merlet, N. and Dore, M. (1987) Chloropicrin Formation in Aqueous Solution: Effect of Nitrites on Precursors Formation During the Oxidation of Organic compounds. *Wat. Res.* **21**, 813-821.

Thies, W. G. and Nelson, E. E. (1982) Control of Phellinus weirii in Douglas-fir stumps by the fumigants chloropicrin, allyl alcohol, Vapam, or Vorlex. *Can. J. For. Res.* **12**, 528-532.

Tobien, T., Cooper, W. J. and Asmus, K. -D. (2000) Removal Simulation for the Radiation Induced Degradation of the Disinfection By-Product Chloroform. In *Natural Organic Matter and Disinfection Byproducts* (Edited by S. Barrett, S. Krasner and G. Amy). American Chemical Society, Symposium Series 761, American Chemical Society, Washington, DC.

Tobien, T., Cooper, W. J., Nickelsen, M. G., Pernas, E., O'Shea, K. E. and Asmus, K. -D. (2000) Odor Control in Wastewater Treatment: The Removal of Thioanisole from Water – A Model Case Study by Pulse Radiolysis and Electron Beam Treatment. *Environ. Sci. Technol.* **34**, 1286-1291.

Treinin, A. and Hayon, E. (1970) Absorption Spectra and Reaction Kinetics of NO_2, N_2O_3, and N_2O_4 in Aqueous Solutions. *J. Am. Chem. Soc.* **92**, 5821-5828.

Trumbore, C. N., Youngblade, W. and Short, D. R. (1988) Modeling of Gamma-Ray Radiolysis at Moderate and Low Solute Concentrations in Aqueous Solutions. *Radiat. Phys. Chem.* **32**, 233-239.

U.S. Department of Health, Education and Welfare (1978) *Bioassay of Chloropicrin for Possible Carcinogenicity, CAS No. 76-06-2, NCI-CG-TR-65 National Institute of Health, National Cancer Institute Carcinogenesis Technical Report Series No. 65.* U. S. Department of Health, Education and Welfare, Washington, DC.

U.S. Environmental Protection Agency (1997) National Primary Drinking Water Regulations: Disinfectants and disinfection byproducts rule. *Federal Register* **65**, 19045-19094

U.S. Environmental Protection Agency (1999) *Alternative Disinfectants and Oxidants Guidance Manual EPA 815-R-99-014.* U.S. Environmental Protection Agency, Office of Water, Washington, DC.

U.S. Food and Drug Administration (1997) Irradiation in the Production, Processing, and Handling of Food; final rules. *Federal Register* **62**, 64102-64121.

von Gunten, U. and Hoigné, J. (1996) Ozonation of Bromide-Containing Waters: Bromate Formation through Ozone and Hydroxyl Radicals. In *Disinfection Byproducts in Water Treatment, The Chemistry of Their Formation and Control* (Edited by R. A. Minear and G. L. Amy). Lewis Publishers, New York.

von Sonntag, C. and Schuchmann, H-P. (1997) Peroxyl Radicals in Aqueous Solutions. In *The Chemistry of Free Radicals* (Edited by Z. Alfassi) John Wiley and Sons, New York.

Wade, E. A., Reak, K. E., Parsons, B. F., Clemes, T. P. and Singmaster, K. A. (2002) Photochemistry of chloropicrin in cryogenic matrices. *Chem. Phys. Lett.* **365**, 473-479.

Wagnière, G. H. (1969) Theoretical aspects of the C-NO and C-NO_2 Bonds. In *The Chemistry of the nitro and nitroso groups, Part 1* (Edited by H. Feuer). Interscience Publishers, John Wiley and Sons, New York.

Wallace, S.C. and Thomas, J. K. (1973) Reactions in micellar systems. *Radiat. Res.* **54**, 49-62.

Wang, Q., Gan, J., Papiernik, S. K. and Yates, S. R. (2000) Transformation and Detoxification of Halogenated Fumigants by Ammonium Thiosulfate. *Environ. Sci. Technol.* **34**, 3717-3721.

Weinberg, H. S., Krasner, S. W., Richardson, S.D. and Thruston, Jr., D. (2002) *The Occurrence of Disinfection Byproducts (DBPs) of Health Concern in Drinking Water: Results of a Nationwide DBP Occurrence Study EPA/600/R-02/068.* U. S. Environmental Protection Agency, National Exposure Research Laboratory, Research Triangle Park, North Carolina.

Weston, R. E. and Schwarz, H. A. (1972) *Chemical Kinetics*. Prentice-Hall, New Jersey.

Whitham, K., Lyons, S., Miller, R., Nett, D., Treas, P., Zante, A., Fessenden, R. W., Thomas, M. D. and Wang, Y. (1995) Linear Accelerator For Radiation Chemistry Research at Notre Dame. In *Proceedings of the 16th Particle Accelerator Conference and International Conference on High Energy Accelerators in Dallas, Texas, May 1-5.* Institute of Electrical and Electronics Engineers, Inc., College Park, Maryland.

Wilhelm, S. N., Shepler K. Lawrence, L. J. and Lee, H. (1996) Environment Fate of Chloropicrin. In *ACS Symposium Series 652 Fumigants: Environmental Fate, Exposure, and Analysis* (Edited by J. N. Seiber, J. E. Woodrow, M. V. Yates, J. A. Knuteson, N. L. Wolfe and S. R. Yates). American Chemical Society, Washington, DC.

Williams, D. T., LeBel, G. L. and Benoit, F. M. (1997) Disinfection byproducts in Canadian drinking water. *Chemosphere* **34**, 299-316.

Woods, R. J. (1998) Radiation Chemistry and Its Application to Environmental Pollution. In *Environmental Applications of Ionizing Radiation* (Edited by W. J. Cooper, R. D. Curry and K. E. O'Shea). John Wiley and Son, New York.

Wright, M. R. (2004) *An Introduction to Chemical Kinetics*. John Wiley and Sons, West Sussex, England.

Wu, D., Wong, D. and Di Bartolo, B. (1980) Evolution of Cl_2^- in aqueous $NaCl^-$ solutions. *J. Photochem.* **14**, 303-310.

Xu, J. M., Gan, J., Papiernik, S. K., Becker, J. O. and Yates, S. R. (2003) Incorporation of Fumigants into Soil Organic Matter. *Environ. Sci. Technol.* **37**, 1288-1291.

Yu, X.-Y., Bao, Z.-C. and Barker, J. R. (2004) Free radical reactions involving $Cl^•$, $Cl_2^{-•}$, and $SO_4^{-•}$ in the 248 nm photolysis of aqueous solutions containing $S_2O_8^{2-}$ and Cl^-. *J. Phys. Chem.* **108**, 295-308.

Zehavi, D. and Rabani, J. (1972) The oxidation of Aqueous Bromide Ions by Hydroxyl Radicals. *J. Phys. Chem.* **76**, 312-319.

Zhang, G. and Hua, I. (2000) Ultrasonic degradation of trichloroacetonitrile, chloropicrin and bromobenzene: Design factors and matrix effects. *Advances in Environmental Research* **4**, 211-218.

Zimek, Z., and Chmielewski (1998)Advanced Accelerator Technology for Environmental Protection. In *Environmental Applications of Ionizing Radiation* (Edited by W. J. Cooper, R. D. Curry and K. E. O'Shea). John Wiley and Son, New York.

Zona, R., Solar, S. and Gehringer, P. (2002) Degradation of 2, 4-dichlorophenooxyactetic acid by ionizing radiation: influence of oxygen concentrations. *Wat. Res.* **36**, 1369-1374.

Appendix

A. COMPUTER PROGRAMS FOR KINETIC ANALYSIS

A.1. Mass Action Kinetic Simulation

Upon completion of the research to determine the rate constants for HNM destruction in water exposed to pulse radiolysis (LINAC) and the quantification of the ion mass produced as a result of steady state irradiation by ^{60}Co, a kinetic model was prepared to simulate the chemical reactions. The kinetic model included a series of chemical reactions to simulate HNMs destruction in water upon exposure to ionizing radiation. A computer program was then used for study of water radiolysis and the destruction of the HNMs. The mechanism was coded into the kinetic computer model. Initially the computer model was used to simulate the degradation mechanism using the derived rate constants. The mechanistic model results were then compared to experimental results at level of HNM the concentration as used in experimentation. The model was then revised to incorporate a lower concentration of HNMs to replicate the concentration of HNM as found in drinking water. Based on the dose constant (k_D) results for lower concentrations an estimate of the EE/O was made.

Three mass action kinetic computer models have been identified in the industry and open literature where they were designed for modeling kinetic reactions in the radiolysis of water. These include MAKSIMA-CHEMIST, FACSIMILI™, and CHEMSIMUL™. Both FACSIMILI™ and CHEMSIMUL™ can be commercially purchased and are supported by their developers. MAKSIMA-CHEMIST was developed by Carver *et al.* (1979), Atomic Energy of Canada Limited and is no longer supported.

Simulations were performed to compute the mass action kinetics of simultaneous chemical reactions. The kinetic computer program will accommodate 200 chemical reactions and up to 60 reactants. The computational analysis used in the program was prepared by Carver *et al.* (1979) based on radiation chemistry kinetics by Schwarz (1962) and differential equation algorithms by Gear (1971).

The MAKSIMA-CHEMIST kinetic computer model included rate constants from radiolysis of water identified in Table 1.3 (Buxton *et al.,* 1988) and those HNM rate constants derived from experimentation. The model also included the concentration of radicals as identified in equation (1.1), radiation dose (eV L^{-1} s^{-1}), time of radiation exposure in seconds, concentration for each of the solutes in moles, the reaction rate constant in units of s^{-1} or $M^{-1}s^{-1}$, and the ionic charge.

The model output provides the concentration of all the reactants as function of both dose and the time step. The relative error in the model predictions is comparable to the number of accurate significant figures in the results (10^{-5}) (Carver *et al.,* 1979) and the relative error of the input data.

The model is based on reaction of chemicals in a given first or second-order reaction. From independent reactions (A.1) and (A.2) with rates constants k_1 and k_2 (Carver *et al.,* 1979):

$$A^- + BC \xrightarrow{k_1} AB + C^- \qquad \text{(A.1)}$$

$$2AB \xrightarrow{k_2} A_2B_2 \qquad \text{(A.2)}$$

Reaction (A.1) removes A^- and BC from the system to form AB and C^- at a rate according to (A.3) (Carver *et al.,* 1979):

$$R_1 = k_1[A^-][BC] \qquad \text{(A.3)}$$

The total net rate of formation of AB from (A.1) and (A.2) (Carver *et al.,* 1979):

$$\frac{d}{dt}[AB] = k_1[A^-][BC] - k_2[AB]^2 \tag{A.4}$$

Instantaneous formation is given by (Carver *et al.,* 1979):

$$[A] = [AB]_0 + \int (\frac{d}{dt}[AB])dt \tag{A.5}$$

Summarizing equations (A.1) through (A.4) gives (Carver *et al.,* 1979):

$$\upsilon_A \mathrm{A} + \upsilon_B \mathrm{B} + \upsilon_C \mathrm{C} \rightarrow \upsilon_D D + \upsilon_E E + \upsilon_F F \tag{A.6}$$

where ν are integers, removes negative reagents A, B, and C from the system to form positive products D, E, and F and a rate according to (Carver *et al.,* 1979):

$$R_i = \pm k_i [A]^{\upsilon_A}[B]^{\upsilon_B}[C]^{\upsilon_C} = \pm k_i \prod_{j=1}^{3} [x_j]^{\upsilon_{x_j}} \tag{A.7}$$

where k_i is the rate constant. In m reactions and p species, the time derivative for the concentration of species x_g would give (Carver *et al.,* 1979):

$$\frac{d[X_g]}{dt} = \sum_{i=1}^{m} \upsilon_{x g_i} \quad \mathrm{R_i} = \sum_{i=1}^{m} \pm k_i \upsilon_{x g_i} \prod_{j=1}^{P_i} [X_{ij}2]^{\upsilon_{x_{ij}}} \tag{A.8}$$

The elements of the Jacobian matrix follows and is used in the predictor-corrector equation (Carver *et al.,* 1979):

$$\frac{\partial}{\partial [x_r]} \frac{\partial [x_r]}{\partial t} = \sum_{i=1}^{m} k_i \upsilon_{x g_i} \upsilon_{x_{ri}} [x_{ri}]^{(\upsilon_{x_{ri}} - 1)} \prod_{\substack{j=1 \\ \neq r}}^{P_i} [x_{ij}2]^{\upsilon_{x_{ij}}} \tag{A.9}$$

Analytic expression for the Jacobian matrix is by equation (A.9) and automatic solution of differential equations with criterion for order of approximation (Gear, 1971). Problems encountered in the solution include an expression for derivatives (rate equation) where they are nonlinear, and they must be done numerically (Carver *et al.,* 1979). As nonlinearity increases small errors will amplify and the individual reaction rates may differ by orders of magnitude. The resolution is by use stiff equation integration. These stiff equations allow for follow fast transients and small integrations where they rapidly increase their time step when initial transients have died out (Carver *et al.,* 1979). Carver *et al.* (1979) identified that the backward differencing method for stiff differential equations effectively avoids the stability constraint on integration by implementation of a stepwise method. This was accomplished by use of the Gear (1971) algorithm that effectively combined this integration with an effective error controlled step size and order selection (Carver *et al.,* 1979).

B. ANALYTICAL METHODS

Precaution was made to secure HNM samples and extreme care was used when sealing and storing samples to assure they are upright and caps were screwed tight. Samples were stored in chilled storage. It was noted that HNMs will not tolerate long periods of storage as they will evaporate. Caution should be used for handling HNMs and strict safety procedures must be used. These compounds are an irritant, toxic, and possibly carcinogenic.

Analytical methods conformed to applicable procedures for the equipment and laboratory equipment use was within date of last calibration. Generally, calibrations were provided with sample blanks and control samples were applied. Analytical methods applied in this research are identified in Table B.1. A detailed description of the methods and procedures follows.

Table B.1. Analytical Methods

Item	Parameter	Method
1	Purity of Sample Distillation	Nuclear Magnetic Resonance
2	HNM residual in the ^{60}Co irradiated samples	Gas Chromatography/ Mass Spectrometry
3	Determination of samples anion (chloride, bromide, nitrate, nitrite) concentrations in the ^{60}Co irradiated samples	Ion Chromatography
4	Intermediate and Final Compound Identification in the ^{60}Co irradiated samples, oxalic acid and formic acid	High Performance Liquid Chromatography

B.1. Nuclear Magnetic Resonance

A Bruker™ Nuclear Magnetic Resonance (NMR) instrument incorporated use of a 400 MHz radio frequency generator. It was designed to pulse the sample and then record the signal given off by the relaxing nuclei. The data obtained was then mathematically treated by Fourier-Transform in an integral digital analyzer. The data was then analyzed to provide information about the molecule under study. The principal of operation was based on the condition where non-identical nuclei exist in different chemical environments, and therefore resonate at different frequencies. The peaks of NMR spectra indicate when a particular nuclei of the molecule was in resonance. The data was then interpolated by computer and the digital results, as percentage of purity, were provided.

B.2. Gas Chromatography Mass Spectrometry

Gas Chromatography Mass Spectrometry (GC/MS) was used to determine the amount of residual halonitromethane remaining in solution after γ-irradiation. Aqueous solutions of ^{60}Co irradiated and control treatments (1 mL) were fortified with an appropriate amount of an internal standard (1, 3 dichloropropane) and liquid-liquid extracted against 1 mL of MTBE by using an orbital shaker. Upon separation of the organic phases, 500 uL of the MTBE extracts were recovered from the vial and placed into a glass insert. After addition of a recovery standard the samples were run on a GC/MS (Finnigan, DSQ Utra-Trace™). The system was equipped with a 30 meter $\times$ 0.25 mm $\times$ 0.25 micron capillary column (Model DB5-MS). Helium was used as a carrier gas at a flow of 1.0 mL $min.^{-1}$ and compounds were eluted from the column by ramping the oven from 45° to 150°C at 15°C per minute (Chen *et al.,* 2002). Care was exercised to not exceed temperature limits for

halonitromethane volatilization. All compounds were quantitated under electron impact ionization (70 eV) in selected ion mode (SIM) with a minimum of three diagnostic ions. A six point calibration curve (0 to 100 ppm) was used to quantitate the HNMs using internal standard method. Calibration curves used for the GC/MS to determine the concentration of HNMs are presented in Figure B.1.

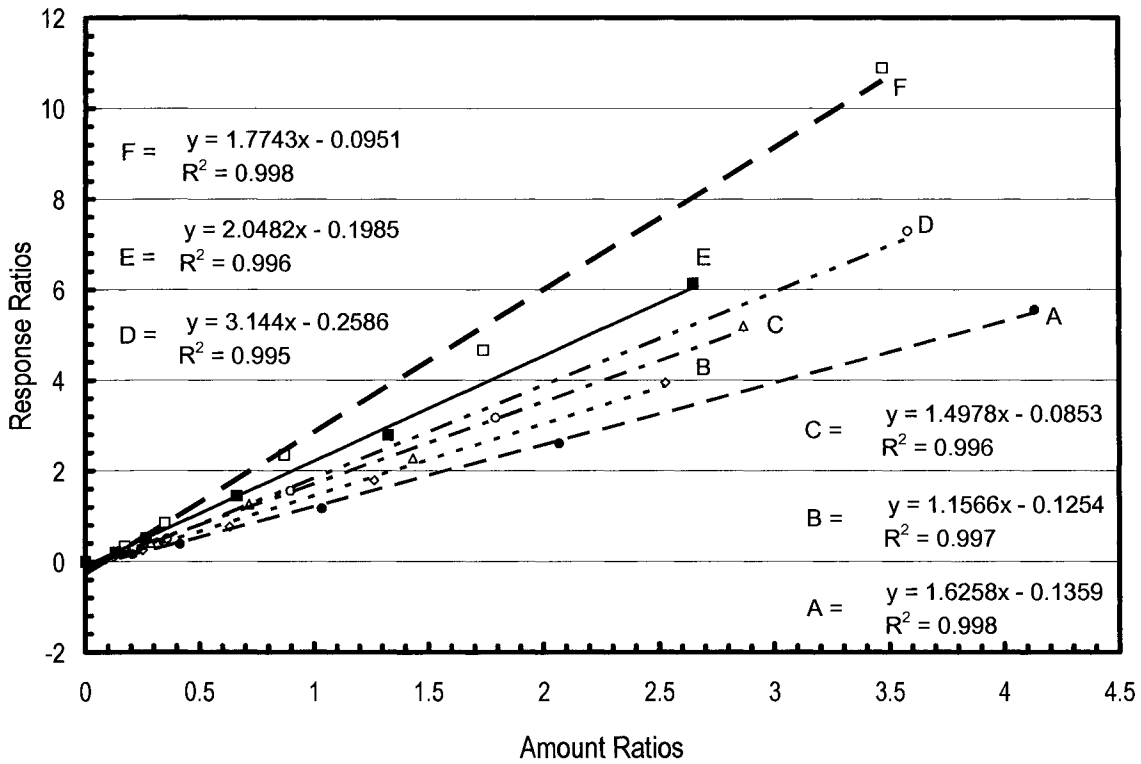

Figure B.1. Calibration curves for GC/MS. Chlorodibromonitromethane (A), chloronitromethane (B), trichloronitromethane (C), bromochloronitromethane (D), dichloronitromethane (E), bromnitromethane (F).

The minimum level of detection for the GC/MC was estimated by investigation of the lowest calibration solution (0.1 ppm) and the results obtained from a calculated ratio of signal to noise (S/N). The integral GC/MS software was used to calculate the height of the peak for the HNM and automatically divide this peak height number by the height of

the average noise to the side of the peak. The lowest sensitivity is based on a minimum signal to noise ratio to detect a peak. This method applied uses a basis for discrimination of the condition that the signal has to be significantly different that the noise (one standard deviation). The S/N ratios were calculated for each of the triplicates of the 0.1 ppm HNM solutions. The S/N values, which ranged between 800 to 8000 depending on the analyte, were then used to back calculate the concentrations in units of ppm and produce a S/N of 10. The minimum detection level (MDL) for each of the HNMs is presented in Table B.2. Based on this method, the overall MDL for all HNMs was approximately 0.03 ppm.

Table B.2. Minimum Level of Detection for GC/MS

Compound	Minimum Detection Level (ppm)	RSD for n=3 (%)
chloronitromethane	0.021	11
dichloronitromethane	0.003	5
trichloronitromethane	0.025	4
bromonitromethane	0.005	12
bromodichloromethane	0.004	5
chlorodibromonitromethane	0.009	6

B.3. High Performance Liquid Chromatography

The High Performance Liquid Chromatography (HPLC) system was used in the analysis of samples for oxalic acid and formic acid concentrations. The HPLC (Hitachi, San Jose, CA) system was equipped with a computer interface (Model D-6000) and ultra-violet detector (Model L-4000H) set at 210 nm. Eluant as 0.1% H_3PO_4 was pumped (L-6200A Intelligent Pump™) at 0.5 mL per minute and the configuration incorporated use of an autosampler (AS-4000 Intelligent™). The system was controlled by the equipment

manufactures computer software (Hitachi D-6000 HPLC Manager™, Version 2, Revision 10). Organic acids were separated using a column (Supelco, Supelcogel™ C-610H) operated at 30°C. A guard column (Supelcogel™ H) and a 50 mm column packed with Amberlyst 15 resin beads were also used. Samples were filtered and placed in 2 mL vials. Reagents used for HPLC analysis include standards that were prepared for organic acid analysis using sodium formate (certified by American Chemical Society, Fisher Scientific, Fair Lawn, NJ, Lot 986590) and oxalic acid disodium salt by (Sigma, St. Louis, MO, Lot 41H0116). A 2000 ppm formate and a 1000 ppm oxalate stock solution were prepared. Standard concentrations consisted of 200 ppm, 20 ppm, and 2 ppm formate, and 100 ppm, 10 ppm, and 1 ppm oxalate. Standards contained both formate and oxalate. All standards were prepared using nano-pure water with resistivity ≥18-MΩcm at 25°C. A blank was also run and prepared from ≥18 MΩcm at 25°C nano-pure water. Limit of detection was approximately 0.02 mM. The calibration standard data for the HPLC is presented in Table B.3.

Table B.3. HPLC standard data for oxalic acid and formic acid

Standard (ppm)	Oxalic Acid (area response)	Formic Acid (area response)
Blank	0	0
20	124843	4244
20	128578	4149
100	409125	48076
100	430677	50747
200	854903	106339
200	885587	111057

Notes:
1. Linear regression analysis of the oxalic acid standard yields the line equation $y = 4146x + 30043$ for $R^2 = 0.9955$
2. Linear regression analysis of the formic acid standard yields the line equation $y = 581.07x - 7878.6$ $R^2 = 0.9985$

B.4. Ion Chromatography

Ion chromatography (IC) for the determination of anion (chloride, bromide, nitrate, and nitrite) concentrations in the ^{60}Co irradiated samples was performed on an ion chromatograph (Dionex, Sunnyvale, CA, USA DX-500™). Components of the Dionex system consisted of a gradient pump (Model GP50), an electrochemical detector (Model ED40), and a thermal compartment (Model AS50). Samples were loaded using a Rheodyne, Cotati, CA, USA six-port valve (Model 9750E-033). A 25 μL loop made from polyether ether ketone (PEEK) tubing was fitted to the six-port valve. Data acquisition and instrument control chromatography were performed using a personal computer with the equipment manufacture's software (Dionex, PeakNet™ Version 5.2).

A Dionex eluent generator (Model EG40) was used and equipped with a cartridge (Model EGC II-KOH), suitable for producing potassium hydroxide eluents. A Dionex (AS17 IonPac™) analytical column 4×250 mm was used to perform ionic separations. A guard column (Model AG17) 4×50 mm was also present. Eluent concentrations through the columns as a function of runtime were: 0 to 3 minutes at 10 mM, 3 to 5 minutes at 10 to 15 mM, 5 to 8 minutes at 15 to 25 mM, 8 to 12 minutes at 25 to 30 mM, and 12 to 15 minutes at the 10 mM concentration. Eluted peaks were integrated and anion concentrations were calculated from standard curves. Each of the original irradiated samples and blank samples (time = 0) were analyzed in triplicate. Quality control standards were run before and after each eight hour day and interspersed every 10^{th} sample during the run.

Chemicals, solutions and samples were prepared and diluted using Class A volumetric glassware and ≥ 18 MΩcm at 25°C nano-pure water. Standards were prepared

using a Dionex seven anion standard. The original concentration of anions in the standard were; 20 mg L^{-1} fluoride, 30 mg L^{-1} chloride, 100 mg L^{-1} nitrite, 100 mg L^{-1} bromide, 100 mg L^{-1} nitrate, 150 mg L^{-1} phosphate, and 150 mg L^{-1} sulfate. Dilutions of the original standard were prepared using serial dilution techniques. The IC calibration standard data for is presented in Table B.4 and Table B.5. Minimum level of detection was identified as 1 ppm.

Table B.4. Ion chromatography standard data for Cl^- and NO_3^-

Standard (ppm)	Cl^- (microSiemens/m)	NO_3^- (microSiemens/m)
Blank	0.0037	0.009
1	0.2178	0.1219
5.0521	1.1445	0.6513
10.0715	2.2952	1.329
20.2674	4.641	2.7217

Notes:
1. Linear regression analysis of the Cl^- standard yields the line equation $y = 0.2296x - 0.0143$ for $R^2 = 1$
2. Linear regression analysis of the NO_3^- standard yields the line equation $y = 0.1352x - 0.024$ for $R^2 = 0.9999$

Table B.5. Ion chromatography standard data for Br^- and NO_2^-

Standard (ppm)	Br^- (microSiemens/m)	NO_2^- (microSiemens/m)
Blank	0.000	0.000
1.000	0.096	0.161
5.052	0.512	0.841
10.072	1.030	1.661
20.267	2.086	3.258

Notes:
1. Linear regression analysis of the Br^- standard yields the line equation $y = 0.1033x - 0.0088$ for $R^2 = 1$
2. Linear regression analysis of the NO_2^- standard yields the line equation $y = 0.1603x - 0.0215$ for $R^2 = 0.9998$

VITA
for
Stuart Kirkham Cole

DEGREES:

Master of Engineering (Civil Engineering), Old Dominion University, Norfolk, Virginia,
December 1995

Bachelor of Science (Civil Engineering), Virginia Military Institute, Lexington, Virginia,
May 1980